DISSERTATION

CALCITONIN GENE RELATED PEPTIDE INVOLVEMENT IN GUT HEALTH AND MODELS OF PARKINSON'S DISEASE

Submitted by

Hayley Nicole Templeton

Department of Biomedical Sciences

In partial fulfillment of the requirements

For the Degree of Doctor of Philosophy

Colorado State University

Fort Collins, Colorado

Spring 2025

Doctoral Committee:

Advisor: Stuart A. Tobet

Brent Myers
Bret Smith
Julie Moreno
Ronald Tjalkens

ABSTRACT

CALCITONIN GENE RELATED PEPTIDE INVOLVEMENT IN GUT HEALTH AND MODELS OF PARKINSON'S DISEASE

The gut plays a central role in maintaining overall health, serving not only as the site of digestion and nutrient absorption but also as a key player in immune function, microbial interactions, and metabolic regulation. Emerging research has highlighted the gut's influence on various diseases, including inflammatory bowel diseases, autoimmune disorders, and neurodegenerative conditions such as Parkinson's disease. Disruptions in intestinal barrier integrity, often referred to as 'leaky gut', have been linked to these conditions, with increased intestinal permeability allowing potentially harmful immunomodulatory substances to enter the bloodstream, triggering inflammation, cellular immune reactivity, and myriad other potential detrimental pathways. Many available models to study gut health lack the cellular diversity and complexity to investigate mechanisms of intestinal barrier dysfunction and epithelial – neural – immune signaling pathways. We developed a device that can maintain the intestinal barrier of intestinal tissue ex vivo for up three days. This was accomplished through the utilization of a dual-flow microfluidic device that uses two gaskets to create individual fluidic channels where luminal and serosal sides of the intestine are separated. The addition of bacterial collagenase to the luminal chamber of this device resulted in a model for investigating 'leaky gut' in the laboratory with recapitulation of important anatomic arrangements and physiologic conditions seen in the in vivo gut wall.

A large proportion of Parkinson's disease patients have impaired intestinal barrier integrity. Gastrointestinal symptoms often precede motor symptoms in Parkinson's disease, indicating early gut involvement. The neuropeptide known as calcitonin gene related peptide

(CGRP) is involved in regulating gut motility, inflammation, and nociception, and has been linked to both neurodegeneration and altered gut function in Parkinson's disease. A hallmark pathology of Parkinson's is the accumulation of the protein alpha synuclein, in both the central and peripheral nervous systems. Investigation of CGRP's involvement in gastrointestinal pathology of Parkinson's revealed elevated levels of CGRP in the colon. Treatment with CGRP resulted in increased alpha synuclein within gut neurons, implicating a role of CGRP in enteric alpha synuclein accumulation. Understanding CGRP's multifaceted role in PD may provide a novel pathway for therapeutic intervention aimed at improving both gut and central nervous system health in neurodegenerative diseases.

ACKNOWLEDGMENTS

Throughout the last 5 years, I've been surrounded by so many incredible people who helped and supported me throughout this journey. Stu – thank you for always pushing me to be a better scientist, researcher, and person. I wouldn't be the scientist I am today without you. A special thank you to Bob Handa who helped and supported me through a difficult change and gave me the courage to continue science. I would also like to thank my committee: Brent, Bret, Julie, and Ron, for all of your advice and support, both scientifically and career related.

Next, I want to thank my lab family. Julietta, Mina, Emily, Connie, Alexis, Brielle, and Luke. You have all become some of my best friends and I wouldn't have been able to complete this without you all. A special shoutout to Luke – I probably wouldn't have studied the best organ ever (the gut) if it wasn't for you. Beyond that, thank you for being an incredible mentor. Your guidance and support were instrumental in helping me complete this journey.

I would also like to express my gratitude to the many other great individuals at CSU who supported me during my time here. River and Taylor – we share a bond that will never break. Zephyr, Erica, Maddie, Sebastian, Tyler, Jordan, Amir, Nik, Sarah – thank you all for being there to vent frustrations, celebrate wins, pick me up when I'm down, and just have a good time with. Not many people can say they enjoy the people they work with, let alone say they're friends 😊 I would also like to thank the fantastic engineers who helped with the microfluidic devices – Ryan and Amanda.

Finally, I would like to thank my family for their support. My husband Brian – thank you so much for your unwavering support throughout my journey. You were always there to cheer me up on hard days and celebrate me on good days. I love and appreciate you more than you know. My family – thank you for supporting me and understanding that asking when I was going

to graduate was a triggering question. Topaz, Midnight, and Sadie – thank you for all of your love and snuggles.

TABLE OF CONTENTS

INTRODUCTION

Gut Involvement in Health and Disease:

Investigations into gut health have exploded in recent years as the role of the microbiome and enteric nervous system have emerged as targets for disease modulating treatments and overall well-being. Not only is the gut responsible for digestion and nutrient absorption but also serves as a key player in immune function, microbial interactions, and the regulation of metabolic processes. Additionally, the gut is intricately connected to the brain through the gut-brain axis, influencing mood, cognition, and even behavior. Disruptions in gut function have been linked to the pathogenesis of a wide range of conditions such as inflammatory bowel diseases (IBD) (Michielan and D'Inca, 2015), autoimmune diseases such as celiac disease (Akobeng et al, 2020; Christovich and Luo, 2022), neurodegenerative disorders such as Alzheimer's and Parkinson's Disease, (Braak et al, 2006; Kim et al, 2019; Holmqvist, 2014; Caradonna et al, 2024) and multiple sclerosis (Schwerdtfeger et al., 2024), and neurodevelopmental disorders such as autism spectrum disorder (Min et al, 2022). With emerging evidence highlighting the gut's role in diseases like Parkinson's disease, understanding mechanisms of gut homeostasis and pathogenesis of disease is essential for developing therapeutic strategies that address both gut-related and systemic health issues.

Intestinal Barrier:

The intestinal barrier separates the contents of the gastrointestinal tract from the underlying tissues and bloodstream, ensuring proper digestion and nutrient absorption while protecting the body from harmful substances. Epithelial cells of the gut physically separate luminal contents from the underlying lamina propria through apical transmembrane mucins and tight junctions (Schwerdtfeger & Tobet, 2020a). Specialized epithelial cells, known as goblet cells, produce and secrete mucin to create a mucosal barrier that protects the mucosa from commensal

microbes and pathogens (Schwerdtfeger & Tobet, 2020b). When the intestinal barrier is compromised, it can lead to increased permeability leading to a condition known as ‘leaky gut’, allowing harmful substances to leak into the bloodstream and underlying lamina propria ultimately triggering immune activation and inflammation. Leaky gut is associated with various diseases, including autoimmune disorders (Akobeng et al, 2020; Christovich and Luo, 2022), inflammatory bowel disease (Michielan and D’Inca, 2015), and neurodegenerative conditions including Parkinson’s Disease (Braak et al, 2006; Kim et al, 2019; Holmqvist, 2014). Maintaining the integrity of the intestinal barrier is essential for overall health, however, models to study the intestinal barrier are limited. Therefore, we have developed devices capable of maintaining the intestinal barrier of intestinal tissue explants for up to 72 hr. The devices discussed in Section 1 maintain the intestinal barrier through the utilization of two gaskets to create individual fluidic channels where luminal and serosal sides of the intestine have separate channels. I worked alongside engineers to maintain tissue health and evaluate relevant physiology. Hopefully these devices will guide the ability to study disease states associated with intestinal barrier dysfunction.

Models for Studying Gut Health:

When designing a device to study intestinal health, it is important to consider the previously employed approaches to studying organ function outside of the body, each with its own strengths and limitations. In vitro models such as 2D monolayers and 3D cell culture systems, using either cell lines or primary progenitor cells, have been developed to model organs like the gastrointestinal (GI) tract (Schwerdtfeger & Tobet, 2019). The integration of microfluidics into 2D culture systems has greatly enhanced their functionality by allowing the application of physical forces such as fluid shear stress, cyclic strain, and mechanical compression (McLean et al., 2018). While these advances have enhanced the modeling of certain GI features, in vitro models still fall short in accurately replicating the full complexity and intricacy of the gut. Key

characteristics such as villi structure, Peyer's patches, the microbiome, active and synchronous contraction of gut smooth muscle, and the intrinsic enteric nervous system are not captured. Without these critical components, these reductionist models can only offer partial representations of GI functions and are therefore unable to accurately predict behavior of cells or organs in living organisms limiting their effectiveness to study the gut with relevance to human health.

Ex vivo models offer an alternative approach, utilizing tissue explants that closely resemble the physiological conditions of in vivo tissues, maintaining 3D architecture, cellular diversity, and biological complexity. The microfluidic organotypic model system discussed in Chapter 1 serves as a bridge between 2D and in vivo systems enabling more accurate recapitulation of in vivo GI conditions such as leaky gut (Richardson et al., 2020; Martinez et al., 2022; Cherwin et al., 2023). By introducing bacterial collagenase into the luminal flow of the device, the epithelial and mucosal barriers of the gut were disrupted resulting in a leaky gut phenotype. The device discussed in Chapter 2 further enhances this system by incorporating transepithelial resistance (TEER) measurements, which allow for real-time monitoring of changes in barrier permeability (Way et al., 2024). The ex vivo culture systems outlined in Section 1 offer methods for investigating physiological, functional, and pathological pathways in the intestinal barrier.

Parkinson's Disease and Calcitonin Gene Related Peptide (CGRP):

While investigating mechanisms of intestinal barrier dysregulation, Parkinson's disease (PD) became of particular interest as a large proportion of PD patients have been reported to have impaired intestinal barrier integrity (Clairembault et al, 2015; Mertsalmi et al, 2017). Parkinson's disease (PD) is the second most widespread neurodegenerative disease, affecting over 1 million people in the United States and over 10 million people worldwide (Maras et al, 2018; Poewe et al, 2017). While motor symptoms are the most well-known, up to 80% of patients with

PD experience pre-motor gastrointestinal (GI) symptoms such as constipation, bloating, and nausea up to 20 years prior to motor symptom onset (de Laue and Breteler, 2006). These gastrointestinal symptoms significantly impact quality of life and can lead to severe complications such as, malnutrition, intestinal obstruction, megacolon, impaired medication effectiveness, and dehydration (Skjaerbaek et al, 2021; Warnecke et al, 2022). These complications are not trivial as they often lead to hospitalization and greatly decrease patients' quality of life. However, the underlying pathophysiology of prodromal gut symptoms in PD is largely unknown. Since these symptoms often arise years before diagnosis, it is critical to determine mechanisms of PD pathology in the gut.

Regardless of whether the origin of PD is in the brain or periphery, it is increasingly recognized as a multi-system disorder that extends beyond the central nervous system (CNS) (Adams et al, 2019; Craig et al, 2021; Bayati et al, 2024; Sun et al, 2019). Growing evidence suggests that immune activation and inflammation, both peripherally and centrally, play significant roles in contributing to neurodegeneration in PD (Harms et al, 2017). When neuropeptides are released from activated fibers this can initiate an inflammatory reaction known as neurogenic inflammation (Jansco and Szolcsanyi, 1967). Several neuropeptides and their involvement in both central and peripheral PD pathology are discussed in Chapter 3. The neuropeptide calcitonin gene related peptide (CGRP) is of particular interest in PD pathology as alterations in CGRP have been closely linked to various disease states that are strongly associated with PD, including IBD (Pascual-Mato, 2024), migraine (Juhasz et al, 2005), and increased enteric and CNS aSyn (Na et al, 2020). Additionally, treatment with CGRP antagonists have been shown to reduce neuroinflammation and aSyn aggregation in mouse brain, further supporting a role for CGRP in PD pathophysiology (Benemei et al, 2009; Na et al, 2020).

CGRP is a 37 amino acid neuropeptide that belongs to the calcitonin family of peptides and exists in two forms – α and β, which share around 90% homology (Russell et al., 2014) and

have nearly identical biological activity (Mulderry et al., 1988; Noguchi et al., 1990). αCGRP is primarily found in sensory peripheral and central nerves while, βCGRP is found primarily in motor enteric neurons (Mulderry et al., 1988). Importantly, both αCGRP and βCGRP are found in the gut and the brain and utilize the same receptors. In the gut, CGRP is involved in regulating nociception, gastric acid secretion, vasodilation, and regulating motility (Ailani et al, 2022). Constipation is the most common GI symptom associated with PD and is often one of the earliest symptoms to appear (Adams-Carr et al, 2016; Cersosimo et al, 2013). Therapeutic interventions targeting CGRP significantly inhibit colonic transit, leading to constipation (Haanes et al, 2020; Ailani et al, 2022), while elevated CGRP is associated with diarrhea suggesting that CGRP plays a role in GI motility. Using the rotenone pesticide model of PD, Chapter 4 demonstrates alterations in colonic CGRP expression associated with increased aSyn in enteric $CGRP^{+}$ neurons and mucosal projecting fibers. Along with its role in gut motility, CGRP is thought to play a large role in the neuro-immune axis by inducing shifts in immune cell recruitment, proliferation, and cytokine release (Assas et al, 2014). Patients with inflammatory bowel disease are reported to have greater risk of developing PD, indicating that gut inflammation may play a role in PD (Mertsalmi et al, 2017; Park et al, 2019). However, the role of intestinal inflammation in aSyn aggregation and neurodegeneration has yet to be fully elucidated. Enteric glia have immune functions and are of particular interest in PD, because they play key roles in supporting and maintain neuronal health. Additionally, both CGRP and aSyn can activate brain glial cells (Afroz et al, 2019; Harms et al, 2017; Grozdanov et al, 2019). Chapter 5 discusses the potential role of alterations in enteric CGRP and aSyn that may result in reactive enteric gliosis that initiates, perpetuates, or worsens PD pathology in the gut. The work presented in section 2 highlights the importance of studying the gut, specifically the neuropeptide CGRP, in neurodegenerative disorders such as PD. Targeting peripheral CGRP signaling pathways may provide a promising therapeutic strategy to reduce enteric aSyn aggregation. Given that CGRP plays a role in both inflammatory and neuroprotective processes,

modulating gut CGRP signaling could have wider implications for treating PD, especially in the early disease stages when peripheral aSyn accumulation may serve as a precursor to disease progression.

References

1 Adams, B. *et al.* Parkinson's Disease: A Systemic Inflammatory Disease Accompanied by Bacterial Inflammagens. *Front Aging Neurosci* **11**, 210 (2019). https://doi.org:10.3389/fnagi.2019.00210

2 Adams-Carr, K. L. *et al.* Constipation preceding Parkinson's disease: a systematic review and meta-analysis. *J Neurol Neurosurg Psychiatry* **87**, 710-716 (2016). https://doi.org:10.1136/jnnp-2015-311680

3 Afroz, S. *et al.* CGRP Induces Differential Regulation of Cytokines from Satellite Glial Cells in Trigeminal Ganglia and Orofacial Nociception. *Int J Mol Sci* **20** (2019). https://doi.org:10.3390/ijms20030711

4 Ailani, J. *et al.* Role of Calcitonin Gene-Related Peptide on the Gastrointestinal Symptoms of Migraine-Clinical Considerations: A Narrative Review. *Neurology* **99**, 841-853 (2022). https://doi.org:10.1212/WNL.0000000000201332

5 Akobeng, A. K., Singh, P., Kumar, M. & Al Khodor, S. Role of the gut microbiota in the pathogenesis of coeliac disease and potential therapeutic implications. *Eur J Nutr* **59**, 3369-3390 (2020). https://doi.org:10.1007/s00394-020-02324-y

6 Assas, B. M., Pennock, J. I. & Miyan, J. A. Calcitonin gene-related peptide is a key neurotransmitter in the neuro-immune axis. *Front Neurosci* **8**, 23 (2014). https://doi.org:10.3389/fnins.2014.00023

7 Bayati, A. *et al.* Modeling Parkinson's disease pathology in human dopaminergic neurons by sequential exposure to alpha-synuclein fibrils and proinflammatory cytokines. *Nat Neurosci* (2024). https://doi.org:10.1038/s41593-024-01775-4

8 Benemei, S., Nicoletti, P., Capone, J. G. & Geppetti, P. CGRP receptors in the control of pain and inflammation. *Curr Opin Pharmacol* **9**, 9-14 (2009). https://doi.org:10.1016/j.coph.2008.12.007

9 Braak, H., de Vos, R. A., Bohl, J. & Del Tredici, K. Gastric alpha-synuclein immunoreactive inclusions in Meissner's and Auerbach's plexuses in cases staged for Parkinson's disease-related brain pathology. *Neurosci Lett* **396**, 67-72 (2006). https://doi.org:10.1016/j.neulet.2005.11.012

10 Caradonna, E. *et al.* The Brain-Gut Axis, an Important Player in Alzheimer and Parkinson Disease: A Narrative Review. *J Clin Med* **13** (2024). https://doi.org:10.3390/jcm13144130

11 Cersosimo, M. G. *et al.* Gastrointestinal manifestations in Parkinson's disease: prevalence and occurrence before motor symptoms. *J Neurol* **260**, 1332-1338 (2013). https://doi.org:10.1007/s00415-012-6801-2

12 Cherwin, A. E. *et al.* Microfluidic organotypic device to test intestinal mucosal barrier permeability ex vivo. *Lab Chip* **23**, 4126-4133 (2023). https://doi.org:10.1039/d3lc00615h

13 Christovich, A. & Luo, X. M. Gut Microbiota, Leaky Gut, and Autoimmune Diseases. *Front Immunol* **13**, 946248 (2022). https://doi.org:10.3389/fimmu.2022.946248

14 Clairembault, T. *et al.* Structural alterations of the intestinal epithelial barrier in Parkinson's disease. *Acta Neuropathol Commun* **3**, 12 (2015). https://doi.org:10.1186/s40478-015-0196-0

15 Craig, D. W. *et al.* RNA sequencing of whole blood reveals early alterations in immune cells and gene expression in Parkinson's disease. *Nat Aging* **1**, 734-747 (2021). https://doi.org:10.1038/s43587-021-00088-6

16 de Lau, L. M. & Breteler, M. M. Epidemiology of Parkinson's disease. *Lancet Neurol* **5**, 525-535 (2006). https://doi.org:10.1016/S1474-4422(06)70471-9

17 Grozdanov, V. *et al.* Increased Immune Activation by Pathologic alpha-Synuclein in Parkinson's Disease. *Ann Neurol* **86**, 593-606 (2019). https://doi.org:10.1002/ana.25557

18 Harms, A. S. *et al.* alpha-Synuclein fibrils recruit peripheral immune cells in the rat brain prior to neurodegeneration. *Acta Neuropathol Commun* **5**, 85 (2017). https://doi.org:10.1186/s40478-017-0494-9

19 Hayley N Templeton, A. T. E., Luke A Schwerdtfeger, Julietta A Sheng, Ronald B Tjalkens, Stuart A Tobet. Sex specific effects of environmental toxin-derived alpha synuclein on enteric neuronal-epithelial interactions. *BioRxiv* (2024). https://doi.org:https://doi.org/10.1101/2024.11.27.625701

20 Holmqvist, S. *et al.* Direct evidence of Parkinson pathology spread from the gastrointestinal tract to the brain in rats. *Acta Neuropathol* **128**, 805-820 (2014). https://doi.org:10.1007/s00401-014-1343-6

21 Jancso, N., Jancso-Gabor, A. & Szolcsanyi, J. Direct evidence for neurogenic inflammation and its prevention by denervation and by pretreatment with capsaicin. *Br J Pharmacol Chemother* **31**, 138-151 (1967). https://doi.org:10.1111/j.1476-5381.1967.tb01984.x

22 Juhasz, G. *et al.* Sumatriptan causes parallel decrease in plasma calcitonin gene-related peptide (CGRP) concentration and migraine headache during nitroglycerin induced migraine attack. *Cephalalgia* **25**, 179-183 (2005). https://doi.org:10.1111/j.1468-2982.2005.00836.x

23 Kim, S. *et al.* Transneuronal Propagation of Pathologic alpha-Synuclein from the Gut to the Brain Models Parkinson's Disease. *Neuron* **103**, 627-641 e627 (2019). https://doi.org:10.1016/j.neuron.2019.05.035

24 Marras, C. *et al.* Prevalence of Parkinson's disease across North America. *NPJ Parkinsons Dis* **4**, 21 (2018). https://doi.org:10.1038/s41531-018-0058-0

25 Martinez, B., Schwerdtfeger, L. A., Richardson, A., Tobet, S. A. & Henry, C. S. (1)H-NMR Profiling of Short-Chain Fatty Acid Content from a Physiologically Accurate Gut-on-

a-Chip Device. *Anal Chem* **94**, 9987-9992 (2022). https://doi.org:10.1021/acs.analchem.1c05146

26 McLean, I. C., Schwerdtfeger, L. A., Tobet, S. A. & Henry, C. S. Powering ex vivo tissue models in microfluidic systems. *Lab Chip* **18**, 1399-1410 (2018). https://doi.org:10.1039/c8lc00241j

27 Mertsalmi, T. H. *et al.* More than constipation - bowel symptoms in Parkinson's disease and their connection to gut microbiota. *Eur J Neurol* **24**, 1375-1383 (2017). https://doi.org:10.1111/ene.13398

28 Michielan, A. & D'Inca, R. Intestinal Permeability in Inflammatory Bowel Disease: Pathogenesis, Clinical Evaluation, and Therapy of Leaky Gut. *Mediators Inflamm* **2015**, 628157 (2015). https://doi.org:10.1155/2015/628157

29 Mulderry, P. K. *et al.* Differential expression of alpha-CGRP and beta-CGRP by primary sensory neurons and enteric autonomic neurons of the rat. *Neuroscience* **25**, 195-205 (1988). https://doi.org:10.1016/0306-4522(88)90018-8

30 Na, H. *et al.* Characterization of the effects of calcitonin gene-related peptide receptor antagonist for Alzheimer's disease. *Neuropharmacology* **168**, 108017 (2020). https://doi.org:10.1016/j.neuropharm.2020.108017

31 Noguchi, K., Senba, E., Morita, Y., Sato, M. & Tohyama, M. Alpha-CGRP and beta-CGRP mRNAs are differentially regulated in the rat spinal cord and dorsal root ganglion. *Brain Res Mol Brain Res* **7**, 299-304 (1990). https://doi.org:10.1016/0169-328x(90)90080-w

32 Park, S. *et al.* Patients with Inflammatory Bowel Disease Are at an Increased Risk of Parkinson's Disease: A South Korean Nationwide Population-Based Study. *J Clin Med* **8** (2019). https://doi.org:10.3390/jcm8081191

33 Parkinson, J. *An Essay on the Shaking Palsy*. (Edwards & Brune Ltd., 1817).

34 Pascal, M. *et al.* The neuropeptide VIP potentiates intestinal innate type 2 and type 3 immunity in response to feeding. *Mucosal Immunol* **15**, 629-641 (2022). https://doi.org:10.1038/s41385-022-00516-9

35 Poewe, W. *et al.* Parkinson disease. *Nat Rev Dis Primers* **3**, 17013 (2017). https://doi.org:10.1038/nrdp.2017.13

36 Richardson, A. *et al.* A microfluidic organotypic device for culture of mammalian intestines ex vivo. *Anal Methods-Uk* **12**, 297-303 (2020). https://doi.org:10.1039/c9ay02038a

37 Russell, F. A., King, R., Smillie, S. J., Kodji, X. & Brain, S. D. Calcitonin gene-related peptide: physiology and pathophysiology. *Physiol Rev* **94**, 1099-1142 (2014). https://doi.org:10.1152/physrev.00034.2013

38 Schwerdtfeger, L. A., Nealon, N. J., Ryan, E. P. & Tobet, S. A. Human colon function ex vivo: Dependence on oxygen and sensitivity to antibiotic. *PLoS One* **14**, e0217170 (2019). https://doi.org:10.1371/journal.pone.0217170

39 Schwerdtfeger, L. A. & Tobet, S. A. Vasoactive intestinal peptide regulates ileal goblet cell production in mice. *Physiol Rep* **8**, e14363 (2020). https://doi.org:10.14814/phy2.14363

40 Schwerdtfeger, L. A. a. M., Federico and Lanser, Toby B. and Ekwudo, Millicent N. and Zurawski, Jonathan and Tauhid, Shahamat and Glanz, Bonnie I. and Chu, Renxin and Bakshi, Rohit and Chitnis, Tanuja and Cox, Laura M. and Weiner, Howard L. and Administrator. Gut Microbiota and Metabolites are Linked to Disease Progression in Multiple Sclerosis. *Cell Press Sneak Peak* (2024). https://doi.org:http://dx.doi.org/10.2139/ssrn.4886559

41 Schwerdtfeger, L. A. a. T., S. A. in *Prescision Medicine for Investigators, Practitioners and Providers* (ed Salomao Faintuch Joel Faintuch) 97-104 (Academic Press, 2020).

42 Skjaerbaek, C., Knudsen, K., Horsager, J. & Borghammer, P. Gastrointestinal Dysfunction in Parkinson's Disease. *J Clin Med* **10** (2021). https://doi.org:10.3390/jcm10030493

43 Sun, C. *et al.* Abnormal subpopulations of peripheral blood lymphocytes are involved in Parkinson's disease. *Ann Transl Med* **7**, 637 (2019). https://doi.org:10.21037/atm.2019.10.105

44 Warnecke, T., Schafer, K. H., Claus, I., Del Tredici, K. & Jost, W. H. Gastrointestinal involvement in Parkinson's disease: pathophysiology, diagnosis, and management. *NPJ Parkinsons Dis* **8**, 31 (2022). https://doi.org:10.1038/s41531-022-00295-x

45 Way, R. *et al.* A microphysiological system for studying barrier health of live tissues in real time. *Commun Eng* **3**, 142 (2024). https://doi.org:10.1038/s44172-024-00285-2

CHAPTER 1 –MICROFLUIDIC ORGANOTYPIC DEVICE TO TEST INTESTINAL MUCOSAL BARRIER PERMEABILITY EX VIVO[1]

Overview:

To protect the body from external pathogens, the intestines have sophisticated epithelial and mucosal barriers. Disruptions to barrier integrity are associated with a variety of disorders such as irritable bowel disease, Crohn's Disease, and celiac disease. One critical component of all barriers are collagens in the extracellular matrix. While the importance of the intestinal barrier is established, current models lack the ability to represent the complex biology that occurs at these barriers. For the current study a microfluidic device model was modified to determine the effectiveness of collagen breakdown to cause barrier disruption. Bacterial collagenase was added for 48 h to the luminal channel of a dual flow microfluidic device to examine changes in intestinal barrier integrity. Tissues exhibited dose-dependent alterations in immunoreactive collagen-1 and claudin-1, and coincident disruption of the epithelial monolayer barrier as indicated by goblet cell morphologies. This ex vivo model system offers promise for further studies exploring factors that affect gut barrier integrity and potential downstream consequences that cannot be studied in current models.

Introduction:

The importance of the intestinal barrier has become more obvious with recent observations of its involvement in disease progression and human health.[1-5] To ensure survival, the gut must maintain a barrier that retains the ability to digest and absorb nutrients while protecting the body from harmful substances.[2, 3] The diverse functions of the intestinal barrier are mediated by complex biochemistry and anatomy including epithelial, immune, neural, and bacterial interactions.[6, 7] Epithelial cells of the gut physically separate luminal contents from the underlying lamina propria through apical transmembrane mucins and tight junctions. Together

[1] Cherwin AE, Templeton HN, Ehrlich AT, Patlin BH, Henry SC, Tobet SA. Microfluidic organotypic device to test intestinal mucosal barrier permeability ex vivo. *Lab on a Chip*. 2023.

with the epithelial barrier, a mucosal barrier prevents unregulated passage of luminal contents into underlying tissue.[8] Disruptions to the epithelial and mucosal layers can lead to alterations in paracellular and transcellular permeability in what is termed as "leaky gut."[2] Leaky gut has been associated with the pathogenesis of conditions such as inflammatory bowel diseases (IBD),[9-11] autoimmune diseases such as celiac disease,[2] neurodegenerative disorders such as Alzheimer's and Parkinson's Disease,[12, 13] and neurodevelopmental disorders such as autism spectrum disorder.[14] Generation of an intestinal model that maintains the complexity of intestinal anatomy, microenvironment, and barrier is necessary to better understand how alterations in barrier integrity may contribute to disease states.

There are currently many approaches to study organ function that each have strengths and weaknesses. In vivo studies have the benefit of maintaining communication across organ systems. The gut is difficult to access in vivo, and probes inserted to monitor changes could disrupt the natural environment. Using an alternative approach such as an ex vivo system can have significant benefits. Ex vivo models using tissue explants represent reasonable physiological similarity to tissue in vivo in terms of 3D structure and biological complexity.[15] They offer a powerful tool for studying cell-cell interactions, cellular responses, and extracellular matrix (ECM) remodeling processes.[16, 17] However, tissue explant models are limited by shortened lifespan of the tissues and challenges in recreating the microenvironment.[16] Simplified approaches to modeling these organs have been done by using in vitro models with 2D[18-20] monolayer or 3D[21, 22] cell culture systems (e.g., using cell lines or primary progenitor cells) to mimic the gastrointestinal (GI) tract. The incorporation of microfluidics with 2D culture systems greatly increased these in vitro systems functionality by allowing for the inclusion of physical forces such as fluid shear stress, cyclic strain, and mechanical compression.[23] These "organ-on-a-chip" models offer utility in high throughput screening approaches for

[1] Cherwin AE, Templeton HN, Ehrlich AT, Patlin BH, Henry SC, Tobet SA. Microfluidic organotypic device to test intestinal mucosal barrier permeability ex vivo. *Lab on a Chip*. 2023.

pharmaceutical, industrial, and toxicological research.[16] However, they fail to model the GI tract as they don't capture the complexity of either the microbiome or the cellular composition of the intestinal wall. Since these models do not have all the components which comprise the barrier, they can only provide partial modeling for conditions such as leaky gut.

To create a paradigm for intestinal microphysiological systems, several approaches[24-26] have incorporated microfluidics, but these models are still missing valuable components for gut health. Models such as the GOFlowChip[25] recapitulate some of the cellular diversity by using host cells that are derived from stem cells combined with inter- and extraluminal flow to carry nutrients and remove waste. However, there is no native microbial population so microbes must be injected into the organoid to have functionality and to study host-microbe interactions.[15] Even when systems include added bacteria, many of these systems do not consider the oxygen gradient that exists within the GI tract. Our previous work showed that low oxygen is required for better preservation of microbiota ex vivo.[27] These systems lacking a microbiome or lacking an appropriate environment for a microbiome are missing a vital component of the cellular ecosystem of the host relevant for studying diseases like leaky gut. Alternatively, organotypic devices which utilized whole tissue explants have a variety of advantages including maintenance of local microbiome and cell diversity.[15, 26, 28] For example, the Intestinal Explant Barrier Chip[26] measured the functionality of porcine and human gut explants in terms of its ability to perform transcellular and paracellular transport of drug compounds over 24 h. Although, questions remain about the integrity of the tissue given that hemotoxylin and eosin staining indicated significant tissue disruption and specific cellular elements were not examined. While these approaches provide valuable information to the study of intestinal physiological processes, they fail to recapitulate important aspects of the complex environment of the intestines.

[1] Cherwin AE, Templeton HN, Ehrlich AT, Patlin BH, Henry SC, Tobet SA. Microfluidic organotypic device to test intestinal mucosal barrier permeability ex vivo. *Lab on a Chip*. 2023.

The model system in the current study serves as a bridge between 2D and in vivo systems currently in use and provides a layer of complexity that aids in investigating the gut barrier—which is necessary to understand conditions such as leaky gut. This study expands the utilization of an ex vivo dual flow microfluidic device to create a model of leaky gut using bacterial collagenase. Bacterial collagenases are enzymes produced by endogenous gut bacteria that have the natural ability to digest collagen, thus contributing to the degradation of the extracellular matrices (ECM).[29] Here, we introduced bacterial collagenase into the luminal flow of the device to disrupt the epithelial and mucosal barriers of the gut, resulting in a leaky gut-like phenotype. We observed changes to gut permeability, collagen type 1 within the ECM, and epithelial cell (goblet cell) morphologies as a result of collagenase exposure. Using an enzyme that can be secreted by commensal bacteria provides a model for future studies of leaky gut. The purpose of this study was to create a model of leaky gut that recreates physiological hallmarks of the disorder enabling future investigation into causative mechanisms.

Materials and Methods:

Device design

The device (Figure 1) was designed in SolidWorks (Dassault Systémes, Vélizy-Villacoublay, France) and manufactured via injection molding (Applied Medical, Rancho Santa Margarita, CA) and consisted of three cyclic olefin copolymer (COC; TOPAS Grade 8007) layers separated by polyurethane gaskets (PORON AquaPro, Rogers Corporation, Chandler, AZ). Details on device design, as well as a video demonstrating device assembly can be found in our previous publication.[27] Briefly, each gasket made individual fluidic channels and tissue was placed in the middle layer where luminal and serosal sides have separate channels. The tissue was placed in the device such that the luminal side of the tissue was facing up when it was

[1] Cherwin AE, Templeton HN, Ehrlich AT, Patlin BH, Henry SC, Tobet SA. Microfluidic organotypic device to test intestinal mucosal barrier permeability ex vivo. *Lab on a Chip*. 2023.

placed inside. A significant modification to the previous design was the use of 50µm pore Nitex mesh (Genesee Scientific, San Diego, CA) that was secured at the bottom of the middle layer with quick-setting epoxy (J-B Weld, Marietta, Georgia, USA) to support the tissue. The luminal side of the tissue had an additional piece of mesh glued onto it so that the full perimeter of the tissue was securely held in place. This mesh had a 2mm diameter hole in the center to allow the media to reach the tissue that wasn't in contact with any glue (Figure 1A). This modification was made to eliminate the use of nicardipine, a calcium channel blocker. Nicardipine was previously used in the media to keep the tissue flat in the device by decreasing intestinal muscle contractions.[27] The use of mesh and epoxy ensured the tissue remained flat in the device even

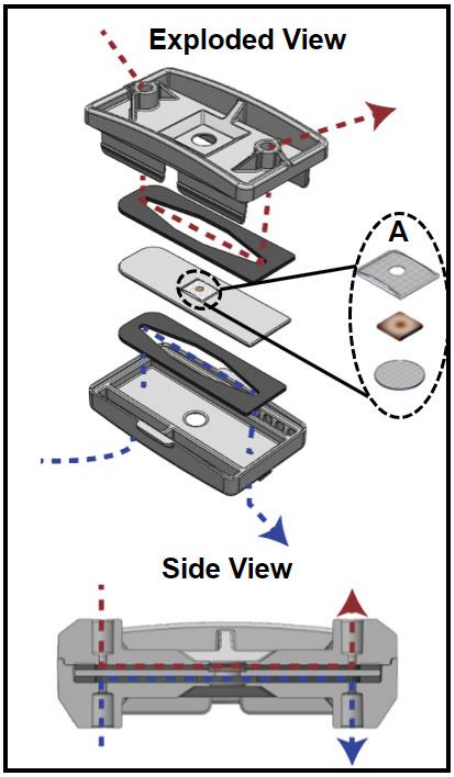

Figure 1. The organotypic microfluidic device. Exploded view of the device with the tissue piece between two gaskets that define flow paths for luminal (above, red) and serosal (below, blue) media flows, respectively. A shows the components held within the middle piece of the device; two mesh pieces provide support above and below the tissue. Below shows a side view of the assembled device, with the flow paths for luminal (above, red) and serosal (below, blue) media flows.

[1] Cherwin AE, Templeton HN, Ehrlich AT, Patlin BH, Henry SC, Tobet SA. Microfluidic organotypic device to test intestinal mucosal barrier permeability ex vivo. *Lab on a Chip*. 2023.

when contractions were occurring. The top mesh piece and the tissue were secured around the edge using cyanoacrylate glue (Loctite Super Glue, Henkel Corporation, Bridgewater, NJ) to help prevent leakage. The top piece of the device had integrated snap-fit fasteners that allowed for quick assembly to decrease the time tissue was without media.

Animals, tissue collection, and device loading

Male C57BL/6 background mice aged 3-4 months were used in all experiments. Animal protocols were approved by the Institutional Animal Care and Use Committee (IACUC) at Colorado State University. Mice were kept on a 12-h light/dark cycle with access to standard chow and water *ad libitum*.

To prepare for tissue collection, mice were deeply anesthetized with isoflurane and terminated via decapitation. The intestines were removed from stomach to colon and immediately placed in 4°C 1x Krebs buffer (in mM: 2.5 KCl, 2.5 $CaCl_2$, 126 NaCl, 1.2 $MgCl_2$, 1.2 NaH_2PO_4) containing 1µl/1mL nicardipine (Sigma Aldrich, St. Louis, MO), an L-type calcium ion channel blocker, to prevent contractions during dissection. Proximal colon was then dissected to remove any remaining mesentery. Using angled vascular scissors, the tissue was cut longitudinally to form a flat piece of tissue which was then cut into ~5mm sections (Figure 1A). Using a small strainer spoon, tissue sections were gently scooped up and transferred to the device. This method allowed the tissue section to remain flat and promoted a smooth transfer to the device. Only a small corner of the tissue needed to be touched with forceps to move the tissue to the device's middle piece. This significantly decreased tissue stretch, which was previously associated with tissue damage.[30] Once the tissue was placed inside the device, the top layer of Nitex mesh was gently placed on top and cyanoacrylate glue was placed around the edges of the mesh. Careful attention was paid to not allow glue to contact the tissue beyond the perimeter. To cure the glue, 1x Krebs buffer was applied. The device was immediately snapped

[1] Cherwin AE, Templeton HN, Ehrlich AT, Patlin BH, Henry SC, Tobet SA. Microfluidic organotypic device to test intestinal mucosal barrier permeability ex vivo. *Lab on a Chip*. 2023.

closed and transferred to a 37°C incubator where the media inlets were connected. The syringe pumps were run at a purge setting for ~10s to fill the device so the tissue was in contact with media in less than 60s after it was removed from the Krebs solution.

Media preparation and experiments

Adult Neurobasal CTS culture media with 2% B27 supplement (Thermo Fisher Scientific, Waltham, WA) and 3% 1 M HEPES buffer (Sigma Aldrich, St. Louis, MO) was used. Experiments to investigate tight junctions and the mucus layer were done with the same media except for lower glucose (4mM versus 25mM) and the omission of phenol red in the culture media. Luminal media contained 0.5 M sodium sulfite (oxygen scavenger) to decrease oxygen levels.[27] The addition of Nitex mesh and cyanoacrylate glue securely held the tissue in place eliminating the need for nicardipine to prevent muscle contractions and maintain tissue viability. Media was loaded in sterile 10 mL syringes and placed in a 37°C incubator to equilibrate and remove air bubbles before experiments. Experiments to analyze barrier permeability after collagenase exposure included luminal media with 0.1% 10kDa dextran fluorescein (Thermo Fisher Scientific, Waltham, WA) for only the last 2 h of the experiment.

Each device had two 10 mL syringes filled with media connected to NE-300 pumps (New era Pump Systems Inc., Farmingdale, NY) that continually flowed media across both luminal and serosal sides of the tissue. For the first 24 h of the experiment, control media was used to allow the tissue to stabilize and to establish a baseline of device performance with an intact, healthy barrier. The flow rate on the luminal side was 250 µL/h, and on the serosal side it was 200 µL/h. The flow rates were optimized using computational fluid dynamics simulations to identify appropriate levels of shear stresses to the tissue surface. After 24 h, the media for the luminal side of the tissue was replaced with collagenase-containing media—control (0 U), low ($5.80*10^{-2}$ U), or high ($1.16*10^{-1}$ U) collagenase (Worthington Biochemical Corporation,

[1] Cherwin AE, Templeton HN, Ehrlich AT, Patlin BH, Henry SC, Tobet SA. Microfluidic organotypic device to test intestinal mucosal barrier permeability ex vivo. *Lab on a Chip*. 2023.

Lakewood, NJ) concentrations. These concentrations were chosen after performing a dosage curve to determine levels of collagenase that showed measurable disruption of the tissue over 48 h without complete destruction. Working stocks of bacterial collagenase were diluted in water and because media is composed mainly of water, control media did not utilize the addition of water as a vehicle.

Following collagenase addition, the device ran for an additional 48 h. After 72 h, the tissue was removed from the device and placed in a small weigh boat. A solution containing 0.5% cetyl pyridium chloride (CPC) in 4% paraformaldehyde (PFA) was then gently pipetted onto the luminal surface of the tissue. After approximately 5 min the tissue was removed from the weigh boat and stored in 0.5% CPC in 4% PFA at 4°C for 24 h. Tissue was then stored in 0.05 M phosphate buffered saline (PBS) at 4°C for sectioning.

Tissue sectioning and histochemistry

Tissue sections were prepared from 1-3 mm sections of colon and submerged in 4% agarose. The tissue was in agarose for a total of 9 min: 5 min on a room temperature shaker, and 4 min at 4°C to ensure polymerization. Once the agarose was hardened, tissue was cut at a thickness of 50 µm on a vibrating microtome (VT1000S; Leica microsystems, Wetzlar, Germany).

For lectin histochemistry and immunohistochemistry, sections were washed in 1x PBS for 10 minutes at 4°C and were then incubated in 0.1M glycine for 30 min at 4°C, followed by three, 5-min PBS washes. Next, tissue was incubated in 0.5% sodium borohydride at 4°C for 15 min, followed by three, 5 min PBS washes. Sections were blocked in PBS with 5% normal goat serum (NGS; Lampire Biological, Pipersville, PA), 1% hydrogen peroxide, and 0.3% Triton X (TX) for 1 h at 4°C with a change of solution at 30 min. Following blocking, sections were placed into primary antisera with PBS containing 5% NGS and 0.3% TX for 3 days. Primary antibodies

[1] Cherwin AE, Templeton HN, Ehrlich AT, Patlin BH, Henry SC, Tobet SA. Microfluidic organotypic device to test intestinal mucosal barrier permeability ex vivo. *Lab on a Chip*. 2023.

used were anti-c-kit (ACK2; Novus Biologicals) at 1:250, Ulex Europaeus Agglutinin I conjugated to Rhodamine (UEA-1; Vector Labs) at a concentration of 0.125µg/mL, anti-claudin-1 (Invitrogen) 1:200, anti-peripherin (Sigma-Aldrich) 1:300, anti-Collagen I (Novus Biologicals) 1:500 and anti-MUC-2 (Novus Biologicals) at 3 µg/mL. Following primary antibody addition, sections were washed at room temperature in PBS with 1% NGS and 0.32% TX four times at 15-min intervals. Sections with anti-peripherin and anti-claudin-1 primary antibodies were incubated for 2 h at room temperature in PBS containing 0.02% TX and Alexa fluor 594 conjugated to secondary antibodies specific to the species of the primary antibodies at a 1:500 dilution. Sections originally incubated with anti-MUC2, anti-collagen I, anti-ACK2 primary antibodies were incubated for 2 h in biotinylated secondary antiserum (anti-rabbit 1:2500 or anti-rat, 1:1000; Jackson ImmunoResearch, West Grove, PA) specific to the species of the primary antibodies and were constituted in PBS with 0.32% TX. Sections were washed four times at 15-min intervals in PBS with 0.02% TX before being placed in their tertiary conjugated antibody (AF 594) constituted in PBS with 0.32% TX for 1 h at room temperature. Sections were then washed in PBS, mounted on slides, and cover slipped with an aqueous mounting medium (Aqua-Poly/Mount, Polysciences, Warrington, PA). More information about primary antibodies can be found in Table S.1.

Tissue imaging and analysis

Images were taken using a Zeiss LSM800 upright confocal laser scanning microscope and a 20x (W Plan-Apochromat 20X/1.0 DIC Vis-ir ∞ /0.17) objective or Olympus BX61 equipped for epifluorescence imaging. All image analyses were performed using Fiji (v1.0; NIH). To quantify the relative fluorescence intensity of 10kDa dextran fluorescein penetration into the tissue, 12 lines were drawn from the luminal surface to the bottom of the crypts and a plot profile of the fluorescence intensity (gray value) across each line was generated; the data from all 12

[1] Cherwin AE, Templeton HN, Ehrlich AT, Patlin BH, Henry SC, Tobet SA. Microfluidic organotypic device to test intestinal mucosal barrier permeability ex vivo. *Lab on a Chip*. 2023.

lines was averaged to produce a representative measure of dextran fluorescein penetration (Figure 3D). Plots of the relative fluorescence of each tissue were compared to relate the permeability to the respective treatment regime, where a higher gray value correlated to more dextran fluorescein within the tissue (Figure 3D). To compare treatment groups to control, a one-way ANOVA was performed.

To analyze mucin 2 immunoreactivity (MUC2-IR), max intensity Z-projections were performed through the center 30 µm of each image stack. Regions of interest (ROI) were defined as 60 x 75µm sections of the apical half a crypt. Three crypts were analyzed per sample. Mean grey value of MUC2-IR was analyzed after performing a Gaussian blur and watershed to eliminate false signal and clearly define cells.

Results and Discussion:

Tissue Health and Barrier Integrity in the Device

We first sought to verify that the modifications to the original device and experimental setup did not compromise tissue health. Following previous protocol,[27] colon explants were kept in the device for 72 h ex vivo without antibiotics and with low dissolved oxygen in the mucosal media and ambient oxygen in the serosal media, producing a gradient across the tissue. A key update to device design in the current study was eliminating the use of nicardipine in the media. Nicardipine is an L-type calcium channel blocker that is commonly used in ex vivo preparations to prevent muscle contractions. Calcium channels play vital roles in several cellular physiological functions by allowing controlled transport of calcium across the plasma membrane.[31] By eliminating the need for nicardipine in our device media, we have eliminated a possible variable of physiological disruption and ensured a more accurate physiological environment.

[1] Cherwin AE, Templeton HN, Ehrlich AT, Patlin BH, Henry SC, Tobet SA. Microfluidic organotypic device to test intestinal mucosal barrier permeability ex vivo. *Lab on a Chip*. 2023.

Colon explants maintained patterned crypts and proper arrangement of submucosal and muscular layers (Figure 2A). A specific type of epithelial cell, known as goblet cells, are responsible for producing and secreting mucus in the colon. Goblet cell mucopolysaccharides were identified via Ulex Europaeus Agglutinin I (UEA-1) conjugated to Rhodamine. Peripherin is a type III intermediate filament protein largely expressed on peripheral neurons and was therefore used to label enteric neurons. Mast cells are important cells of the innate immune system and were labeled using an antibody known as ACK2 that recognizes c-kit receptors found on the surface of mast cells. Immunohistochemistry (IHC) showed maintenance of neural (peripherin), epithelial (UEA-1), and immune (ACK2) cell populations in control tissue after 72 h in the device (Figure 2C-E). The mucosal barrier of the colon is composed of two layers-an inner layer firmly attached to epithelial cells and a loose outer layer. To ensure that constant flow over the tissue did not remove the mucous layer, tissue was fixed in 0.5% CPC in 4% PFA to preserve the inner mucus layer by maintaining the glycosaminoglycans in the extracellular space.[32] UEA-1 labeling of mucopolysaccharides confirmed maintenance of the inner mucosal layer after 72 h in the device (Figure 2D). We previously confirmed that luminal and serosal flows remained independent over 72 h by including fluorescein in only luminal media; only luminal effluents were found to have a measurable amount of fluorescence, confirming that the barrier was still intact.[27] Figure 2B shows relative fluorescence of the luminal and serosal effluents, respectively, for the last 2 h of the experiment where the luminal media contained 10 kDa MW dextran fluorescein. The relative fluorescence units (RFUs) were determined using a plate reader (PerkinElmer, USA), where the RFU value of a blank sample (serosal media that was not used in a device) was subtracted. The data plotted is an average from three replicates.

[1] Cherwin AE, Templeton HN, Ehrlich AT, Patlin BH, Henry SC, Tobet SA. Microfluidic organotypic device to test intestinal mucosal barrier permeability ex vivo. *Lab on a Chip*. 2023.

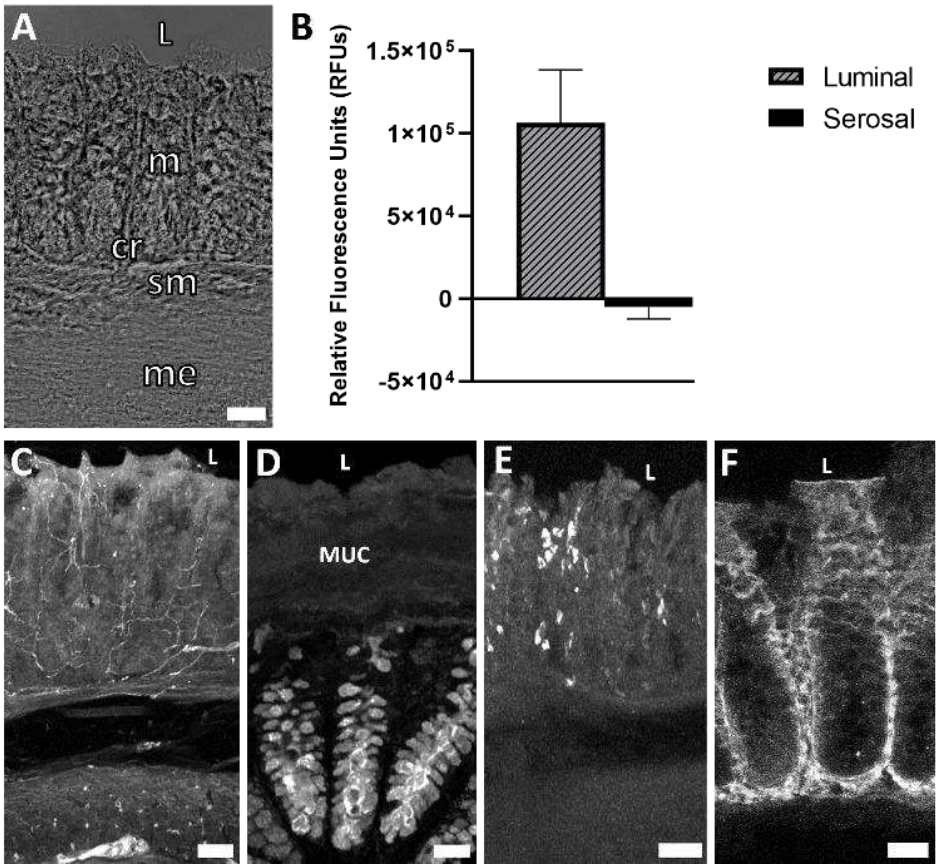

Figure 2. Device maintained tissue health and barrier function without nicardipine over 72 h. A) Brightfield image showing maintenance of colon morphology. **B)** Relative fluorescence of 10kDa dextran fluorescein in the luminal and serosal effluents from the device from the last 2 h of the experiment. **C)** Peripherin labeled nerve fibers in crypts, mucosal plexus, and myenteric plexus. **D)** Maintenance of epithelial cells and inner mucosal layer indicated by UEA-1^{+} material. **E)** Maintenance of immune cells indicated by ACK2^{+} mast cells in lamina propria. **F)** Maintenance of tight junctions indicated by claudin-1 immunoreactivity. L=lumen, MUC=mucus layer, m=mucosa, sm=submucosa, me=muscularis externa, cr=crypt, scale bars are 50µm for A, C, & E, scale bar is 25µm for D & F.

Only measurable fluorescence was detected in the luminal channel, confirming that the barrier was still intact after 72 h in the device.

Effect of Collagenase on Barrier Permeability

We next sought to determine if tissue treated with collagenase could serve as a model for leaky gut and determine its impact on barrier permeability. A key physiological hallmark of leaky gut is increased epithelial permeability indicated by increased passage of luminal

[1] Cherwin AE, Templeton HN, Ehrlich AT, Patlin BH, Henry SC, Tobet SA. Microfluidic organotypic device to test intestinal mucosal barrier permeability ex vivo. *Lab on a Chip*. 2023.

molecules across epithelial cells into underlying lamina propria.[33] To investigate this, 10 kDa molecular weight dextran fluorescein was included in the luminal media for the last 2 h of the experiment. Dextran fluorescein does not covalently attach to anything within the tissue but can freely diffuse. Analysis of epithelial and mucosal tissues revealed some diffusion of dextran fluorescein into the epithelial layer of all tissue explants, with collagenase-treated tissue showing greater fluorescence intensity into the underlying mucosa (Figure 3B-C). The relative fluorescence of each tissue was measured using Fiji (v1.0; NIH), where a higher gray value correlated to more diffusion of dextran fluorescein into the tissue; the average gray value from each treatment group (n=3) is shown in Figure 3D, where the fluorescence values from the first 140 μm starting from the luminal edge of the tissue toward the crypt base were averaged and shown as a single bar per treatment group. Not all tissue sections were equal in crypt length, so 140 μm was chosen as a depth that would give a meaningful amount of dextran fluorescein penetration into the crypts for all tissue sections. The high collagenase treatment group showed the highest gray levels, and the control group had the lowest. From these results, we concluded that collagenase increased permeability of the gut barrier.

[1] Cherwin AE, Templeton HN, Ehrlich AT, Patlin BH, Henry SC, Tobet SA. Microfluidic organotypic device to test intestinal mucosal barrier permeability ex vivo. *Lab on a Chip*. 2023.

Another physiological indication of increased epithelial permeability is alterations in tight junction proteins. Tight junctions function to prevent passage of molecules and ions between epithelial cells. Claudins are a specific type of tight junction protein that can be classified as

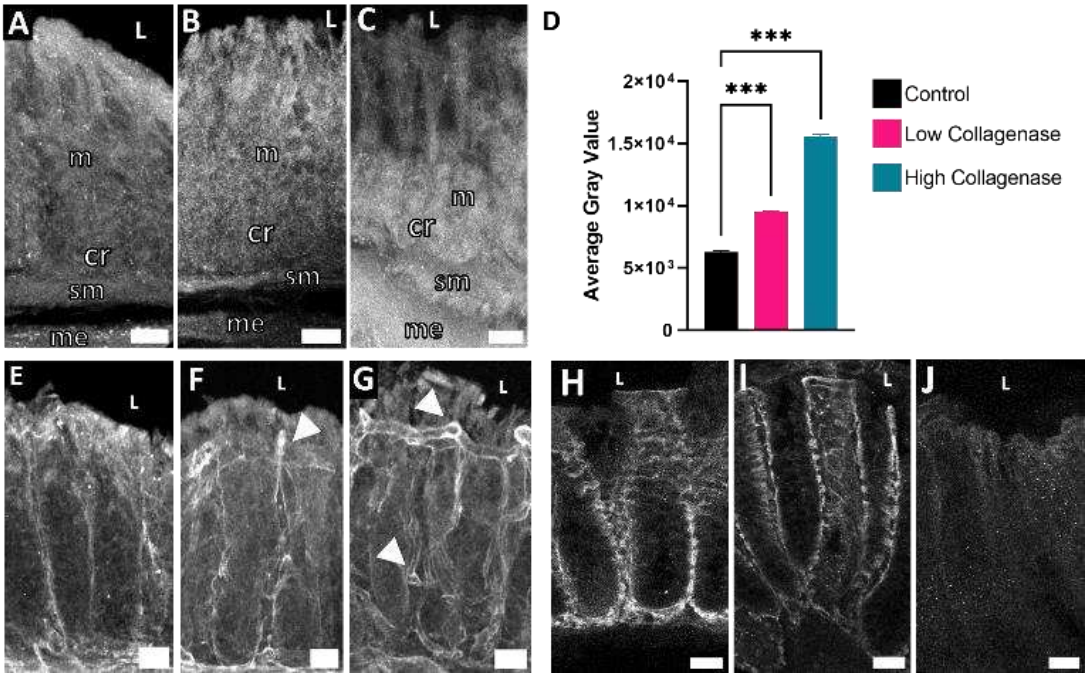

Figure 3. Collagenase exposure altered dextran fluorescein penetration and type 1 collagen morphology indicative of increased barrier permeability. A) Tissue exposed to media containing no collagenase had minimal dextran fluorescein penetration into the mucosa. **B)** Tissue exposed to low levels of collagenase had increased dextran fluorescein penetration into the mucosa. **C)** Tissue exposed to high levels of collagenase had increased dextran fluorescein into the mucosa and into the submucosa. **D)** Average fluorescence intensity of 10 kDa dextran fluorescein penetration into the first 140 µm of the tissue moving from luminal edge towards serosa across treatment groups. **E)** Type 1 collagen immunoreactivity (COL1-IR) showed distinct vertical crimping pattern with no tortuosity in media with no collagenase. **F)** Exposure to low levels of collagenase exhibited some COL1-IR tortuosity. **G)** Exposure to high levels of collagenase increased COL1-IR tortuosity and decreased vertical crimping. Arrows indicate tortuous COL1**. H)** Tissue not exposed to collagenase exhibits clear claudin-1 immunoreactivity around epithelial cells indicating maintenance of tight junctions. **I)** Exposure to low levels of collagenase moderately decreased claudin-1 immunoreactivity. **J)** Exposure to high levels of collagenase dramatically decreased claudin-1 immunoreactivity. L= lumen, m=mucosa, sm=submucosa, cr=crypt, me=muscularis externa, scale bars are 50µm.

sealing/tight or pore-forming. In leaky gut, the expression of sealing claudins have been shown to decrease.[34] We examined claudin-1, which is broadly expressed in the intestinal epithelium

[1] Cherwin AE, Templeton HN, Ehrlich AT, Patlin BH, Henry SC, Tobet SA. Microfluidic organotypic device to test intestinal mucosal barrier permeability ex vivo. *Lab on a Chip*. 2023.

and thought to have an essential role in tight junction integrity.[35, 36] Explants that were exposed to collagenase had decreased claudin-1 immunoreactivity compared to control (Figure 3H-J) indicative of impaired barrier integrity.

To further explore effects of collagenase on barrier integrity, type 1 collagen (COL1), one of the most abundant types of collagen in the extracellular matrix (ECM) was assessed by immunohistochemistry. Collagenase enzymes play a large role in ECM remodeling. Increased collagenase enzyme activity and uncontrolled remodeling of the ECM is distinctive in fibrotic and inflammatory bowel diseases.[37, 38] In healthy intestinal mucosa, collagen exhibits a wavy pattern referred to as "crimping" with fibers oriented in the vertical direction.[39] Increases in collagen tortuosity (twistedness) in vascular collagen is associated with increased remodeling and increased fragility of the ECM.[40, 41] Explants that were exposed to collagenase (Figure 3F-G) had decreased crimping and increased COL1 tortuosity, suggesting that collagenase treatment maladaptively impacted COL1 in colon mucosa. Proper functioning of the ECM is essential to intestinal barrier integrity and our results demonstrate that collagenase disrupts COL1 which may have serious consequences to barrier integrity.

Effect of Collagenase on the Epithelial Cell Lining

Our next objective was to investigate the impact of collagenase on epithelial cells that form the intestinal barrier. Due to their distinctive characteristics and important roles in barrier maintenance we chose to investigate specialized epithelial cells known as goblet cells. Goblet cells produce and secrete mucus and were identified by labeling their mucopolysaccharides using fluorescently labeled Ulex europaeus agglutinin 1 (UEA-1) that recognizes terminal α-linked fucose residues. Goblet cells were further characterized by mucin 2 (MUC2), the most abundant mucin core protein for glycosylation in the colon that is produced and secreted by goblet cells. Collagenase-treated explants showed striking differences in goblet cell morphology,

[1] Cherwin AE, Templeton HN, Ehrlich AT, Patlin BH, Henry SC, Tobet SA. Microfluidic organotypic device to test intestinal mucosal barrier permeability ex vivo. *Lab on a Chip*. 2023.

mucus layer thickness, and MUC2 immunoreactivity as a function of collagenase exposure (Figure 4). Healthy goblet cells have a characteristic goblet-like shape with the apical portion of the cell shaped like a cup and the basal portion shaped like a stem. The apical portion is distended as it contains mucin granules that are released into the lumen. Compared to control

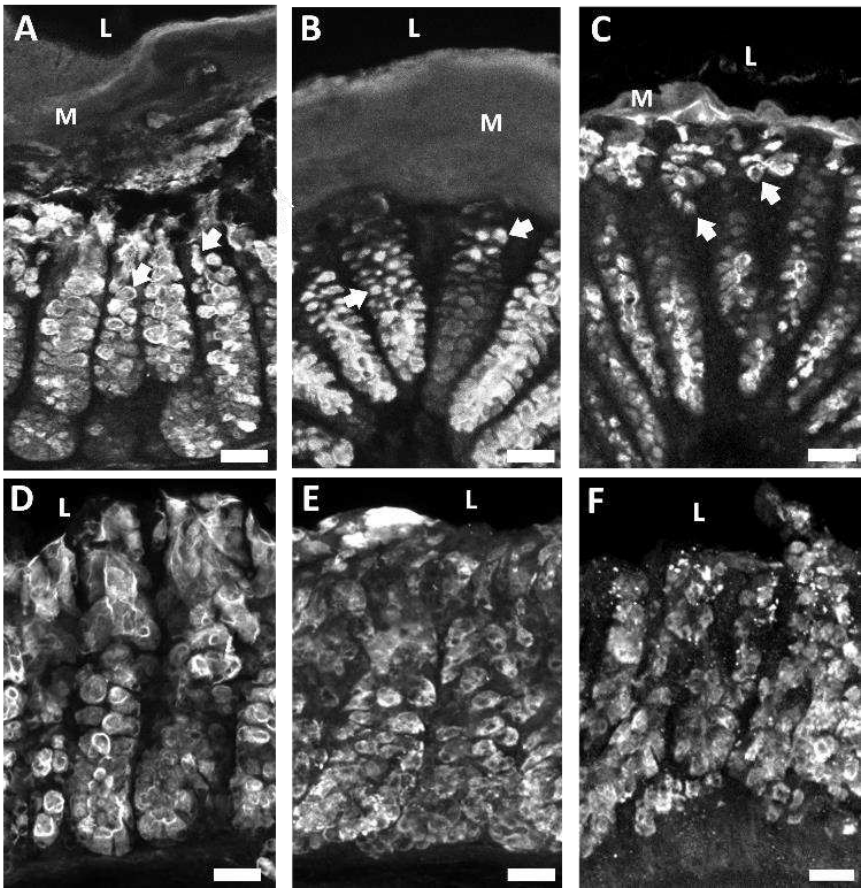

Figure 4. Collagenase treatment altered goblet cell morphology and mucus layer thickness as indicated by UEA-1 mucopolysaccharide labeling and decreased mucin 2 immunoreactivity (MUC2-IR). A) Tissue exposed to media containing no collagenase exhibited healthy goblet cell morphology with "goblet" shaped goblet cells indicated by white arrows. The mucus layer remained intact. **B)** Goblet cell shape became more circular when exposed to low levels of collagenase and the mucus layer remained intact. **C)** Goblet cells lost their distinct shape when exposed to high levels of collagenase and the mucus layer decreased in thickness. **D)** Apical MUC2-IR in tissue not exposed to collagenase. **E)** Apical MUC2-IR decreased in a dose dependent manner when exposed to low collagenase and **F)** high collagenase. Arrows indicate alterations in goblet cells morphology, M=mucus layer, L= lumen, scale bars are 25µm.

[1] Cherwin AE, Templeton HN, Ehrlich AT, Patlin BH, Henry SC, Tobet SA. Microfluidic organotypic device to test intestinal mucosal barrier permeability ex vivo. *Lab on a Chip*. 2023.

(Figure 4A), collagenase treated goblet cells lost their characteristic “goblet” shape becoming more circular (Figure 4B) or devoid of distinct shape (Figure 4C). Compared to control (Figure 4A), high collagenase treated tissue had a much thinner mucous layer (Figure 4C) indicative of an impaired mucosal barrier. Compared to control (Figure 4D), apical MUC2-IR decreased by 25% with low collagenase treatment (Figure 4E) and decreased by 31% with high collagenase treatment (Figure 4F). Alterations to goblet cell shape and MUC2 content is correlated with intestinal barrier disruption.[42] These results suggest that collagenase negatively impacted barrier epithelial cells and mucus production confirming that collagenase is a promising model for leaky gut.

Conclusions and Outlook:

The organotypic microfluidic device in the current study preserved intestinal health and morphology indicated by labeling of neurons, epithelial cells, and immune cells comparable to in vivo tissue. Importantly, the device maintained tissue health and barrier function over 72 h without inhibiting muscle contractions with nicardipine. This model provides novel opportunities to examine the intestinal barrier ex vivo to better understand disease states associated with leaky gut. The penetration of fluorescent molecules into the mucosa of collagenase-treated tissue suggests that collagenase increased epithelial barrier permeability. This is supported by the decrease in claudin-1 (tight junction) immunoreactivity suggestive of increased paracellular permeability and alterations to type 1 collagen (COL-1) structure, where collagenase-treated tissue showed increased COL-1 tortuosity and decreased vertical crimping indicative of extracellular matrix fragility. We also observed marked differences in goblet cells, where exposure to collagenase appears to disrupt the morphology and decrease apical mucin 2 immunoreactivity. Changes in shape and content of goblet cells likely affect the thickness of the mucus layer, further compromising the integrity of the intestinal barrier.

[1] Cherwin AE, Templeton HN, Ehrlich AT, Patlin BH, Henry SC, Tobet SA. Microfluidic organotypic device to test intestinal mucosal barrier permeability ex vivo. *Lab on a Chip*. 2023.

While bacterial collagenase altered epithelial and mucosal barrier structure, it is important to understand how these changes in barrier function may lead to disease states. The results outlined here demonstrate that this system works to recreate the effects of a leaky gut, in terms of physiologic hallmarks such as increased epithelial permeability. While the data doesn't identify the mechanistic causes of leaky gut, it has laid a foundation for future work to expand upon to address the problem from a more causative perspective. Results from our previous study[27] confirmed the presence of Gram-positive and Gram-negative bacteria in ex vivo murine colon explants after 72 h in the device and demonstrated that an oxygen gradient is necessary for preservation of a physiologically relevant bacterial community. Future experiments will be able to investigate the effects of specific microbiome components (e.g., bacteria) that secrete collagenases, such as *Enterococcus faecalis*,[43] within the tissue to gain a more comprehensive understanding of the mechanisms involved in leaky gut. In the longer run, investigations of the impact of leaky gut on colon tissue ex vivo will allow for detailed studies of neuronal and immune cell populations that could lead to a better understanding of the steps leading to problematic pathology.

Ultimately, we hope to make this device translational to humans to further understanding of intestinal disease processes. Pig intestine is similar to human intestinal tissue in size and structure, so a series of preliminary experiments were performed with pig intestine. Compared to mouse intestine, pig intestine is much thicker resulting in substantially stronger muscle contractions. Unfortunately, these contractions pulled the tissue out of the device. When we removed the muscle layer, we were able to keep pig intestine flat and alive for 72 h. However, this is not ideal as many enteric neurons and some immune cells reside in the muscle layers. Long-term goals include improving the mechanisms for clamping stronger, thicker tissue within the device so that similar studies can be performed with completely intact porcine and human

[1] Cherwin AE, Templeton HN, Ehrlich AT, Patlin BH, Henry SC, Tobet SA. Microfluidic organotypic device to test intestinal mucosal barrier permeability ex vivo. *Lab on a Chip*. 2023.

tissue explants. We have previously obtained human tissue explants to study,[44] so future iterations of the device could very realistically include human tissue for more translatable studies. Results from future studies will be essential to enhance understanding of human gut health.

*Amanda E. Cherwin & Hayley N. Templeton contributed equally to this work

[1] Cherwin AE, Templeton HN, Ehrlich AT, Patlin BH, Henry SC, Tobet SA. Microfluidic organotypic device to test intestinal mucosal barrier permeability ex vivo. *Lab on a Chip*. 2023.

References:

1 C. Stolfi, C. Maresca, G. Monteleone and F. Laudisi, *Biomedicines*, 2022, **10**, 289.

2 A. S. Stewart, S. Pratt-Phillips and L. M. Gonzalez, *Journal of Equine Veterinary Science*, 2017, **52**, 10-22.

3 M. Vancamelbeke and S. Vermeire, *Expert Review of Gastroenterology & Hepatology*, 2017, **11**, 821-834.

4 W. M. Miner-Williams and P. J. Moughan, *Nutrition Research Reviews*, 2016, **29**, 40-59.

5 S. S. Ghosh, J. Wang, P. J. Yannie and S. Ghosh, *Journal of the Endocrine Society*, 2020, **4**.

6 J. M. Wells, O. Rossi, M. Meijerink and P. v. Baarlen, *PNAS*, 2010, **108**, 4607-4614.

7 Y. Guo, X. Chen, P. Gong, G. Li, W. Yao and W. Yang, *International Journal of Molecular Sciences*, 2023, **24**, 4089.

8 S. Yang and M. Yu, *Journal of Inflammation Research*, 2021, **14**, 3171-3183.

9 A. Michielan and R. D'Incà, *Mediators of Inflammation*, 2015, DOI: 10.1155/2015/628157.

[1] Cherwin AE, Templeton HN, Ehrlich AT, Patlin BH, Henry SC, Tobet SA. Microfluidic organotypic device to test intestinal mucosal barrier permeability ex vivo. *Lab on a Chip*. 2023.

10 L. Antoni, S. Nuding, J. Wehkamp and E. F. Stange, *World Journal of Gastroenterology*, 2014, **20**, 1165-1179.

11 S. Jäger, E. F. Stange and J. Wehkamp, *Langenbeck's Archives of Surgery*, 2013, **398**, 1-12.

12 M.C. Houser and M. G. Tansey, *NPJ Parkinson's Dis*, 2017, DOI: 10.1038/s41531-016-0002-0.

13 S. Ryman, A. A. Vakhtin, S. P. Richardson and H. C. Lin, *Journal of Neurology*, 2023, **270**, 746-758.

14 S. Min, N. Than, Y. C. Shin, G. Hu, W. Shin, Y. M. Ambrosini and H. J. Kim, *Scientific Reports*, 2022, **12**.

15 I. C. McLean, L. A. Schwerdtfeger, S. A. Tobet and C. S. Henry, *Lab on a Chip*, 2018, **18**, 1399-1410.

16 A. D. a. T. Gaber, International Journal of Molecular Sciences, 2020, **21**.

17 I. R. Powley, M. Patel, G. Miles, H. Pringle, L. Howells, A. Thomas, C. Kettleborough, J. Bryans, T. Hammonds, M. MacFarlane and C. Pritchard, *British Journal of Cancer*, 2020, **122**, 735-744.

[1] Cherwin AE, Templeton HN, Ehrlich AT, Patlin BH, Henry SC, Tobet SA. Microfluidic organotypic device to test intestinal mucosal barrier permeability ex vivo. *Lab on a Chip*. 2023.

18 P. d. Haan, M. J. C. Santbergen, M. v. d. Zande, H. Bouwmeester, M. W. F. Nielen and E. Verpoorte, *Nature Scientific Reports*, 2021, **11**.

19 H. J. Kim, D. Huh, G. Hamilton and D. E. Ingber, *Lab on a Chip*, 2012, **12**, 2165-2174.

20 K. Kulthong, L. Duivenvoorde, B. Z. Mizera, D. Rijkers, G. t. Dam, G. Oegema, T. Puzyn, H. Bouwmeester and M. v. d. Zande, *RSC Advances*, 2018, **8**, 32440-32453.

21 M. B. Esch, J. H. Sung, J. Yang, C. Yu, J. Yu, J. C. March and M. L. Shuler, *Biomedical Microdevices*, 2012, **14**, 895-906.

22 W. Shin and H. J. Kim, *PNAS*, 2018, **115**, E10539-E10547.

23 S. N. Bhatia and D. E. Ingber, *Nature Biotechnology*, 2014, **32**, 760-772.

24 K.-Y. Shim, D. Lee, J. Han, N.-T. Nguyen, S. Park and J. H. Sung, *Biomed Microdevices*, 2017, **19**.

25 B. Sidar, B. R. Jenkins, S. Huang, J. R. Spence, S. T. Walk and J. N. Wilking, *Lab on a Chip*, 2019, **19**, 3552-3562.

26 H. E. Amirabadi, J. M. Donkers, E. Wierenga, B. Ingenhut, L. Pieters, L. Stevens, T. Donkers, J. Westerhout, R. Masereeuw, I. Bobeldijk-Pastorova, I. Nooijen and E. v. d. Steeg, *Lab on a Chip*, 2022, **22**, 326-342.

[1] Cherwin AE, Templeton HN, Ehrlich AT, Patlin BH, Henry SC, Tobet SA. Microfluidic organotypic device to test intestinal mucosal barrier permeability ex vivo. *Lab on a Chip*. 2023.

27 A. Richardson, L. A. Schwerdtfeger, D. Eaton, I. Mclean, C. S. Henry and S. A. Tobet, *Analytical Methods*, 2020, **12**, 297-303.

28 C. M. Leung, P. d. Haan, K. Ronaldson-Bouchard, G.-A. Kim, J. Ko, H. S. Rho, Z. Chen, P. Habibovic, N. L. Jeon, S. Takayama, M. L. Shuler, G. Vunjak-Novakovic, O. Frey, E. Verpoorte and Y.-C. Toh, *Nature Reviews*, 2022, **2**.

29 A. S. Duarte, A. Caorreia and A. C. Esteves, *Critical Reviews in Microbiology*, 2016, **42**, 106-126.

30 S. Park, H. J. Chun, Y. D. Kwon, B. Keum, Y. S. Seo, Y. S. Kim, Y.-T. Jeen, S. H. Um, C. D. Kim, H. S. Ryu, J. H. Lee and Y.-s. Chae, *Gut and Liver*, 2008, **2**, 199-204.

31 D. Cooper and M. Dimri, *Journal*, 2022.

32 N. Prasadarao, S. A. Tobet and F. B. Jungalwala, *The Journal of Histochemistry and Cytochemistry*, 1990, **38**, 1193-1200.

33 D. Hollander, *Current Gastroenterology Reports*, 1999, **1**, 410-416.

34 V. Garcia-Hernandez, M. Quiros and A. Nusrat, *Annals of the New York Academy of Sciences*, 2017, **1397**, 66-79.

[1] Cherwin AE, Templeton HN, Ehrlich AT, Patlin BH, Henry SC, Tobet SA. Microfluidic organotypic device to test intestinal mucosal barrier permeability ex vivo. *Lab on a Chip*. 2023.

35 B. J. Saeedi, D. J. Kao, D. A. Kitzenberg, E. Dobrinskikh, K. D. Schwisow, J. C. Masterson, A. A. Kendrick, C. J. Kelly, A. J. Bayless, D. J. Kominsky, E. L. Campbell, K. A. Kuhn, G. T. Furuta, S. P. Colgan and L. E. Glover, *Molecular Biology of the Cell*, 2015, **26**, 2151-2384.

36 M. Furuse, M. Hata, K. Furuse, Y. Yoshida, A. Haratake, Y. Sugitani, T. Noda, A. Kubo and S. Tsukita, *Journal of Cell Biology*, 2002, **156**, 1099-1111.

37 A. Derkacz, P. Olczyk, K. Olczyk and K. Komosinska-Vassev, *J Clin Med*, 2021, **10**, 1122.

38 T. R. Cox and J. T. Erler, *Dis Model Mech*, 2011, **4**, 165-178.

39 C. Zhu, L. Yin, J. Xu, X. Yang, H. Wang, X. Xiang, H. Liu and K. Liu, *Biomolecules*, 2022, **12**, 1683.

40 H. C. Han, *J Vasc Res*, 2012, **49**, 185-197.

41 J. Xu and G. P. Shi, *Biophys Acta*, 2014, **1842**, 2106-2119.

42 Y. S. Kim and S. B. Ho, *Curr Gastroenterol Rep*, 2010, **12**, 319-330.

43 B. D. Shogan, N. Belogortseva, P. M. Luong, A. Zaborin, S. Lax, C. Bethel, M. Ward, J. P. Muldoon, M. Singer, G. An, K. Umanskiy, V. Konda, B. Shakhsheer, J. Luo, R. Klabbers,

[1] Cherwin AE, Templeton HN, Ehrlich AT, Patlin BH, Henry SC, Tobet SA. Microfluidic organotypic device to test intestinal mucosal barrier permeability ex vivo. *Lab on a Chip*. 2023.

L. E. Hancock, J. Gilbert, O. Zaborina and J. C. Alverdy, *Science Translational Medicine*, 2015, DOI: 10.1126/scitranslmed.3010658.

[1] Cherwin AE, Templeton HN, Ehrlich AT, Patlin BH, Henry SC, Tobet SA. Microfluidic organotypic device to test intestinal mucosal barrier permeability ex vivo. *Lab on a Chip*. 2023.

CHAPTER 2 –A MICROPHYSIOLOGICAL SYSTEM FOR STUDYING BARRIER HEALTH OF LIVE TISSUES IN REAL TIME[2]

Overview:

Epithelial cells create barriers that protect many different components in the body from their external environment. Increased gut barrier permeability (leaky gut) has been linked to several chronic inflammatory diseases. Understanding the cause of leaky gut and effective interventions are elusive due to the lack of tools that maintain tissue's physiological environment while elucidating cellular functions under various stimuli ex vivo. Here we present a microphysiological system that records real-time barrier permeability of mouse colon in a physiological environment over extended durations. The system includes a microfluidic chamber; media composition that preserves microbiome and creates necessary oxygen gradients across the barrier; and integrated sensor electrodes for acquiring transepithelial electrical resistance (TEER). Our results demonstrate that the system can maintain tissue viability for up to 72 h. The TEER sensors can distinguish levels of barrier permeability when treated with collagenase and low pH media and detect different thickness in the tissue explant.

Introduction:

Barrier tissues composed of epithelial monolayers are the body's first line of defense for protecting a mammalian host from its external environment[1]. These barriers help maintain cellular and tissue homeostasis[1,2,3]. Disruption of the intestinal barrier has been implicated in pathologies including inflammatory bowel disease (IBD)[4], neurodegenerative disorders[5,6], and numerous others[7,8,9]. Consequently, there is a demand for measuring the integrity of cellular barriers, prompting researchers to turn to techniques such as Transepithelial/transendothelial electrical resistance (TEER). TEER measurements represent the electrical resistance of the cellular barrier in real time and is a widely accepted measure of barrier integrity[3]. Traditionally,

[2] Way R, Templeton HN, Ball D, Cheng M, Tobet SA, Chen T. A microphysiological system for studying barrier health of live tissues in real time. *Communications Engineering*. 2024.

TEER has been used on cell monolayers, devoid of the complex three dimensional and heterogenous cellular environment of barrier tissues in vivo. Thus, there is a need for a microphysiological system that maintains the cellular complexity of the in vivo barrier tissue while maintaining the ability to measure barrier breakdown with TEER over the course of a full experiment.

Classically, epithelial barrier integrity is interrogated via fluorescently labeled probes to visualize the paracellular flux across the epithelial layer[10,11,12,13,14,15]. However, the importance of real-time data on barrier integrity during an experiment has led to an increased desire for using TEER to examine epithelial barrier properties. A widely used device for TEER measurements is the Transwell[2,16], where a cell monolayer is grown inside of a well-plate and TEER is measured using two “chopstick” electrodes. Transwells are desirable for their simplicity, cost, and high throughput. However, Transwells are not suited for in-depth investigations of cellular barrier function because of the simplified in vitro model without media flow and high variability from chopstick electrodes. To bolster the functionality and physiological representation of in vitro models, organ-on-a-chip (OoC) devices have been employed. These are more advanced devices containing engineered organ tissues and incorporating microfluidics to ensure continuous supply of fresh media containing vital nutrients and accounting for physical force faced by epithelia such as cyclic strain, fluid sheer stress, and mechanical stretching[11,17]. The results from the experiments using both Transwell and OoC devices have enhanced our understanding of the transepithelial transport process, however, they do not replicate the cellular complexity of the intact tissue barrier in vivo[2,8,13,14,18].

To create a better physiological model some researchers have moved towards ex vivo tissue explant devices. The Ussing chamber was one of the first and most commonly used tools to

[2] Way R, Templeton HN, Ball D, Cheng M, Tobet SA, Chen T. A microphysiological system for studying barrier health of live tissues in real time. *Communications Engineering*. 2024.

assess epithelial permeability in ex vivo experiments by measuring paracellular flux using electrical measurements. The Ussing chamber was originally designed to understand the phenomenon of active NaCl transport across frog skin[19,20]. This technique set the groundwork and created the first model for epithelial ion permeability. More modern designs of Ussing systems have accommodated many different types of epithelial barriers found inside animals. These barriers include skin, intestinal, esophageal, and more[3,20,21,22,23]. Common shortcomings of current Ussing chamber designs include the use of expensive benchtop equipment; static media within the chamber; low throughput; and bulky experimental setup. Static media makes it difficult to maintain viability of live ex vivo tissue for an extended period of time inside of devices. With reduced tissue viability, experiments using live tissues in an Ussing chamber have often been limited to under 3 h[20,24]. Due to the limited viability and lack of tissue equilibrium, there are limited interrogations that can be performed on the tissue and long-term affects cannot be addressed.

The intestinal barrier as live tissue is coordinated across complex biomaterials (e.g., mucus) and cellular elements that range from bacteria in the intestinal lumen to multiple epithelial cell types on the surface of the gut wall and cell types inside the wall that include, immune, stromal, neural, and muscle cells. Ex vivo models maintain these complex interactions providing a much more realistic physiological model than cell culture, epithelial monolayers, or OoC. One crucial distinction between cell culture and live tissue models lies in the variety of cell types and biological structures present within the model[14]. The most common intestinal in vitro models are comprised of immortalized Caco-2 cells that originated from a human intestinal tumor[3]. These cells are useful for absorption studies and are capable of forming tight junctions between cells in the monolayer, but lack many of the other structures that intestinal epithelium have[3,20]. There have also been OoC devices with intestinal organoid models cultured from stem cells[8,14].

[2] Way R, Templeton HN, Ball D, Cheng M, Tobet SA, Chen T. A microphysiological system for studying barrier health of live tissues in real time. *Communications Engineering*. 2024.

Intestinal organoid models can add a layer of epithelial cell diversity in the formation of intestinal villi and crypts, but still lack important cell components such as the immune, neuronal, or muscle systems present in vivo[14].

The ex vivo model is capable of providing cellular diversity closest to that in vivo, however, the challenge of maintaining the tissues viability over the course of an experiment has hindered the effectiveness of many current devices. Enhancing tissue viability is essential in crafting ex vivo models that mimic physiological conditions more accurately. This enables researchers to extend experimentation durations, thereby capitalizing on the benefits of enhanced cellular diversity across various experimental setups. Advancements in microfluidic device design and appropriate media composition have allowed live tissue inside a microphysiological chamber to maintain cellular heterogeneity and other key health markers over a long-term experiment (>48 h)[12,14,25,26]. Microfluidics create a more accurate physical microenvironment for the live tissue explant (e.g., fluid flow and shear stress) and the media composition provides the tissue with appropriate nutrient diffusion and oxygen gradients[14]. Existing devices capable of long-term explant viability are limited to data observed after the tissue is removed from the device, 48 h or more after it was dissected from the animal[12,25]. Incorporating TEER measurements inside such microphysiological devices increase the temporal resolution of changes in barrier function that might be caused by external perturbations (e.g., infection or chemical irritation). Without real-time TEER measurements in ex vivo models, tissue would need to be taken and removed from the experiment setup at multiple time points to assess barrier integrity. This would result in the use of more animals to obtain enough tissue to perform long time point experiments (i.e., 72 h) and would greatly increase labor and time to achieve results.

[2] Way R, Templeton HN, Ball D, Cheng M, Tobet SA, Chen T. A microphysiological system for studying barrier health of live tissues in real time. *Communications Engineering*. 2024.

This paper presents a microphysiological system for ex vivo tissues capable of longer-term viability and real-time TEER measurement with integrated sensors and electronics. The difficulties of using ex vivo tissue (e.g., leaking, intestinal wall damage, etc.,) has limited the number of systems capable of integrating these two crucial attributes. However, incorporation of ex vivo tissue in TEER measurements is necessary to create a model that most accurately represents in vivo conditions. If key components of a barrier system are missing in drug development, the drug may not perform as well in vivo. With most of the complex interactions maintained in the biological model and the ability to measure TEER throughout an experiment, this system is equipped to investigate essential biological questions and hypotheses for drug discovery and developmental research when compared to in-vitro models.

Overall, our contribution is threefold: first, the microphysiological system is capable of keeping intestinal tissue explants viable for up to 72 h by utilizing physiologically relevant media and microfluidic channels. Within the media, there is an oxygen gradient, a prebiotic to maintain the hosts natural microbiome, and a normoglycemic environment. Second, the TEER measurement of the ex vivo tissue is supported by integrated electrodes and backend electronics to record real-time TEER measurements throughout the entirety of the experiment at a user-specified interval, thus, allowing users to observe the evolution of barrier integrity in real time. Third, the system architecture is scalable allowing multiple microfluidic chambers to be connected to the system at a time, allowing for multiple controlled experiments using live tissues from the same donor. The proposed device is designed for intestinal tissue slices extracted from a mouse. However, the chamber design can be easily adapted to other barrier tissues.

[2] Way R, Templeton HN, Ball D, Cheng M, Tobet SA, Chen T. A microphysiological system for studying barrier health of live tissues in real time. *Communications Engineering*. 2024.

Materials and Methods:

Microfluidic Chamber Design

The microfluidic chamber (Fig. 5a–e), to be referred to as chamber for short, was designed using CAD (Autodesk, Inc) and fabricated using Anycubics UV sensitive resin and SLA printer. To avoid harmful effects from uncured resin, each chamber is fully cured using UV light and thoroughly rinsed with isopropyl alcohol. It is further sterilized in a low-temperature autoclave. The chamber consists of two halves assembled to hold the tissue and make connections to the integrated TEER electrodes. Each half chamber is composed of the following (Fig. 5a): the chamber body; two 1 mm thick PDMS layers for holding the electrode chip in place; one gold electrode chip; an aluminum clamp; and a printed circuit board (PCB) with spring headers that connect to the electrode chip. The fully assembled chamber (Fig. 5b) consists of two halves, the top half has spikes to hold the tissue tight when the chamber is sealed; the bottom half has corresponding openings for these spikes and is where the tissue is placed before closing the chamber. Figure 5c shows how the tissue explant positioned on the bottom half chamber, before and after the experiment. When the tissue is enclosed in the device, the chamber spikes puncture around the outer edge of the tissue but leaves the center untouched. A PDMS layer is placed over the spikes of the top chamber to create a flush seal against the tissue and prevent leaks between the chamber halves after the chamber is closed. A fully assembled chamber is shown in Fig. 5d, e in the front and the back view of the device, respectively.

Tubing is connected to each chamber half through Luer lock connectors. Media is pumped into the chamber using custom-designed syringe pumps where users can specify start and stop time points throughout the experiment period. With the tissue positioned over the circular opening

[2] Way R, Templeton HN, Ball D, Cheng M, Tobet SA, Chen T. A microphysiological system for studying barrier health of live tissues in real time. *Communications Engineering*. 2024.

between the chamber halves, a barrier is formed between the two media flows, one for the

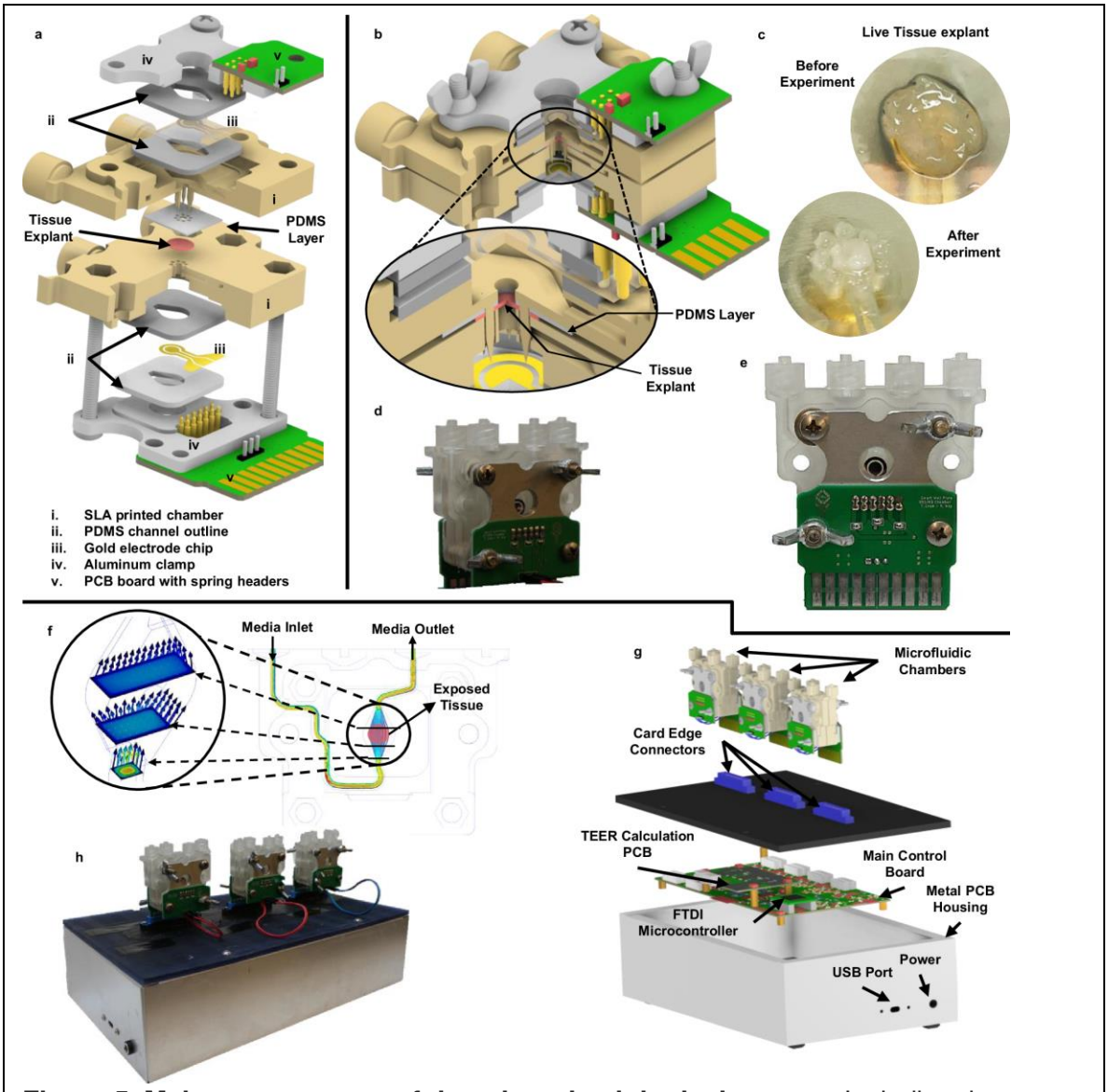

Figure 5. Major components of the microphysiological system. Including the microfluidic chamber (**a**–**f**) and the system-level housing (**g**–**h**). **a** Expanded view of a full chamber, with all components labeled. **b** Closed chamber with a closeup view of the tissue and PDMS clamped between two chamber halves. **c** Tissue explant before and after the experiment. **d**, **e** The actual manufactured chamber assembled (front and back, respectively). **f** Flow simulation through the chamber's microfluidics. **g** Expanded view of the microphysiological system. **h** The manufactured and fully assembled system with three chambers connected the system.

serosal side and the other for the luminal side of the tissue. The microfluidic path flows over the opening on each side exposing the tissue to the media composition. Providing balanced flow for

[2] Way R, Templeton HN, Ball D, Cheng M, Tobet SA, Chen T. A microphysiological system for studying barrier health of live tissues in real time. *Communications Engineering*. 2024.

the tissue inside the chamber is important for controlling shear stress and extending tissue viability[10,13,20]. The chamber was designed using 3D fluid simulations (CFD, Autodesk Inc) to make the media flow over the tissue area with uniform velocity as possible. Figure 5f shows an example of the flow simulations performed during design.

Each chamber half has its own PCB breakout board that connects to the glass chip electrodes through gold spring headers. The spring headers are compressed against the chip during assembly. The PCB on the top half chamber has external wire connectors for connecting to the bottom halve PCB. The bottom PCB includes a card edge connector that is plugged into the top of the enclosure for the microphysiological system (see section “System Overview below”). The chamber, when plugged into the system, is oriented vertically, making the media flow in from the bottom and out above the tissue (Fig. 5f). This orientation helps push air bubbles to the top and get them pushed out of the media outlet during experiments. Air bubbles can injure the tissue and cause large deviations for the TEER measurement.

Animals, tissue collection, and media preparation

In all experiments, male C57BL/6 background mice aged 3–4 months were used. Mice were kept on a 12 h light/dark cycle with access to standard chow and water ad libitum. Animal protocols were approved by the Institutional Animal Care and Use Committee (IACUC) at Colorado State University under United States Department of Agriculture (USDA) guidelines. Mice were deeply anesthetized with isoflurane and terminated via decapitation to prepare for tissue collection. The intestines were removed and immediately placed in 4 °C 1x Krebs buffer (in mM: 2.5 KCl, 2.5 $CaCl_2$, 126 NaCl, 1.2 $MgCl_2$, 1.2 NaH_2PO_4). To prevent contractions during dissection, the Krebs buffer contained 1 µl 1 mL^{-1} nicardipine (Sigma Aldrich, St. Louis, MO), an L-type calcium ion channel blocker. Colon was then dissected to remove any remaining

[2] Way R, Templeton HN, Ball D, Cheng M, Tobet SA, Chen T. A microphysiological system for studying barrier health of live tissues in real time. *Communications Engineering*. 2024.

mesentery. For experiments in which muscle was removed, a 26 G needle was used to gently tease away the muscle layer on the mesenteric edge of the tissue. Tissue was then cut longitudinally using angled vascular scissors to form flat pieces of tissue around ~5 mm. Adult Neurobasal media was custom made in house with 2% B27 supplement (ThermoFisher scientific, Waltham, WA), 4 mM glucose, 3% 1 M HEPES buffer (Sigma Aldrich, St. Louis, MO), without phenol red. To help maintain the gut microbiome, luminal media contained 0.4 mg ml^{-1} inulin (soluble fiber) and 0.5 M sodium sulfite (oxygen scavenger) to decrease oxygen levels[17]. The serosal media had ambient levels of oxygen creating an oxygen gradient across the tissue which we previously demonstrated[15] is necessary for preservation of microbiome. After 24 h, luminal media for control tissue was not changed. Treatment group luminal media contained $5.80*10^{-2}$ U of broad spectrum bacterially sourced collagenase (Worthington Biochemical, Lakewood, NJ) or was treated with hydrochloric acid (HCl) to acidify the pH to 2. After completion of experiments, 0.05 M phosphate buffered saline (PBS) containing 0.5% cetylpyridinium chloride (CPC) was gently pipetted onto the tissue to preserve the mucus layer[12]. The tissue was then gently removed from the device and placed in 4% paraformaldehyde (PFA) containing 0.5% CPC at 4 °C for 24 h. Tissue was stored in PBS at 4 °C until sectioning.

Tissue sectioning and histochemistry

Detailed methodology can be found in our previous publication[12]. Briefly, 1–3 mm sections of colon were submerged in agarose until polymerization. Tissue was then cut on a vibrating microtome (VT100S; Leica microsystems, Wetzlar, Germany) at a thickness of 50 µm. For lectin and immunohistochemistry, sections were first washed in 1x PBS, then incubated in 0.1 M glycine followed by PBS washes and incubated in 0.5% sodium borohydride followed by PBS

[2] Way R, Templeton HN, Ball D, Cheng M, Tobet SA, Chen T. A microphysiological system for studying barrier health of live tissues in real time. *Communications Engineering*. 2024.

washes. Sections were then blocked in PBS with 5% normal goat serum (NGS; Lampire Biological, Pipersville, PA), 1% hydrogen peroxide, and 0.3% Triton X (TX). Next, sections were placed in PBS containing 0.3% TX and 5% NGS with the appropriate lectin or antibody for 2 days. The lectin used was Ulex Europaeus Agglutinin I conjugated to Rhodamine (UEA-1; Vector Labs) at a concentration of 0.125 µg mL^{-1}. Primary antibodies used were anti-claudin1 (Invitrogen) 1:200 and anti-peripherin (Sigma-Aldrich) 1:300. After lectin or primary antibody incubation, sections were washed in PBS with 1% NGS. Sections incubated in primary antibody were then incubated with PBS containing 0.02% TX and Alexa Fluor 594 conjugated to secondary antibodies specific to the species of the primary antibodies at a 1:500 dilution. Finally, sections were washed in PBS, mounted on slides, and cover slipped. Images were taken using a Zeiss LSM800 upright confocal laser scanning microscope and a 20x (W Plan-Apochromat 20X/1.0 DIC Vis-ir ∞ /0.17) objective or an Olympus BH2 brightfield microscope.

Results and Discussion:

Tissue viability

Tissue health was maintained in the device with barrier integrity over 72 h. Colon explants maintained proper arrangement of mucosal, submucosal, muscular layers, and patterned crypts and the inner mucosal layer remained intact confirming maintenance of the mucosal barrier (Fig. 6a(i)). To protect the body from potential pathogens, healthy intestinal tissue must maintain sophisticated epithelial and mucosal barriers. Specialized epithelial cells, known as goblet cells, are crucial to barrier maintenance as they are responsible for producing and secreting mucin. Goblet cells were characterized due to their essential roles in maintenance of the barrier. Goblet cell mucopolysaccharides were identified by binding *Ulex europaeus* agglutinin I (UEA-1) conjugated to rhodamine. After 72 h in the microphysiological system, goblet cells retained their

[2] Way R, Templeton HN, Ball D, Cheng M, Tobet SA, Chen T. A microphysiological system for studying barrier health of live tissues in real time. *Communications Engineering*. 2024.

distinct shape (Fig. 6a(v), arrows) comparable to tissue taken directly after sacrifice that never went into the device (in vivo tissue) (Fig. 6a(iv), arrows). A hallmark indicator of intestinal tissue damage in several disorders is a decrease in number of goblet cells[28]. Goblet cells arise from progenitor cells at the base of colonic crypts. As they migrate apically, they mature and acquire the ability to synthesize and secrete mucopolysaccharides[29]. Since mature goblet cells are located in the upper third of crypts[30], they are potentially more susceptible to morphological changes. Therefore, the number of goblet cells in the upper third of crypts (apical crypt) were analyzed to further confirm tissue health. There were no statistically significant differences in the number of apical goblet cells between in vivo and ex vivo tissue (Fig. 6) indicating that 72 h ex vivo tissue was likely comparable in health to in vivo tissue. To further assess barrier integrity, tight junctions were examined. Tight junctions adhere epithelial cells together forming a physical barrier between cells to prevent unwanted passage of ions and molecules between epithelial cells. Claudins are a specific type of tight junction protein that help form the backbone of tight junctions. Claudin-1 is widely expressed in the intestinal epithelium and has essential roles in tight junction integrity. After 72 h in the device, clear claudin-1 immunoreactivity remained around epithelial cells (Fig. 6a(iii)) similar to in vivo tissue (Fig. 6a(ii)) further indicating maintenance of tissue health and barrier integrity.

[2] Way R, Templeton HN, Ball D, Cheng M, Tobet SA, Chen T. A microphysiological system for studying barrier health of live tissues in real time. *Communications Engineering*. 2024.

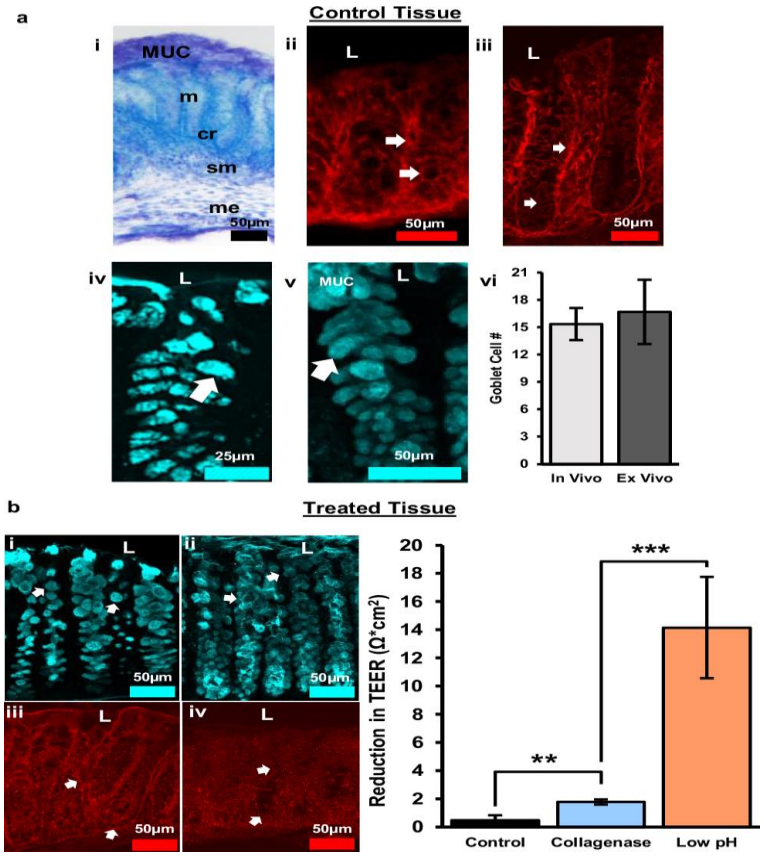

Figure 6. Tissue health was maintained over 72 h in the device and monitored after media treatment. a Control tissue after 72 h experiment. (i) Tol blue staining showing maintenance of colon morphology, MUC = mucus layer, m = mucosa, cr = crypt, sm = submucosa, me = muscularis externa. (ii) Claudin-1 immunoreactivity in vivo. (iii) Claudin-1 immunoreactivity in 72 h ex vivo shows maintenance of tight junctions between epithelial cells and crypts. (iv) UEA-1$^+$ material in vivo. (v) UEA-1$^+$ material ex vivo confirming maintenance of epithelial cells and mucus layer. (vi) Quantification of goblet cell number per apical crypt in in vivo vs. ex vivo tissue, $n = 3$, error bars show the standard error. **b** Collagenase treated, and acidic luminal media resulted in alterations in goblet cell morphology and tight junction expression indicative of increased barrier permeability. (i) Goblet cells labeled with UEA-1 become circular after collagenase treatment. (ii) Acidic media resulted in loss of goblet cell shape and sloughing off of cells near the lumen. (iii) Alterations in tight junction protein expression (claudin-1) following collagenase treatment. (iv) Claudin-1 expression decreased considerably with exposure to acidic media indicative of substantial barrier disruption. (v) The bar graph shows a distinct reduction in transepithelial electrical resistance (TEER) after exposure to different media composition. The difference in TEER was measured from 24 to 48 h mark after the tissue was enclosed in the device, with the media change occurring at 24 h. The three media compositions consist of a control media, collagenase treated media, and low pH media (more details about media composition in *"Animals, Tissue Collection, and Media Preparation"*). L = lumen, TEER values are normalized to the membrane surface area of the chamber, 0.0314 cm^2. Control: $n = 4$, Collagenase: $n = 10$, Low pH: $n = 3$, error bars show standard error, $^{**}p < 0.005$; $^{***}p < 0.0001$.

[2] Way R, Templeton HN, Ball D, Cheng M, Tobet SA, Chen T. A microphysiological system for studying barrier health of live tissues in real time. *Communications Engineering*. 2024.

Using TEER to measure changes in barrier permeability

Changes in TEER were correlated with physiological signs of barrier impairment, such as alterations to epithelial cells, the mucus layer, and tight junction proteins. To induce a disruption to barrier permeability, the luminal side of colon tissue was treated with collagenase or acidic media. Bacterial collagenases are enzymes secreted by endogenous bacteria in the intestines that degrade collagen. Increased collagenase can break down tight junctions between epithelial cells, as well as break down the extracellular matrix of epithelial cells[31]. This leads to increased intestinal permeability and provides a model for the development of leaky gut syndrome[32]. We have previously shown that bacterial collagenase in luminal media can be used as a model to create leaky gut by disrupting epithelial cell (goblet cell) morphology and decreasing tight junction (claudin-1) expression[12]. Increased barrier permeability was shown by an increased reduction in TEER with collagenase treatment over time (Fig. 6b(v)). To confirm that reductions in TEER correlated with physiological characteristics of increased intestinal permeability, goblet cells, and claudin-1 were examined. Following collagenase treatment, goblet cells became more circular in shape (Fig. 6b(i)) and claudin-1 immunoreactivity was moderately decreased (Fig. 6b(iii)) indicating barrier impairment.

To assess whether changes in TEER matched changes in physiological changes, acidic media (pH 2) was added to the luminal side of tissue to induce substantial damage to the intestinal barrier. Cells need to maintain a pH of 7.4 to function properly. Lowering the pH to 2.0 leads to increased epithelial cell death and alterations in cellular processes creating drastic increases in permeability. This was confirmed with goblet cells losing distinct shape and sloughing off near the lumen (Fig. 6b(ii)). Claudin-1 immunoreactivity dramatically decreased indicating substantial loss of tight junctions (Fig. 6b(iv)). These dramatic changes in epithelial cell and claudin-1

[2] Way R, Templeton HN, Ball D, Cheng M, Tobet SA, Chen T. A microphysiological system for studying barrier health of live tissues in real time. *Communications Engineering*. 2024.

morphology correlate with the significant reduction of TEER following acidic pH treatment (Fig. 6b(v)).

Differences in tissue explant detected by TEER:

Cut muscle vs. muscle intact

To determine whether distinct tissue components contributed differentially to TEER, the muscle layer was dissected away. Thereby removing the muscularis externa, a major subepithelial structure of the colon. TEER was measured after 24 h inside the chamber, allowing sufficient time for the tissue to equilibrate to its new environment. Removal of the muscle layer decreased TEER by about 39% (Fig. 7a). This result is consistent with previous reports that have performed experiments to study the contribution of sub epithelial resistance. The values reported have ranged from 15% to 80% of the total epithelial resistance is concentrated in the sub epithelium, depending on the location in the intestine as well as the animal[23,27,33,34,35]. Research using rat jejunum has shown a much larger contribution to total resistance done by the sub epithelium (78–80%)[23,33]. Whereas measurements on the ileum, colon, and rectum in both rats and mice have showed much lower contributions (15–45%)[27,34,35]. This is consistent with the results found here using mouse colon.

[2] Way R, Templeton HN, Ball D, Cheng M, Tobet SA, Chen T. A microphysiological system for studying barrier health of live tissues in real time. *Communications Engineering*. 2024.

Confirmation of total muscle dissection was done by Toluidine blue staining, as seen in Fig. 7a(ii) when compared to tissue with the muscle intact (Fig. 7a(i)). Demonstrating the TEER calculated with the muscle dissected is an accurate representation of the epithelial resistance alone and has little to no contribution from subepithelial resistances. This demonstration is lacking from all previous research studying the contribution of subepithelial resistance by subepithelial stripping or dissection[42,43,44]. These images alongside the TEER measurements provide new evidence for the contribution of subepithelial resistance to total epithelial resistance.

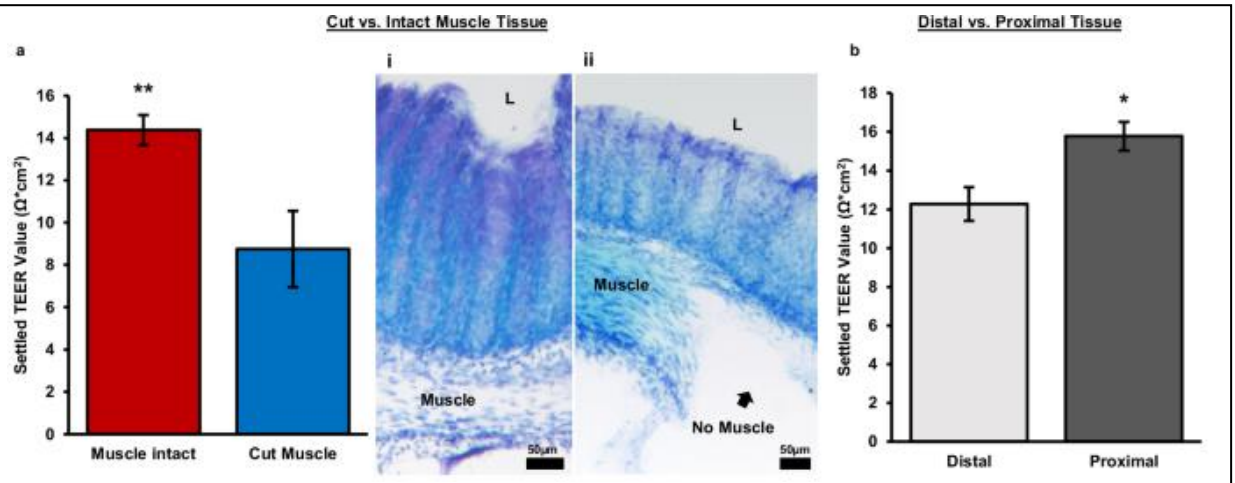

Fig. 7: Physical differences in tissue explant. a This bar chart shows the difference in settled transepithelial electrical resistance (TEER) value of tissues explants with the muscle intact vs. with the muscle removed. The settled TEER value is taken 24 h after the tissue is enclosed in the chamber. (i) Tol blue staining of tissue with intact muscle. (ii) Tol blue staining tissue with muscle removed, L = lumen. **b** Settled TEER values for different regions of mouse colon tissue. Proximal tissue was defined as the three pieces of tissue closest to the cecum and distal tissue was defined as the two pieces farthest from the cecum and closest to the rectum. Each tissue piece was approximately 5 mm in length. The settled TEER value was taken approximately 24 h after the tissue had been enclosed in the device. Muscle intact: $n = 15$, Cut muscle: $n = 7$, Distal: $n = 6$, Proximal: $n = 9$, error bars show standard error, $^{**}P < 0.005$, $^{*}P < 0.01$.

Proximal vs. distal colon

The position within the colon is another possible factor contributing to differences among tissue explant slices. Previous research on mouse colon tissue has shown that the proximal tissue has

[2] Way R, Templeton HN, Ball D, Cheng M, Tobet SA, Chen T. A microphysiological system for studying barrier health of live tissues in real time. *Communications Engineering*. 2024.

a higher baseline TEER value compared to mid or distal slices[21]. After compiling data from our own experiments, we found that our TEER results are consistent with previously reported data on tissues located in different sections of the colon. We observed about a 19% decrease in TEER in the distal colon compared to the proximal colon (Fig. 7b).

Highlights of system performance

Table 1 Comparison of epithelial barrier investigation devices

	Biological Sample		Electrical Permeability				Chamber/System Design	
	Sample Type	Demonstrated Tissue Viability	TEER capable?	Electrode Type	Stimulus Signal	Measurement Electronics	Microfluidics Support	Throughput
Transwell[2,16]	Cell monolayer	-	Yes	Ag/AgCl "stick" electrodes	DC	Commercial Benchtop	No	96
Liang et al. [13]	Cell monolayer (canine kidney)	-	Yes	Integrated glass chip	Up to 10 MHz	Commercial Benchtop	Yes	1
Helm et al. [18]	Cell monolayer (Caco-2)	-	Yes	Polycarbonate substrate electrode chips	Up to 100 kHz	Commercial Benchtop	Yes	1
Fernandes et al. [35]	Cell monolayer (GI tract and airway)	-	Yes	Integrated glass chip	Up to 100 kHz	Custom-built	One side only	8
Navicyte[21]	Mouse and human intestinal tissue	<3 h	Yes	Ag/AgCl "stick" electrodes	DC	Commercial Benchtop	No	6
Clarke et al. [20]	Mouse colon tissue	3 h	Yes	Ag/AgCl electrodes connected by salt bridge	DC	Commercial Benchtop	No	1
Calvo et al. [27]	Frog epithelial tissue	-	Yes	Integrated "stick" electrodes	Up to 100 kHz	Custom-built	No	1
Dawson et al. [25]	Human intestine tissue	72 h	No	-	-	-	Yes	1
Poenar et al. [22]	Porcine esophageal tissue	48	Yes	Integrated "stick" electrodes	DC	Commercial Benchtop	Yes	1
Cherwin et al. [12] & Richardson et al. [15]	Mouse colon tissue	72 h	No	-	-	-	Yes	1
Amirabadi et al. [26]	Porcine & human colon tissue	24 h	No	Optical Fiber Sensor	-	-	Yes	1
This Work	Mouse colon tissue	72 h	Yes	Integrated glass chip	Up to 5 kHz	Custom-built	Yes	3

To showcase the distinctive qualities of our system, we compared it with existing devices for studying epithelial transport based on several key attributes, such as sample type, tissue

[2] Way R, Templeton HN, Ball D, Cheng M, Tobet SA, Chen T. A microphysiological system for studying barrier health of live tissues in real time. *Communications Engineering*. 2024.

viability duration, TEER measurement capability, experiment throughput, and more. The comparison is shown in Table 1. All of these attributes are important for evaluating different epithelial transport systems, and highlighting the differences between Transwell, OoC, and ex vivo devices.

The top four rows of the table show existing in vitro devices (Transwell and OoC). These systems are intended for studying cultured cell monolayers. In addition to providing TEER measurements, they also provide high throughput of up to 96 wells. Unlike the Transwell system, most of the OoC systems provide microfluidic support to maintain cell viability. One of their biggest weaknesses is their lack of realistic biological model to better represent rich biological processes in live tissues.

The remaining rows in Table 1 are existing ex vivo systems. Our proposed system is in the bottom row. Some of the existing ex vivo systems are capable of TEER measurements, but they can only maintain tissue viability for a short period of time (<3 h). The ex vivo devices that are capable of maintaining tissue viability for longer period of time (up to 72 h) are not capable of TEER measurements or any other real-time tissue integrity feedback measurements. Furthermore, the existing ex vivo systems can only support one tissue measurement at a time, making experiments requiring replicates more difficult and time consuming. In contrast, our proposed system is designed to perform real-time TEER measurements on multiple tissue explants at the same time, with the capability of maintaining tissue viability for up to 72 h. These advances in capabilities will make studies targeting a specific organ, requiring extended experiment time period of interrogation, and replicates from the same animal, easier and more feasible.

[2] Way R, Templeton HN, Ball D, Cheng M, Tobet SA, Chen T. A microphysiological system for studying barrier health of live tissues in real time. *Communications Engineering*. 2024.

Conclusion:

This paper presents a highly integrated microphysiological system for studying live tissue barrier permeability of mouse colon. The unique design of the microfluidic chamber is capable of securing an explant of mouse colon tissue between two independent media pathways creating a micro physiological environment inside the chamber comparable to the environment in vivo. The use of proper media provides nutrients, support gut microbiome, and create important oxygen gradients across the tissue to keep tissue viability for an extended period of time. After 72 h in the chamber, the tissue explants displayed an inner mucus layer, robust goblet cells, and evident tight junction function along the length of the epithelial layer. These characteristics all serve as strong indicators of sustained barrier integrity. This preservation of tissue viability addresses an important drawback in existing live tissue barrier permeability devices.

Integrated electrode chips allow the microfluidic chamber to successfully characterize barrier permeability using TEER measurements in real time. The plug-and-play nature of the system design simplifies the experiment setup and allows for all chambers to be re-usable and universal. Unlike most existing systems where bulky and expensive benchtop equipment is needed to perform experiments, the integrated support electronics made the overall system small enough to fit into an incubator. Furthermore, architectural scalability allows multiple chambers to be connected to the system enabling multiple controlled experiments using samples from the same donor. The use of the system is further enhanced by a custom-built GUI which was developed to allow each experiment to be customizable and ran from any host computer.

[2] Way R, Templeton HN, Ball D, Cheng M, Tobet SA, Chen T. A microphysiological system for studying barrier health of live tissues in real time. *Communications Engineering*. 2024.

In conclusion, this microphysiological system has the potential to open new avenues to investigate barrier health of live tissues. Real time permeability measurements are crucial to developing more accurate ex vivo tissue models for studying the health and chemical responses of barrier tissues.

[2] Way R, Templeton HN, Ball D, Cheng M, Tobet SA, Chen T. A microphysiological system for studying barrier health of live tissues in real time. *Communications Engineering*. 2024.

References:

1. Moens, E. & Veldhoen, M. Epithelial barrier biology: good fences make good neighbours. *Immunology* **135**, 1–8 (2012).

2. Walter, F. R. *et al.* A versatile lab-on-a-chip tool for modeling biological barriers. *Sensors and Actuators B: Chemical* **222**, 1209–1219 (2016).

3. Srinivasan, B. *et al.* TEER Measurement Techniques for In Vitro Barrier Model Systems. *SLAS Technology* **20**, 107–126 (2015).

4. Michielan, A. & D'Incà, R. Intestinal Permeability in Inflammatory Bowel Disease: Pathogenesis, Clinical Evaluation, and Therapy of Leaky Gut. *Mediators Inflamm* **2015**, 628157 (2015).

5. Houser, M. C. & Tansey, M. G. The gut-brain axis: is intestinal inflammation a silent driver of Parkinson's disease pathogenesis? *NPJ Parkinsons Dis* **3**, 3 (2017).

6. Ryman, S., Vakhtin, A. A., Richardson, S. P. & Lin, H. C. Microbiome-gut-brain dysfunction in prodromal and symptomatic Lewy body diseases. *J Neurol* **270**, 746–758 (2023).

7. Fasano, A. Leaky Gut and Autoimmune Diseases. *Clinic Rev Allerg Immunol* **42**, 71–78 (2012).

8. Lechuga, S., Braga-Neto, M. B., Naydenov, N. G., Rieder, F. & Ivanov, A. I. Understanding disruption of the gut barrier during inflammation: Should we abandon traditional epithelial cell lines and switch to intestinal organoids? *Front. Immunol.* **14**, 1108289 (2023).

9. Esnafoglu, E. *et al.* Increased Serum Zonulin Levels as an Intestinal Permeability Marker in Autistic Subjects. *The Journal of Pediatrics* **188**, 240–244 (2017).

10. Benson, K., Cramer, S. & Galla, H.-J. Impedance-based cell monitoring: barrier properties and beyond. *Fluids and Barriers of the CNS* **10**, 5 (2013).

[2] Way R, Templeton HN, Ball D, Cheng M, Tobet SA, Chen T. A microphysiological system for studying barrier health of live tissues in real time. *Communications Engineering*. 2024.

11. Leung, C. M. *et al.* A guide to the organ-on-a-chip. *Nat Rev Methods Primers* **2**, 1–29 (2022).

12. Cherwin, A. E. *et al.* Microfluidic organotypic device to test intestinal mucosal barrier permeability *ex vivo*. *Lab Chip* 10.1039.D3LC00615H (2023) doi:10.1039/D3LC00615H.

13. Liang, F. *et al.* A microfluidic tool for real-time impedance monitoring of in vitro renal tubular epithelial cell barrier. *Sensors and Actuators B: Chemical* **392**, 134077 (2023).

14. McLean, I. C., Schwerdtfeger, L. A., Tobet, S. A. & Henry, C. S. Powering *ex vivo* tissue models in microfluidic systems. *Lab Chip* **18**, 1399–1410 (2018).

15. Richardson, A. *et al.* A microfluidic organotypic device for culture of mammalian intestines *ex vivo*. *Anal. Methods* **12**, 297–303 (2020).

16. Leonard, F., Collnot, E.-M. & Lehr, C.-M. A three-dimensional coculture of enterocytes, monocytes and dendritic cells to model inflamed intestinal mucosa in vitro. *Mol Pharm* **7**, 2103–2119 (2010).

17. Trujillo-de Santiago, G., Lobo-Zegers, M. J., Montes-Fonseca, S. L., Zhang, Y. S. & Alvarez, M. M. Gut-microbiota-on-a-chip: an enabling field for physiological research. *Microphysiol Syst* **2**, 7 (2018).

18. Helm, M. W. van der *et al.* Non-invasive sensing of transepithelial barrier function and tissue differentiation in organs-on-chips using impedance spectroscopy. *Lab Chip* **19**, 452–463 (2019).

19. Ussing, H. H. & Zerahn, K. Active transport of sodium as the source of electric current in the short-circuited isolated frog skin. *Acta Physiol Scand* **23**, 110–127 (1951).

20. Clarke, L. L. A guide to Ussing chamber studies of mouse intestine. *American Journal of Physiology-Gastrointestinal and Liver Physiology* **296**, G1151–G1166 (2009).

[2] Way R, Templeton HN, Ball D, Cheng M, Tobet SA, Chen T. A microphysiological system for studying barrier health of live tissues in real time. *Communications Engineering*. 2024.

21. Thomson, A. *et al.* The Ussing chamber system for measuring intestinal permeability in health and disease. *BMC Gastroenterol* **19**, 98 (2019).

22. Poenar, D. P., Yang, G., Wan, W. K. & Feng, S. Low-Cost Method and Biochip for Measuring the Trans-Epithelial Electrical Resistance (TEER) of Esophageal Epithelium. *Materials (Basel)* **13**, 2354 (2020).

23. Fromm, M., Schulzke, J. D. & Hegel, U. Epithelial and subepithelial contributions to transmural electrical resistance of intact rat jejunum, in vitro. *Pflugers Arch* **405**, 400–402 (1985).

24. Ghiselli, F., Rossi, B., Piva, A. & Grilli, E. Assessing Intestinal Health. In Vitro and Ex vivo Gut Barrier Models of Farm Animals: Benefits and Limitations. *Front Vet Sci* **8**, 723387 (2021).

25. Dawson, A. *et al.* A microfluidic chip based model for the study of full thickness human intestinal tissue using dual flow. *Biomicrofluidics* **10**, 064101 (2016).

26. Eslami Amirabadi, H. *et al.* Intestinal explant barrier chip: long-term intestinal absorption screening in a novel microphysiological system using tissue explants. *Lab Chip* **22**, 326–342 (2022).

27. Gitter, A. H., Fromm, M. & Schulzke, J.-D. Impedance analysis for the determination of epithelial and subepithelial resistance in intestinal tissues. *Journal of Biochemical and Biophysical Methods* **37**, 35–46 (1998).

28. Kim, Y. S. & Ho, S. B. Intestinal Goblet Cells and Mucins in Health and Disease: Recent Insights and Progress. *Curr Gastroenterol Rep* **12**, 319–330 (2010).

29. Yang, S. & Yu, M. Role of Goblet Cells in Intestinal Barrier and Mucosal Immunity. *JIR* **Volume 14**, 3171–3183 (2021).

[2] Way R, Templeton HN, Ball D, Cheng M, Tobet SA, Chen T. A microphysiological system for studying barrier health of live tissues in real time. *Communications Engineering*. 2024.

30. Merzel, J. & Almeida, M. L. P. Maturation of goblet cells of the mouse small intestine as shown by the uptake of ^{35} S-sodium sulfate. *Anat. Rec.* **177**, 519–524 (1973).

31. Duarte, A. S., Correia, A. & Esteves, A. C. Bacterial collagenases - A review. *Crit Rev Microbiol* **42**, 106–126 (2016).

32. Aleman, R. S., Moncada, M. & Aryana, K. J. Leaky Gut and the Ingredients That Help Treat It: A Review. *Molecules* **28**, 619 (2023).

33. Hemlin, M., Jodal, M., Lundgren, O., Sjövall, H. & Stage, L. The importance of the subepithelial resistance for the electrical properties of the rat jejunum *in vitro*. *Acta Physiologica Scandinavica* **134**, 79–88 (1988).

34. Tai, Y.-H. & Tai, C.-Y. The conventional short-circuiting technique under-short-circuits most epithelia. *J. Membrain Biol.* **59**, 173–177 (1981).

35. Gitter, A. H., Bendfeldt, K., Schulzke, J. D. & Fromm, M. Trans/paracellular, surface/crypt, and epithelial/subepithelial resistances of mammalian colonic epithelia. *Pflugers Arch - Eur J Physiol* **439**, 477–482 (2000).

[2] Way R, Templeton HN, Ball D, Cheng M, Tobet SA, Chen T. A microphysiological system for studying barrier health of live tissues in real time. *Communications Engineering*. 2024.

CHAPTER 3 –GUT NEUROPEPTIDE INVOLVEMENT IN PARKINSON'S DISEASE[3]

Overview

Parkinson's disease (PD) is a neurodegenerative disorder affecting over 10 million people worldwide. A key pathological feature of PD is the accumulation of misfolded α-synuclein (aSyn) protein in the substantia nigra pars compacta (SNpc). Aggregation of aSyn can form Lewy Bodies that contribute to dopaminergic neuron degeneration and motor symptoms such as tremor, rigidity, and bradykinesia. Beyond the central nervous system (CNS), aSyn aggregates have been detected in peripheral tissues, including the gastrointestinal (GI) tract, suggesting a link between peripheral aSyn and non-motor PD symptoms. GI symptoms, often preceding motor symptoms by up to 20 years, highlight the potential bidirectional communication between the central nervous system and the enteric nervous system (gut-brain axis) in PD. Although microbiome alterations and intestinal inflammation have been associated with PD, functional impact of these alterations on gut-brain signaling or aSyn aggregation remain unclear. Intestinal neuropeptides are key modulators of gut-brain communication, alter immune response to pathogens and environmental toxins, and may contribute to function of the luminal gut barrier. Dysregulation of gut neuropeptide signaling including vasoactive intestinal peptide (VIP), neuropeptide Y (NPY), calcitonin gene related peptide (CGRP) and substance P (SP) have been associated pathologic effects of PD in animal models. Despite their potential role in pathogenesis and disease modulation, gut derived neuropeptide influences on PD are under explored. This manuscript reviews current knowledge surrounding microbial metabolite and immune influences on gut neuropeptide signaling, aSyn aggregation in the enteric nervous

[3]Templeton HA, Tobet SA & Schwerdtfeger LA. Gut Neuropeptide Involvement in Parkinson's Disease. American *Journal of Physiology Gastrointestinal and Liver Physiology. Under Review*.

system, and downstream neuroimmune pathway alterations within the context of PD and its mouse models.

Introduction

Parkinson's disease (PD) is a neurodegenerative disease that affects over 10 million people worldwide[1,2], driven by an accumulation of misfolded α-synuclein (aSyn) protein in midbrain basal ganglia, specifically, the substantia nigra pars compacta (SNpc). Aggregated aSyn may contribute to degeneration of dopaminergic neurons in the SNpc, resulting in motor symptoms including tremor, rigidity, bradykinesia, and postural and gait impairment[3,4]. Beyond the central nervous system (CNS), aSyn aggregates have been found in several peripheral tissues including the urinary tract, cardiovascular system, and the gastrointestinal (GI) tract, all of which may contribute to the diverse and complex non-motor symptomology of PD[5]. Peripheral prodromal symptoms can provide early indicators of future disease, some with predictive validity up to 20 years prior to motor symptom onset[6,7]. A substantial percentage of PD subjects experience pre-motor GI issues, including constipation, bloating, and nausea[8-11] that are correlated with severity of motor symptoms in PD. Additionally, GI symptoms such as bowel incontinence and constipation can be predictive of cognitive outcomes in PD[12]. Altered microbial composition[13] and related gut barrier degradation[14] can lead to an inflamed mucosal immune environment, likely playing a role in elevated peripheral aSyn[15]. Furthermore, CNS aSyn can shuttle to the intestine[16,17] and from the intestine to the brain trans-synaptically[16,18,19], supporting the role of the gut-brain axis as a bidirectional mediator of aSyn with potential involvement in PD disease severity and etiology.

[3]Templeton HA, Tobet SA & Schwerdtfeger LA. Gut Neuropeptide Involvement in Parkinson's Disease. American *Journal of Physiology Gastrointestinal and Liver Physiology. Under Review.*

Small bioactive molecules known as neuropeptides may play significant roles in the development of PD pathology[20]. Dysregulation of several neuropeptides including vasoactive intestinal peptide (VIP), neuropeptide Y (NPY), and substance P (SP) is correlated with classical CNS pathology observed in PD, however there appears to be a protective role for some, such as glucagon like peptide-1 (GLP-1), CGRP, and VIP[21-26]. Neuropeptides can mediate gut-brain communication, immune function, and overall neural – immune, and neural – epithelial homeostasis. Animal models for investigating damage to dopaminergic neurons in the nigrostriatal pathway include exposure to pesticides and herbicides such as rotenone[27,28] and paraquat[29], as well as neurotoxins such as 6-Hydroxydopamine (6-OHDA)[30], and 1-methyl-4-phenyl-1,2,3,6-tetrahydropyridine (MPTP)[31]. Furthermore, transgenic mouse strains including A53T[32] and E46 / 3K[33] provide animals with pan-neuronal human aSyn and result in the development of motor disorders with age. Investigations harnessing these models coupled with human epidemiologic and clinical studies identify changes in several neuropeptides that play may roles in the development and progression of PD.

Gastrointestinal Symptomatology and Microbial Metabolite Shifts in PD

GI dysfunction has been recognized as a feature of PD since the disorder was first described in detail by James Parkinson. In his 1817 “An Essay on the Shaking Palsy,” Parkinson included a case report highlighting GI symptoms such as constipation and increased mucus when passing feces[34]. Even with early descriptions of non-motor symptoms, diagnostic criteria for PD has remained centered around motor dysfunction with the cardinal signs being bradykinesia, tremor and rigidity[35]. A surge of scientific interest in non-motor and specifically GI symptomology arose with early PD clinical trials that found increased prevalence of GI side effects following

[3]Templeton HA, Tobet SA & Schwerdtfeger LA. Gut Neuropeptide Involvement in Parkinson’s Disease. American *Journal of Physiology Gastrointestinal and Liver Physiology. Under Review*.

treatments like levodopa[36]. In the late 1980s and early 1990s, clinical studies involving PD and GI interactions began to increase[37-41], but it was not until after 2000 that the search for explanations concerning the potential role of the peripheral nervous system (PNS) and GI involvement in PD pathogenesis gained momentum[42-44]. Constipation is often one of the earliest PD symptoms seen in up to 80% of PD subjects[9 45,46] and heavily impacts quality of life[47]. Furthermore, dysphagia and abdominal pain are often reported to worsen when antiparkinsonian medications are stopped[48,49]. Other common GI symptoms in PD include drooling, dry mouth[50], impaired gastric emptying, bloating, vomiting[9,10], and small intestinal bacterial overgrowth (SIBO)[51-54]. These symptoms are routinely reported differently across sex[55,56] and while men are twice as likely to develop the disease, females experience faster disease progression, higher mortality, and more severe GI symptoms[47,57]. Despite this, many PD focused investigations fail to include sex as a biological variable, an omission that should be rectified moving forward as a field. GI symptoms in PD pose significant health risks including malnutrition, intestinal obstruction, and impaired medication effectiveness[58,59], underscoring the importance of understanding mechanisms driving GI symptomology.

Altered gut function in PD is influenced by microbiota and their metabolites[60-67] which can alter neuropeptide release. Robust shifts in specific taxa are observed in PD compared to healthy individuals, with potentially beneficial genera including *Lactobacillus, Akkermansia,* and *Bifidobacterium* being enriched in PD[68]. Roles of potentially pathogenic microbes in PD, including *Alistipes,* are emerging[69]. Microbial transformation of food products including fibers and host-derived compounds like bile acids result in bioactive microbially derived metabolites that are critical for intestinal function. Numerous studies have shown decreased levels of short chain fatty acids (SCFAs) in PD stool[70,71], which are bacterial products involved in maintenance

[3]Templeton HA, Tobet SA & Schwerdtfeger LA. Gut Neuropeptide Involvement in Parkinson's Disease. American *Journal of Physiology Gastrointestinal and Liver Physiology. Under Review*.

of gut epithelial barrier and immune health[72]. SCFAs may influence intestinal homeostasis by regulating neuropeptide production and secretion. Addition of acetate, propionate, or butyrate to a flat-sheet preparation of rat colon increased CGRP release by 2-3 fold[73]. SCFA treatment also increased mRNA expression of GLP-1R in cultured chicken duodenal epithelial cells and elevated GLP-1 content in culture medium[74]. SCFA influence on gut neuropeptide secretion is intriguing, as both SCFAs and neuropeptides are critical in regulation of the intestinal barrier [75,76] [77-80] and influencing both mucosal and CNS immunity[81-84]. Oral administration of SCFAs have been investigated as driving CNS dysfunction in animal models of PD by altering microglial gene expression and anatomic structure[71]. While this study shows one route for peripheral modulation of central microglial function, it is important to consider the blood brain barrier (BBB) and accessibility of peripheral metabolites to the CNS. While many microbial derived metabolites can cross the BBB[85], the effect of SCFAs observed by Sampson et al., was likely driven by immature microglia in germ-free animal models[86] that become more activated when exposed to any microbial metabolites, rather than SCFAs specifically. Other investigations have found decreased butyrate in PD fecal and serum samples while observing elevated microbial derived metabolites like p-cresol and phenylacetylglutamine[64,87], which correlated with stool consistency and constipation[64]. Non-human primate models of PD show decreased levels of potentially beneficial microbially derived metabolites including secondary bile acids, phosphocholines, and sphingomyelins in serum and stool[88]. Together, these studies demonstrate an altered intestinal environment that supports microbiota to produce varied metabolic profiles in PD compared to healthy controls.

[3]Templeton HA, Tobet SA & Schwerdtfeger LA. Gut Neuropeptide Involvement in Parkinson's Disease. American *Journal of Physiology Gastrointestinal and Liver Physiology. Under Review.*

Gut-Brain Axis Involvement in Alpha Synuclein Pathology

PD has been postulated to begin with perturbations to the olfactory or gastrointestinal systems that induce pathologic aSyn that reaches the CNS[44]. In support of this, aggregated aSyn has been found throughout the GI tract in PD subjects[42,89-93]. A commonly used mouse model for synucleinopathies, A53T human aSyn transgenic mice display signs of GI dysfunction that precede motor abnormalities and CNS aSyn pathology by at least 6 months[94]. Motor symptoms in rats can be recapitulated via injection of pre-formed aSyn fibrils into the intestinal wall. Gut aSyn moves along the vagus nerve, to the dorsal motor nucleus of the vagus (DVM) and into the SNpc[19], a process abolished by vagotomy[18]. Pathological aSyn can propagate bidirectionally between the brain and gut via the vagus nerve[16]. Four months after injection of aSyn pre-formed fibrils (PFFs) into the duodenal wall, phosphorylated aSyn pathology was increased in the DMV and several brain areas including the SNpc[16]. Fibrils of aSyn injected into the striatum can propagate anterograde to the colon within one month, primarily via the vagus nerve[17]. These findings support the hypothesis of bi-directional vagal transmission of aSyn between the gut and brain, and mechanisms by which gut derived aSyn reaches the vagus remains an area of ongoing investigation. Specialized enteric epithelial cells known as enteroendocrine cells (EECs), which produce a range of peptide hormones, connect to enteric nerves that synapse with vagal neurons, creating a gut-brain circuit[95,96]. Mucosal EECs express aSyn and connect with aSyn- containing neurons[97]. Recent work has used mucosa specific, cre-inducible aSyn mouse line to show that subdiaphragmatic vagotomy results in a lack of aSyn in vagal (nodose) ganglia that is present in non-vagotomized mice, suggesting that gut mucosal aSyn can spread to the CNS via the vagus nerve[98]. In further support of vagal involvement in PD, epidemiologic studies have suggested that truncal vagotomy may lower PD risk[99,100].

[3]Templeton HA, Tobet SA & Schwerdtfeger LA. Gut Neuropeptide Involvement in Parkinson's Disease. American *Journal of Physiology Gastrointestinal and Liver Physiology. Under Review.*

However, these studies are done in relatively small populations and anti-parkinsonian drug treatment is likely confounding[101]. Vagal involvement in PD has spurred investigation into non-pharmacological interventions such as transcutaneous auricular vagus nerve stimulation (taVNS) which may improve gait impairment[102,103]. Vagus stimulation likely impacts autonomic vagal projections to the gut, a pathway that has profound effects on enteric neuropeptide production, mucosal immune populations, and the microbiome. These studies highlight the importance of exploring the impact of VNS on gastrointestinal function with respect to neuropeptide signaling in health and diseased states.

Gut to CNS aSyn shuttling may occur through alternate routes beyond vagal trafficking. Nigrostriatal or enteric injections of human aSyn Lewy body extracts into non-human primates resulted in both nigrostriatal and enteric pathology without aSyn pathological lesions in the vagal nerve[104], suggesting that the vagus nerve may not be necessary for transmission of aSyn. McFleder and colleagues[105] injected an adeno-associated virus (AAV) encoding the human A53T-mutated form of aSyn directly into the SNpc of transgenic mice expressing the photoconvertible protein Dendra 2. This system was used to demonstrate that CD11c+ cells exited the brain and traveled to the ileum carrying brain derived human aSyn, suggesting that aSyn can be trafficked humorally between the brain and gut (**Figure 8**) [105]. CD11c+ cell populations interact intimately with enteric neurons and glial cells and have numerous neuropeptide receptors[106-108]. Peripheral immune populations could therefore serve as an enteric neuropeptide modifiable population with capacity to transport aSyn systemically.

[3]Templeton HA, Tobet SA & Schwerdtfeger LA. Gut Neuropeptide Involvement in Parkinson's Disease. American *Journal of Physiology Gastrointestinal and Liver Physiology. Under Review.*

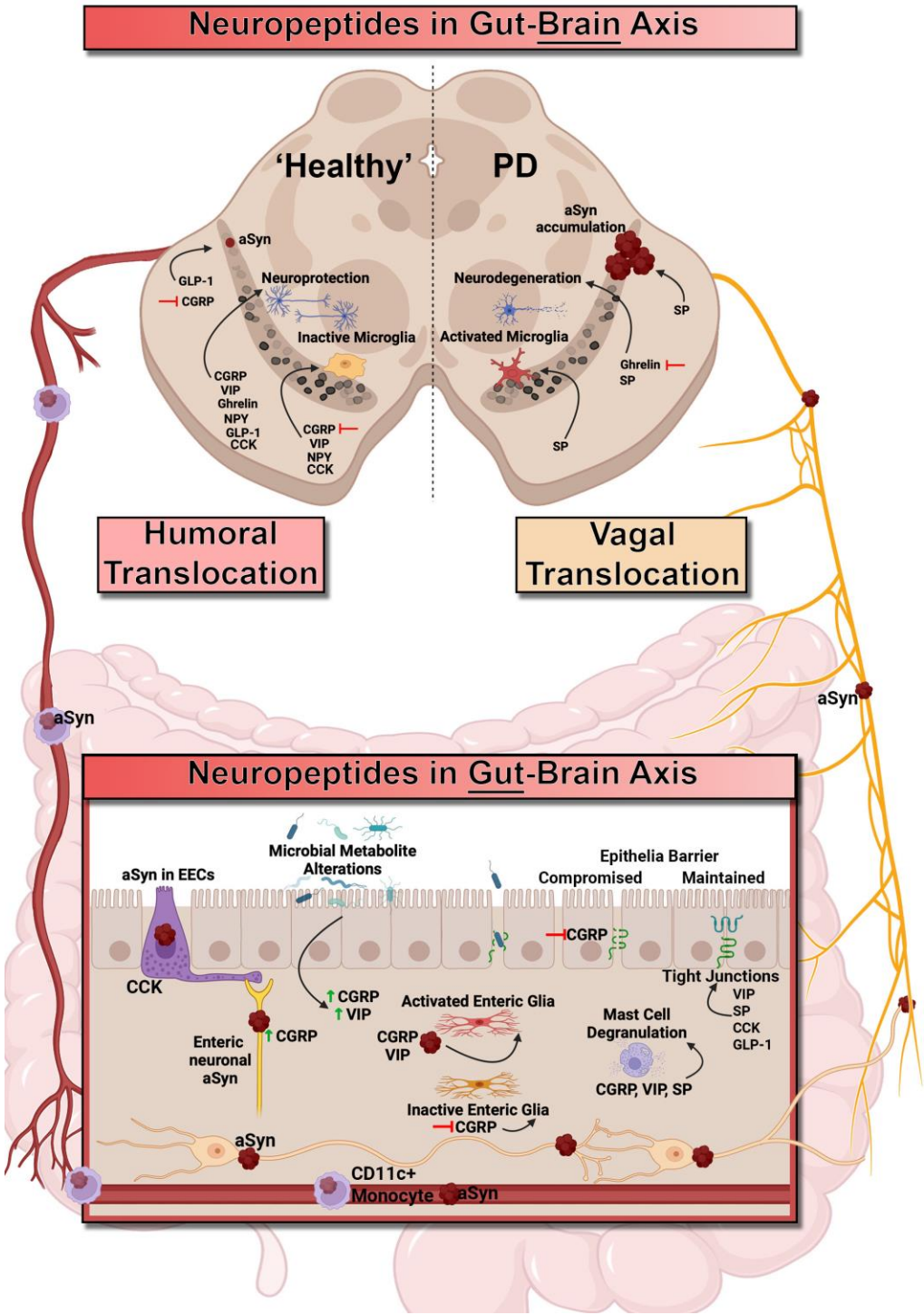

Figure 8. Schematic representation of gut-brain signaling involvement in Parkinson's disease within the context of neuropeptides.

[3]Templeton HA, Tobet SA & Schwerdtfeger LA. Gut Neuropeptide Involvement in Parkinson's Disease. American *Journal of Physiology Gastrointestinal and Liver Physiology. Under Review.*

Neuropeptides and the Gut-Brain Axis

Neuropeptides regulate a diverse array of physiological processes and are key players in nervous system signaling with peripheral organs. Neuropeptides can serve as neurotransmitters to exert local effects in the gut, act as neuromodulators to influence CNS regulatory centers and as hormones impacting the immune system throughout the body[109]. Dysregulation of neuropeptide synthesis and secretion have been linked to various gastrointestinal disorders including irritable bowel syndrome (IBS) and inflammatory bowel disease (IBD)[110-112]. Similarly, neuropeptide dysregulation plays an important role in the development and/or neuroprotection of CNS PD pathology[20]. Neuropeptides including SP, VIP, and CGRP have been implicated in the pathophysiology of PD and its GI symptoms[113-119]. All three of these neuropeptides influence motility and epithelial cell secretion in the GI tract, and dysregulation of their secretion or synthesis can contribute to symptoms like constipation, gastroparesis, and abdominal pain, which are common in PD subjects[120-129]. In addition to these roles, neuropeptides regulate immune cell differentiation and cytokine production. CGRP, SP, and VIP can either enhance or suppress the activity of several immune cells including, T cells, B cells, macrophages, and mast cells to increase or decrease cytokine production, immune cell migration, proliferation, or maturation[130-134]. Appropriate neuropeptide immune signaling ensures an appropriate immune response while preventing excessive inflammation[82-84,135]. Neuropeptides also contribute to maintenance of the intestinal epithelial barrier by regulating cell proliferation, migration, and repair[75-80,136]. Together, these neuropeptides play an important role in homeostasis of immune, neuronal, and epithelial processes. Disruption in neuropeptide function, particularly in the enteric system, may be a key factor in the pathophysiology of PD (**Figure 9, Table 2**).

[3]Templeton HA, Tobet SA & Schwerdtfeger LA. Gut Neuropeptide Involvement in Parkinson's Disease. American *Journal of Physiology Gastrointestinal and Liver Physiology. Under Review*.

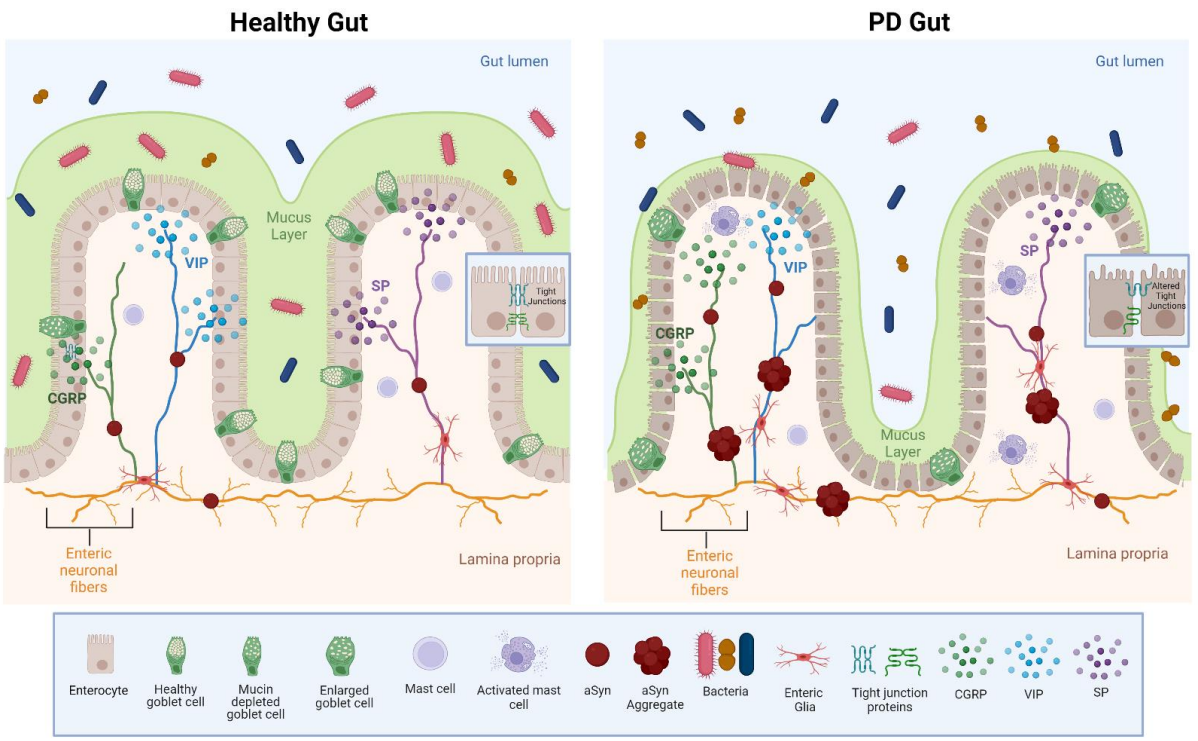

Figure 9. Schematic representation of neuropeptide signaling in healthy versus Parkinson's Disease gut wall. Created with BioRender.

Calcitonin Gene Related Peptide (CGRP)

CGRP is a 37 amino acid peptide that has several functions in the gut involving nociception, gastric acid secretion, vasodilation, and regulating motility[125]. Along with its diverse functions in the gut, CGRP plays a role in migraines with elevated serum CGRP levels during migraine attack[126,137,138]. Migraine is associated with GI comorbidities such as nausea and vomiting, and anti-CGRP therapies for migraine have side effects of constipation and nausea[125]. Migraine is connected to PD, with migraine subjects at a greater risk of developing PD[123,126,127]. Centrally, CGRP receptors are often localized on dopaminergic neurons[139] and when administered directly into the rat brain regions including, the ventral tegmental area and lateral ventricles, CGRP

[3]Templeton HA, Tobet SA & Schwerdtfeger LA. Gut Neuropeptide Involvement in Parkinson's Disease. American *Journal of Physiology Gastrointestinal and Liver Physiology. Under Review.*

affects dopamine release and metabolism in several brain regions including the SN and striatum[140,141]. In addition, CGRP reduced MPP+ induced mitochondrial toxicity and protected a midbrain subpopulation of cultured immature dopamine cells while CGRP reduced mitochondrial toxicity of aSyn overexpressing cells PC12-aSyn cells[114]. Peripherally, intraperitoneal injections of a CGRP receptor antagonist BIBN 4096 BS in a 5XFAD mouse model of Alzheimer's Disease (AD) decreased aSyn levels in the whole brain homogenates and reduced markers of neuroinflammation in the p38 MAPK and NFkB signaling pathways[113] indicating that CGRP likely plays a role in modulation of PD neuroinflammation. Furthermore, BIBN reduced neuronally driven mast cell degranulation in co-cultures of human submucosal plexus neurons with mast cells[142]. These results suggest that CGRP may promote aSyn accumulation and subsequent PD pathology, however a potential protective effect of the neuropeptide in adult dopamine neurons in vivo cannot be ruled out.

Vasoactive Intestinal Peptide (VIP) and Pituitary Adenylate Cyclase Activating Polypeptide (PACAP)

VIP and PACAP are vasoactive peptides with substantial sequence homology[143] that bind to vasoactive intestinal peptide (VPAC) receptors 1 and 2[144], with minor differential functional capacity based on peptide or PACAP isoform[145]. In the gut, VIP is involved in vasodilation[146], intestinal contractility[128], inflammation[82], nociception[120], gastric acid secretion[121] and regulation of goblet cell proliferation[76]. Both VIP and PACAP have neuroprotective and immunomodulatory properties in the CNS[147-150] and the intestine[151]. In an MPTP model of PD, administration of VIP decreased MPTP induced dopaminergic neuronal loss and prevented activation of microglia in the SNpc, suggesting a neuroprotective role[152]. Similar effects were seen in the 6-OHDA rat

[3]Templeton HA, Tobet SA & Schwerdtfeger LA. Gut Neuropeptide Involvement in Parkinson's Disease. American *Journal of Physiology Gastrointestinal and Liver Physiology. Under Review*.

model of PD where intraperitoneal VIP injections resulted in increased tyrosine hydroxylase (TH) neuron counts and spine density in the striatum[23]. PACAP pretreatment in the substantia nigra protected dopaminergic neurons in a 6-OHDA model of PD[115] and intravenous PACAP treatment following paraquat toxicity recovered paraquat induced TH neuronal loss[116]. Neurotoxic models of PD result in central dopaminergic denervation often associated with impairment of GI motility[153-155] suggesting that central dopaminergic cell loss may result in neurochemical changes affecting the ENS. Additionally, PD patients experiencing chronic constipation have decreased expression of VIP in submucosal neurons compared to healthy controls[156]. In the distal ileum and proximal colon, 6-OHDA treatment resulted in elevated nNOS immunoreactive neuron populations[157] an effect in a subpopulation of nNOS cells that co-express VIP/PACAP in myenteric neurons. This study did not observe any effect of 6-OHDA treatment on myenteric ChAT immunoreactive neurons[158], pointing to enteric neurons as primary targets rather than vagal. These neuropeptide effects were concurrent with decreased colonic motility in 6-OHDA treated rats and points towards local enteric nervous alterations with regional specificity in PD models.

Substance P (SP)

Similarly to CGRP and VIP, SP is involved in modulation of GI motility, inflammation, and nociception[124]. SP plays a role in inflammatory bowel disease and migraine that have been implicated in PD[124,159]. In the brain, the substantia nigra contains the highest immunoreactive density of SP neurons particularly in axon terminals that are presynaptic to dopaminergic neurons[160,161] with cell bodies likely located in the striatum and globus pallidus[162-166]. Postmortem analysis of PD brain samples revealed significantly reduced levels of SP[117].

[3]Templeton HA, Tobet SA & Schwerdtfeger LA. Gut Neuropeptide Involvement in Parkinson's Disease. American *Journal of Physiology Gastrointestinal and Liver Physiology. Under Review.*

Whether this was due to targeted SP neuronal death or coincident with overall cell death in the SN is unclear. In contrast, a 6-OHDA rat model of PD revealed that loss of dopaminergic neurons resulted in increased baseline extracellular levels of SP in the substantia nigra reticulata, suggesting that SP may be released from striatonigral SP endings in response to loss of target dopaminergic neurons in the substantia nigra[118] Following intra-striatal 6-OHDA lesions, nigral SP content increased along with activation of microglia and astrocytes, and breakdown of the BBB. This effect was further exacerbated with intra-striatal SP but was reduced with the NK1 receptor agonists N-acetyl-L-tryptophan or L-333,060. These results suggest that SP induced neurogenic inflammation contributes to dopaminergic degeneration[167]. In PD subjects, aggregates of aSyn in the GI tract and DMV are often co-localized with SP, suggesting that SP-positive neurons are peripheral sites of degeneration[168]. Serum SP is elevated in PD subjects and increased with severity of motor impairments[119]. SP has been shown to increase in serum and brain tissue during CNS neuroinflammatory events[169-171] and during GI inflammation in conditions such as ulcerative colitis and inflammatory bowel disease[83]. Following 6-OHDA intranigral injection, myenteric plexus SP increased in the rat colon associated with enhancement of tachykininergic motility. Additionally, there was an increase in inflammatory processes including infiltration of eosinophils and mast cells, and elevated tumor necrosis factor-a (TNFa) and IL-1b in colonic tissue, indicating that central nigrostriatal dopaminergic degeneration is followed by bowel inflammation associated with increased myenteric SP[172]. Few studies have shown the anatomic localization of aSyn in enteric neuronal populations in humans. One investigation demonstrated that a vast majority of SP immunoreactive cells in guinea pig and human colon that contained aSyn were also reactive for the vesicular acetylcholine transporter (VAChT)[173]. This suggests that enteric SP producing

[3]Templeton HA, Tobet SA & Schwerdtfeger LA. Gut Neuropeptide Involvement in Parkinson's Disease. American *Journal of Physiology Gastrointestinal and Liver Physiology. Under Review.*

VAChT neurons are targeted by aSyn accumulation making them vulnerable in PD. Together, the increase of SP in CNS and PNS inflammatory events may play a role in PD neurodegeneration with high potential for central mechanisms to dominate.

Ghrelin

Ghrelin, a hormone primarily produced by the stomach, is most well-known for its role in stimulation of appetite[174,175]. That said, Ghrelin also regulates gastrointestinal motility[176] and gastric acid secretion[177] and may have a neuroprotective role in the context of PD. Levels of active (acylated) and total ghrelin are lower during fasting in PD subjects compared to healthy controls[178]. In the A53T human aSyn transgenic mouse model, loss of cholinergic neurons in the DMV was accompanied by reduced plasma ghrelin levels, a decreased gastric emptying rate, and small intestinal propulsion rate, suggesting PD GI dysfunction may be associated with reduced ghrelin levels[179]. Furthermore, administration of acylated ghrelin attenuated MPTP induced decreases in TH neuronal number and volume in the nigrostriatal pathway[180], limited striatal dopamine depletion[181], and improved motor performance on the rotarod[182]. Similar protective effects were seen in a rotenone model, where ghrelin counteracted rotenone-induced nigrostriatal dopaminergic cell loss[183,184]. Genetic ablation of the ghrelin receptor, growth hormone secretagogue receptor (GHSR), exacerbated nigral dopaminergic neuronal loss and reduced striatal dopamine levels following MPTP treatment[181]. Injection of GSHR into the substantia nigra of wildtype mice produced PD-like dysfunction in motor coordination[185]. These studies point towards lowered levels of ghrelin being involved in dopaminergic cell loss in nigrostriatal pathways in PD as well as regulating GI dysfunction, likely driven by cholinergic neuronal loss in the DMV.

[3]Templeton HA, Tobet SA & Schwerdtfeger LA. Gut Neuropeptide Involvement in Parkinson's Disease. American *Journal of Physiology Gastrointestinal and Liver Physiology. Under Review.*

Neuropeptide Y (NPY)

NPY is widely distributed throughout the central and peripheral nervous systems and is expressed by a majority of enteric neurons with routine co-expression with VIP and nNOS[186]. Antagonizing NPY receptors (Y_1 and Y_2) results in reduced colonic motility and elevated electrolyte secretion[187]. NPY and other Y receptor binding peptides (e.g., peptide YY) can also modulate mucosal IgA+ lymphocyte response to LPS[188]. In the CNS, NPY can modulate neurogenesis[189-191] and neurotransmitter release[192,193], two potentially protective pathways in PD. In support of this, cerebrospinal fluid of PD subjects had lower NPY levels than healthy controls[194]. Human PD brains showed increases in NPY mRNA expression in striatal brain regions, but it is unclear if elevated expression was due to disease progression or a result of drug treatment[195].This elevation of NPY induces the loss of neurons in the nigro-striatal dopamine pathway[196,197], supported by the 6-OHDA toxicity models in which NPY preserved dopaminergic neurons of the nigrostriatal pathway[198] and inhibited microglia activation[199].

Glucagon-Like Peptide-1 (GLP-1)

GLP-1 is a peptide hormone produced and released from intestinal L-cells to help regulate blood sugar, slows gastric emptying, and suppresses appetite[200]. Emerging evidence suggests that GLP-1 may have a neuroprotective role in PD. Administration of GLP-1 and a GLP-1 agonist, exendin-4 (Ex-4), into the left ventricle of MPTP treated mice resulted in improved motor function, preserved numbers of TH+ cells in the SN, and preserved levels of dopamine and metabolite ratios in the SN[201]. Additionally, treatment with GLP-1 receptor agonist liraglutide attenuated MPTP dyskinesia and preserved TH expression in SN[202], suggesting that increased central GLP-1 may protect against nigrostriatal dopaminergic loss. In contrast, following

[3]Templeton HA, Tobet SA & Schwerdtfeger LA. Gut Neuropeptide Involvement in Parkinson's Disease. American *Journal of Physiology Gastrointestinal and Liver Physiology. Under Review.*

treatment with the GLP-1 analogue, exenatide, mice with olfactory bulb injections of aSyn pre-formed fibrils had increases in pathological aSyn and activated microglia in the anterior olfactory nucleus and the perirhinal cortex[203] (Bergkvist et al., 2023). However, when pre-formed fibrils were injected into the striatum, treatment with GLP-1 agonist NLY01 resulted in decreased phosphorylated aSyn and increased TH+ neurons in the substantia nigra[204]. These findings indicate that the location of neuronal insult and GLP-1 analogue likely influence whether GLP-1 will exhibit neuroprotective or neurodegenerative properties. In further support of a neuroprotective role for GLP-1, human neuroblastoma cells treated with MPP+ and then exposed to GLP-1 and GLP-2 (teduglutide) agonists were protected from MMP+ mitochondrial damage[205]. GLP-1 may also play a protective role in the gut. When exposed to MPTP, a mouse strain that received oral administration of an engineered strain of commensal bacteria to continually express GLP-1, MG1363-pMG36e-GLP-1, exhibited reductions in locomotor impairments, suppressed microglia activation, and increased TH+ neurons.[206]. Following intraperitoneal injection with a GLP-1 analogue, Liraglutide, MPTP treated mice and A53T$^{(+/-)}$ mice had restored levels of colonic tight junction proteins occludin and ZO-1, decreased levels of inflammatory markers such as inducible nitric oxide synthase (iNOS) and TNFa, reduction in colonic aSyn, and decreased loss of colonic TH+ neurons[207]. These results suggest that GLP-1 plays a role in intestinal barrier regulation and mucosal immunity, two common readouts seen in PD subjects. Compared to household controls, PD patients exhibited diminished GLP-1 secretion in response to a meal[208] suggesting that enteric GLP-1 secretion may be decreased in PD patients, yet causal factors driving this alteration remain to be seen.

[3]Templeton HA, Tobet SA & Schwerdtfeger LA. Gut Neuropeptide Involvement in Parkinson's Disease. American *Journal of Physiology Gastrointestinal and Liver Physiology. Under Review.*

Cholecystokinin (CCK)

CCK is produced and secreted by intestinal I cells to stimulate gallbladder contraction and pancreatic secretion aiding in digestion[209]. Additionally, CCK is expressed in dopaminergic neurons of the substantia nigra.[210] Administration of the CCK analogue, liraglutide restored TH+ neuron number and decreased glial activation in the substantia nigra in MPTP treated mice[211]. It has been proposed that CCK may have neuroprotective effects in PD and is increased following L-DOPA treatment. When 6-ODHA lesioned rats were treated with prolonged L-DOPA, CCK levels measured by radioimmunoassay (RIA) were increased in the striatum and substantia nigra[212]. Additionally, following 6-OHDA lesioning, two peptides derived from CCK precursors were increased in the lesioned side of L-DOPA treated brains[213]. CCK has also been shown to play a critical role in regulation of the intestinal barrier and mucosal inflammatory response. Rats pre-treated with CCK prior to LPS administration exhibited increased expression of colonic tight junction proteins occludin, claudin-1, and junctional adhesion molecule (JAM-A) and decreased production of mucosal pro-inflammatory cytokines TNF-α, IL-1β, IL-6 and IFN-γ[214]. In two models of PD, MPTP treatment and A53T$^{(+/-)}$ mice, intraperitoneal injection of a CCK analogue resulted in restored levels of colonic tight junction proteins occludin and ZO-1, decreased levels of inflammatory markers such as inducible nitric oxide synthase (iNOS) and TNFa, reduction in colonic aSyn, and decreased loss of colonic TH+ neurons[207]. Additionally, chronic injection of MPTP resulted in mRNA and protein levels of CCK to be significantly decreased in mouse colon compared to vehicle-treated group suggesting that decreased enteric CCK is associated with PD pathology[215].

[3]Templeton HA, Tobet SA & Schwerdtfeger LA. Gut Neuropeptide Involvement in Parkinson's Disease. American *Journal of Physiology Gastrointestinal and Liver Physiology. Under Review.*

Table 2. Neuropeptides reported to have CNS and/or gut effects.

Neuropeptide	Biological Sample	Direction	Main CNS Effect	Main Gut Effect	CNS Reference	Gut Reference
CGRP	Human saliva, plasma, tear fluid, CSF	⇧	Neurogenic inflammation of dura and increased migraine symptoms	Diarrhea, vomiting, nausea, stomach pain	Durham, 2006 Scher et al., 2014 Allani et al., 2022 Goadsby and Edvinsson, 1990 Cady et al., 2009 Kamm et al., 2019 Van Dongen et al., 2017	Falkenberg et al., 2020
	Human plasma	⇩	Migraine symptoms resolve	Constipation	Juhasz et al., 2005	Holzer and Holzer-Petsche, 2021
	Mouse brain, serum, intestine	⇩	Decreased aSyn and neuroinflammation	Decreased barrier integrity	Na et al., 2022	Ning et al., 2023
VIP	Mouse brain, intestine	⇧	Increased TH neuron counts and spine density in striatum. Reduced dopaminergic cell loss in SNpc	Ameliorated colitis induced epithelial damage	Korkmaz et al., 2012	Conlin et al., 2009
	Mouse intestine	⇩	NA	Reduced goblet cell quantities and proliferation	Delgado and Ganea, 2003	Schwerdtfeger and Tobet, 2020 Wu et al., 2015
SP	Human serum	⇧	Increased motor impairment	NA	Schirinzi et al., 2021	
	Mouse brain and intestine	⇧	NA	Protective in colitis - prevents decrease of ZO-1		Hwang et al., 2017

Neuropeptide Influence on Enteric Neuroepithelial Components of Disease

The gut mucosa is in constant contact with the external environment. For this reason, the gut has a formidable intestinal barrier to protect the body from pathogens and external toxins, while retaining its primary function of digestion and absorption of nutrients. Epithelial cells of the gut physically separate luminal contents from the underlying lamina propria through a layer of mucus and interepithelial tight junctions[216]. Specialized epithelial cells, known as goblet cells, produce and secrete mucin core proteins bound to a complex of glycosaminoglycans[76], creating a mucus layer that prevents luminal microbiota and contents from passively reaching the epithelial barrier. Together the mucus layer and epithelial barrier regulate entry into underlying gut wall tissue. Enteric neuropeptides help to ensure tight regulation of this barrier through modulation of epithelial cell secretion[75,76] and tight junction protein regulation[77-80].

Dysregulation of gut barrier integrity has been described in PD subjects and multiple animal models and may contribute to disease progression. Increased intestinal

[3]Templeton HA, Tobet SA & Schwerdtfeger LA. Gut Neuropeptide Involvement in Parkinson's Disease. American *Journal of Physiology Gastrointestinal and Liver Physiology. Under Review.*

permeability[217,218] and barrier structural alterations[219] have been correlated with increased mucosal aSyn[15]. Similar findings were reported when intraperitoneal injections of lipopolysaccharide (LPS), a classic means for barrier disruption[220], increased intestinal permeability and aSyn immunoreactivity in mouse colon, mirroring conditions seen in PD subjects[221]. Murine rotenone models of PD have shown increased aSyn in the myenteric plexus as well as revealed increased intestinal permeability, decreased tight junction expression[222] and alterations in goblet cell size and number[28]. Neuropeptides play a significant role in regulation of the intestinal barrier and many PD subjects exhibit abnormal expression of both central and peripheral neuropeptides suggesting that alterations in enteric neuropeptides may contribute to neuroepithelial GI pathology associated with PD.

Enteric neuropeptides regulate epithelial cell functions ranging from proliferation, response to damage, and secretion. Recently, a study demonstrated that Designer Receptor Exclusively Activated by Designer Drugs (DREADD) activation of CGRP nociceptor Nav1.8 fibers stimulated mucin release from goblet cells resulting in thickening of the mucus layer[75]. However, a CGRP receptor antagonist, BIBN4096, did not completely prevent mucus emptying from goblet cells suggesting that mucin release from goblet cells is not solely mediated by CGRP. Nociceptive Nav1.8+ neurons also express VIP and SP that have been shown to communicate with goblet cells. Proliferation of goblet cells is regulated by VIP, and antagonizing VIP receptors leads to decreased goblet cell proliferation in the mouse ileum[76]. Mice deficient in VIP (VIPKO) also exhibit a reduction in goblet cell quantities and show defects in overall epithelial cell proliferation and migration, with increased barrier permeability[136]. SP is also involved in epithelial cell proliferation and migration and SP stimulation of cultured rat epithelial

[3]Templeton HA, Tobet SA & Schwerdtfeger LA. Gut Neuropeptide Involvement in Parkinson's Disease. American *Journal of Physiology Gastrointestinal and Liver Physiology. Under Review*.

cells (IEC-6 cells) increased epithelial migration, an effect that was blocked by a SP receptor antagonist, Neurokinin receptor 1 (NK1R)[223].

Along with influencing epithelial cell function, several neuropeptides regulate tight junction and epithelial barrier permeability. Transmembrane tight junction proteins like occludins and claudins anchor barrier epithelial cells close together, while cytoplasmic proteins including zona occludens (ZO)-1, -2, and -3, link tight junctions to intracellular machinery ensuring structural and functional connectivity[224]. Immunohistochemistry and western blots of colonic biopsies from PD subjects showed abnormal distribution and decreased expression of occludin and ZO-1[219,225]. Rotenone models develop increased barrier permeability, due in part to decreased expression of colonic ZO-1, occludin, and claudin-1[222,226] and altered to goblet cell morphology[28]. VIP is involved in modulation of several enteric tight junction proteins and treating a colonic epithelial and neuronal co-culture with VIP led to an increase in ZO-1 expression[78]. Following in vivo *Citrobacter rodentium* induced colitis, intraperitoneal injections of VIP ameliorated colitis induced epithelial damage, rescuing epithelial cell and ZO1 disruption, suggesting a regulatory role of VIP in epithelial barrier permeability[77]. Conversely, CGRP knockout mice show a damaged intestinal barrier with decreased tight junction protein levels after LPS treatment[79]. In a dextran sodium sulfate (DSS) induced mouse model of colitis, intravenous injections of SP rescued the decreased ZO-1 expression observed in vehicle treated animals[80] indicating a protective role of SP. Together, VIP, CGRP, and SP are among the more well investigated and important enteric neuropeptides that work to maintain a healthy gut barrier, a critical function with pathogenic implications for GI symptomology in PD subjects and associated cellular and cytokine inflammatory profiles.

[3]Templeton HA, Tobet SA & Schwerdtfeger LA. Gut Neuropeptide Involvement in Parkinson's Disease. American *Journal of Physiology Gastrointestinal and Liver Physiology. Under Review.*

Neuropeptide Influence on Enteric Immune Components of Disease

PD is a multi-system disorder, not restricted to the CNS, irrespective of whether its origin is in the brain or periphery[227-230]. Accumulating evidence in support of this points towards peripheral and CNS immune activation and inflammation as actively contributing to neurodegeneration[231]. The mucosal immune system of the GI tract is a key regulator of peripheral immune response to environmental and microbial analytes and signals bi-directionally with the enteric nervous system[132,232,233]. Peripheral nerves play an active role in modulating immune responses and the pathology of inflammatory diseases. Neuropeptides released from enteric sensory nerves can influence mast cell activation, vascular responses[133,134], neutrophil chemotaxis[130], and T helper cell differentiation[131]. These neuropeptide-induced responses, which resemble inflammatory reactions, have been termed "neurogenic inflammation"[135]. Gut inflammation has been reported in subjects with PD, and those with inflammatory bowel disease (IBD) are at greater risk of developing PD[234,235]. Fibrils or aSyn activate monocytes and microglial cells, triggering expression of MHCII[231,236]. Given that dysregulated immune signaling is central to IBD[237] and changes in neuropeptides have been linked to IBD and PD, it is possible that chronic gut inflammation is involved in aSyn pathology in CNS and PNS neurons. Further supporting this, intestinal resident Th17 cells with stem-like properties can differentiate into a more pathogenic phenotype and migrate centrally[238], and pathogenicity of gut Th17 cells can be modulated by microbial metabolites[239]. Enteric neuronal fibers and enteric glia directly interact with lamina propria immune cells, including mast cells[132], and B- and T- cells[240,241], among others. Dysregulation of several neuropeptides including CGRP[81], VIP[82], and SP[83,84] have been linked to intestinal inflammation and CNS alterations in PD, but their exact roles in neurodegenerative disorders remain largely unexplored.

[3]Templeton HA, Tobet SA & Schwerdtfeger LA. Gut Neuropeptide Involvement in Parkinson's Disease. American *Journal of Physiology Gastrointestinal and Liver Physiology. Under Review.*

Nociceptive neurons, many of which produce multiple neuropeptides, are likely involved in the GI inflammation seen in PD. Diverse immune populations express neuropeptide receptors including receptor activity modifying protein 1 (RAMP1) and calcitonin-like binding receptor (CLR), VIP receptors including VPAC1/2, and the SP receptor NK1R. Expression of these neuropeptide receptors is common in peripheral and central immune populations including on mast cells[242], T and B lymphocytes[243], macrophages[244], and microglia[245]. Alterations in CGRP have been closely linked to various disease states that are strongly associated with PD, including IBD[81], migraine[246], and increased enteric and CNS aSyn[28,113]. There are two forms of CGRP, αCGRP and βCGRP, which share ~90% sequence homology. The biological activity of the two isoforms is nearly identical[247], however αCGRP predominates in sensory nerves while βCGRP predominates in motor neurons[248,249]. Importantly, both CGRP isoforms utilize the same receptors which are found in the brain and intestines. Migraine subjects are at greater risk of developing PD[123,126,127], and biofluid CGRP levels are elevated[246,250-253] during migraine attacks. Increased CGRP during migraine likely leads to neurogenic inflammation by triggering mast cells leading to increased vasodilation of the dura[254]. Most CGRP therapies for migraine have poor blood brain barrier permeability, further supporting a peripheral role of CGRP in migraine[255] and anti-CGRP therapeutic related constipation and other GI symptoms[122,129]. In a rotenone model of PD, increased αCGRP immunoreactivity was observed in apical colonic crypts along with elevated aSyn levels in αCGRP+ neurons and fibers, suggesting that enteric αCGRP dysregulation may contribute to aSyn aggregation[28]. CGRP antagonists decreased neuroinflammation and aSyn aggregation in mouse brain, further supporting a role of CGRP in PD pathophysiology[113,256].

[3]Templeton HA, Tobet SA & Schwerdtfeger LA. Gut Neuropeptide Involvement in Parkinson's Disease. American *Journal of Physiology Gastrointestinal and Liver Physiology. Under Review*.

Mast cells are granulated tissue-resident cells that are upregulated in the colonic mucosa of IBS subjects[257] and may drive metabolic alterations in degenerating neurons in the PD brain[258]. Mast cells are distributed throughout the GI mucosa where they have a close anatomical association with nerve endings from sensory and autonomic neurons forming a bi-directional communication network between the gut and CNS[132,259,260]. Upon CGRP, VIP, or SP binding, mast cells degranulate, releasing inflammatory mediators such as histamine, tryptase, and serotonin. In turn, sensory neurons produce CGRP, VIP, and SP promoting mast cell activation in a positive feedback loop[261]. Histamine is involved in local immune responses to attract other immune cells and acts as a neurotransmitter in the CNS. PD subjects have higher levels of histamine in brain[262], blood[263], and cerebral spinal fluid (CSF)[264]. When PD subjects were given a histamine receptor antagonist, nizatidine, symptoms of functional dyspepsia were improved[265] and gastric emptying was significantly shortened improving gastroparesis[266]. Histamine likely plays a role in PD immune pathology, even if this increase is secondary to the primary immune pathogenic route.

Microglia have emerged as key players in PD neuroinflammation and disease progression[267-272]. Microglia have CGRP[245], VIP[273,274], and SP[171] receptors, and are CNS immune sentinels which release inflammatory mediators (e.g. TNF-α, IL-1B, IL-6) in response to insult or pathologic agents. aSyn fibrils can initiate microglial/macrophage activation and microgliosis in the peripheral and central immune systems[231,236] likely driving tissue damage, neuroinflammation, and subsequent neurodegeneration[236]. The brains of PD subjects have increased levels of activated microglia in areas with increased pathologic aSyn[275] and it is plausible that neuropeptides may exert neuroprotective or neurotoxic effects through microglia. In murine models, VIP[152] and CGRP[276] inhibited the production of LPS-induced TNF-α, nitric

[3]Templeton HA, Tobet SA & Schwerdtfeger LA. Gut Neuropeptide Involvement in Parkinson's Disease. American *Journal of Physiology Gastrointestinal and Liver Physiology. Under Review.*

oxide, and IL-6 from microglia. Furthermore, CGRP is strongly linked to increased pain sensitivity and administration of CGRP stimulated spinal cord microglia[251] while antagonizing CGRP reduced anatomical appearance of microglial activation[277]. Administration of SP to MPP+ or LPS midbrain neuron-glia co-cultures enhanced microglial activation potentially enhancing neurotoxicity of dopaminergic neurons in the brain[278]. Enteric neuropeptides such as CGRP, VIP, and SP and their receptors play a significant role in modulating immune cell and epithelial barrier function in health and disease.

Conclusions

Gut neuropeptides play a significant role in PD through their involvement in the regulation of GI function and neuro-immune activation. Key neuropeptides such as SP, VIP, and CGRP are implicated in the pathophysiology of PD and in exacerbation of PD related GI symptoms. These neuropeptides influence the motility and function of the GI tract, and their dysregulation can contribute to constipation, gastroparesis, and abdominal pain, common complaints among PD subjects, and in particular women with the disease. Changes in neuropeptide signaling may impact the neuroinflammatory processes associated with PD, potentially exacerbating disease progression and affecting the overall management of the condition. Understanding the role of gut neuropeptides in PD can provide insights into novel therapeutic approaches aimed at alleviating GI symptoms and possibly modifying disease progression.

[3]Templeton HA, Tobet SA & Schwerdtfeger LA. Gut Neuropeptide Involvement in Parkinson's Disease. American *Journal of Physiology Gastrointestinal and Liver Physiology. Under Review*.

References

1 Marras, C. *et al.* Prevalence of Parkinson's disease across North America. *NPJ Parkinsons Dis* **4**, 21 (2018). https://doi.org:10.1038/s41531-018-0058-0

2 Poewe, W. *et al.* Parkinson disease. *Nat Rev Dis Primers* **3**, 17013 (2017). https://doi.org:10.1038/nrdp.2017.13

3 Berardelli, A., Rothwell, J. C., Thompson, P. D. & Hallett, M. Pathophysiology of bradykinesia in Parkinson's disease. *Brain* **124**, 2131-2146 (2001). https://doi.org:10.1093/brain/124.11.2131

4 Kalia, L. V. & Lang, A. E. Parkinson's disease. *Lancet* **386**, 896-912 (2015). https://doi.org:10.1016/S0140-6736(14)61393-3

5 Stefanis, L. alpha-Synuclein in Parkinson's disease. *Cold Spring Harb Perspect Med* **2**, a009399 (2012). https://doi.org:10.1101/cshperspect.a009399

6 Kouli, A., Torsney, K. M. & Kuan, W. L. in *Parkinson's Disease: Pathogenesis and Clinical Aspects* (eds T. B. Stoker & J. C. Greenland) (2018).

7 Berg, D. *et al.* Prodromal Parkinson disease subtypes - key to understanding heterogeneity. *Nat Rev Neurol* **17**, 349-361 (2021). https://doi.org:10.1038/s41582-021-00486-9

8 de Lau, L. M. & Breteler, M. M. Epidemiology of Parkinson's disease. *Lancet Neurol* **5**, 525-535 (2006). https://doi.org:10.1016/S1474-4422(06)70471-9

9 Fasano, A., Visanji, N. P., Liu, L. W., Lang, A. E. & Pfeiffer, R. F. Gastrointestinal dysfunction in Parkinson's disease. *Lancet Neurol* **14**, 625-639 (2015). https://doi.org:10.1016/S1474-4422(15)00007-1

10 Travagli, R. A., Browning, K. N. & Camilleri, M. Parkinson disease and the gut: new insights into pathogenesis and clinical relevance. *Nat Rev Gastroenterol Hepatol* **17**, 673-685 (2020). https://doi.org:10.1038/s41575-020-0339-z

11 Valkovic, P. *et al.* Pain in Parkinson's Disease: A Cross-Sectional Study of Its Prevalence, Types, and Relationship to Depression and Quality of Life. *PLoS One* **10**, e0136541 (2015). https://doi.org:10.1371/journal.pone.0136541

12 Jones, J. D., Rahmani, E., Garcia, E. & Jacobs, J. P. Gastrointestinal symptoms are predictive of trajectories of cognitive functioning in de novo Parkinson's disease. *Parkinsonism Relat Disord* **72**, 7-12 (2020). https://doi.org:10.1016/j.parkreldis.2020.01.009

13 Schwerdtfeger, L. A. *et al.* Akkermansia mono-colonization modulates microglia and astrocytes in a strain specific manner. *J Neuroinflammation* **22**, 94 (2025). https://doi.org:10.1186/s12974-025-03417-3

14 Dumitrescu, L. *et al.* Serum and Fecal Markers of Intestinal Inflammation and Intestinal Barrier Permeability Are Elevated in Parkinson's Disease. *Front Neurosci* **15**, 689723 (2021). https://doi.org:10.3389/fnins.2021.689723

15 Forsyth, C. B. *et al.* Increased intestinal permeability correlates with sigmoid mucosa alpha-synuclein staining and endotoxin exposure markers in early Parkinson's disease. *PLoS One* **6**, e28032 (2011). https://doi.org:10.1371/journal.pone.0028032

16 Van Den Berge, N. *et al.* Evidence for bidirectional and trans-synaptic parasympathetic and sympathetic propagation of alpha-synuclein in rats. *Acta Neuropathol* **138**, 535-550 (2019). https://doi.org:10.1007/s00401-019-02040-w

17 Wang, K. *et al.* Gut dysfunction may be the source of pathological aggregation of alpha-synuclein in the central nervous system through Paraquat exposure in mice. *Ecotoxicol Environ Saf* **246**, 114152 (2022). https://doi.org:10.1016/j.ecoenv.2022.114152

18 Kim, S. *et al.* Transneuronal Propagation of Pathologic alpha-Synuclein from the Gut to the Brain Models Parkinson's Disease. *Neuron* **103**, 627-641 e627 (2019). https://doi.org:10.1016/j.neuron.2019.05.035

19 Holmqvist, S. *et al.* Direct evidence of Parkinson pathology spread from the gastrointestinal tract to the brain in rats. *Acta Neuropathol* **128**, 805-820 (2014). https://doi.org:10.1007/s00401-014-1343-6

20 Tabikh, M. *et al.* Parkinson disease: Protective role and function of neuropeptides. *Peptides* **151**, 170713 (2022). https://doi.org:10.1016/j.peptides.2021.170713

21 Chen, L., Liu, C., Xue, Y. & Chen, X. Y. Several neuropeptides involved in parkinsonian neuroprotection modulate the firing properties of nigral dopaminergic neurons. *Neuropeptides* **99**, 102337 (2023). https://doi.org:10.1016/j.npep.2023.102337

22 Zheng, Y., Zhang, L., Xie, J. & Shi, L. The Emerging Role of Neuropeptides in Parkinson's Disease. *Front Aging Neurosci* **13**, 646726 (2021). https://doi.org:10.3389/fnagi.2021.646726

23 Korkmaz, O., Ay, H., Ulupinar, E. & Tuncel, N. Vasoactive intestinal peptide enhances striatal plasticity and prevents dopaminergic cell loss in Parkinsonian rats. *J Mol Neurosci* **48**, 565-573 (2012). https://doi.org:10.1007/s12031-012-9781-x

24 Svenningsson, P., Palhagen, S. & Mathe, A. A. Neuropeptide Y and Calcitonin Gene-Related Peptide in Cerebrospinal Fluid in Parkinson's Disease with Comorbid Depression versus Patients with Major Depressive Disorder. *Front Psychiatry* **8**, 102 (2017). https://doi.org:10.3389/fpsyt.2017.00102

25 Mosley, R. L. *et al.* A Synthetic Agonist to Vasoactive Intestinal Peptide Receptor-2 Induces Regulatory T Cell Neuroprotective Activities in Models of Parkinson's Disease. *Front Cell Neurosci* **13**, 421 (2019). https://doi.org:10.3389/fncel.2019.00421

26 Olson, K. E. *et al.* Selective VIP Receptor Agonists Facilitate Immune Transformation for Dopaminergic Neuroprotection in MPTP-Intoxicated Mice. *J Neurosci* **35**, 16463-16478 (2015). https://doi.org:10.1523/JNEUROSCI.2131-15.2015

27 Cannon, J. R. *et al.* A highly reproducible rotenone model of Parkinson's disease. *Neurobiol Dis* **34**, 279-290 (2009). https://doi.org:10.1016/j.nbd.2009.01.016

28 Hayley N Templeton, A. T. E., Luke A Schwerdtfeger, Julietta A Sheng, Ronald B Tjalkens, Stuart A Tobet. Sex specific effects of environmental toxin-derived alpha synuclein on enteric neuronal-epithelial interactions. *BioRxiv* (2024). https://doi.org:https://doi.org/10.1101/2024.11.27.625701

29 Ossowska, K. *et al.* A slowly developing dysfunction of dopaminergic nigrostriatal neurons induced by long-term paraquat administration in rats: an animal model of preclinical stages of Parkinson's disease? *Eur J Neurosci* **22**, 1294-1304 (2005). https://doi.org:10.1111/j.1460-9568.2005.04301.x

30 Ungerstedt, U. & Pycock, C. Functional correlates of dopamine neurotransmission. *Bull Schweiz Akad Med Wiss* **30**, 44-55 (1974).

31 Petroske, E., Meredith, G. E., Callen, S., Totterdell, S. & Lau, Y. S. Mouse model of Parkinsonism: a comparison between subacute MPTP and chronic MPTP/probenecid treatment. *Neuroscience* **106**, 589-601 (2001). https://doi.org:10.1016/s0306-4522(01)00295-0

32 Giasson, B. I. *et al.* Neuronal alpha-synucleinopathy with severe movement disorder in mice expressing A53T human alpha-synuclein. *Neuron* **34**, 521-533 (2002). https://doi.org:10.1016/s0896-6273(02)00682-7

33 Nuber, S. *et al.* Abrogating Native alpha-Synuclein Tetramers in Mice Causes a L-DOPA-Responsive Motor Syndrome Closely Resembling Parkinson's Disease. *Neuron* **100**, 75-90 e75 (2018). https://doi.org:10.1016/j.neuron.2018.09.014

34 Parkinson, J. *An Essay on the Shaking Palsy*. (Edwards & Brune Ltd., 1817).

35 in *Parkinson's Disease: Pathogenesis and Clinical Aspects* (eds T. B. Stoker & J. C. Greenland) (2018).

36 Parkes, J. D., Zilkha, K. J., Knill-Jones, R. P., Clements, P. J. & Baxter, R. L-dopa and amantadine hydrochloride in Parkinson's disease. *Int Z Klin Pharmakol Ther Toxikol* **4**, 356-360 (1971).

37 Wakabayashi, K., Takahashi, H., Takeda, S., Ohama, E. & Ikuta, F. Parkinson's disease: the presence of Lewy bodies in Auerbach's and Meissner's plexuses. *Acta Neuropathol* **76**, 217-221 (1988). https://doi.org:10.1007/BF00687767

38 Wakabayashi, K., Takahashi, H., Ohama, E. & Ikuta, F. Parkinson's disease: an immunohistochemical study of Lewy body-containing neurons in the enteric nervous system. *Acta Neuropathol* **79**, 581-583 (1990). https://doi.org:10.1007/BF00294234

39 Bushmann, M., Dobmeyer, S. M., Leeker, L. & Perlmutter, J. S. Swallowing abnormalities and their response to treatment in Parkinson's disease. *Neurology* **39**, 1309-1314 (1989). https://doi.org:10.1212/wnl.39.10.1309

40 Jost, W. H. & Schimrigk, K. Constipation in Parkinson's disease. *Klin Wochenschr* **69**, 906-909 (1991). https://doi.org:10.1007/BF01798536

41 Edwards, L., Quigley, E. M., Hofman, R. & Pfeiffer, R. F. Gastrointestinal symptoms in Parkinson disease: 18-month follow-up study. *Mov Disord* **8**, 83-86 (1993). https://doi.org:10.1002/mds.870080115

42 Braak, H., de Vos, R. A., Bohl, J. & Del Tredici, K. Gastric alpha-synuclein immunoreactive inclusions in Meissner's and Auerbach's plexuses in cases staged for Parkinson's disease-related brain pathology. *Neurosci Lett* **396**, 67-72 (2006). https://doi.org:10.1016/j.neulet.2005.11.012

43 Braak, H. *et al.* Staging of brain pathology related to sporadic Parkinson's disease. *Neurobiol Aging* **24**, 197-211 (2003). https://doi.org:10.1016/s0197-4580(02)00065-9

44 Braak, H., Rub, U., Gai, W. P. & Del Tredici, K. Idiopathic Parkinson's disease: possible routes by which vulnerable neuronal types may be subject to neuroinvasion by an unknown pathogen. *J Neural Transm (Vienna)* **110**, 517-536 (2003). https://doi.org:10.1007/s00702-002-0808-2

45 Heinzel, S. *et al.* Update of the MDS research criteria for prodromal Parkinson's disease. *Mov Disord* **34**, 1464-1470 (2019). https://doi.org:10.1002/mds.27802

46 Goldman, J. G. & Postuma, R. Premotor and nonmotor features of Parkinson's disease. *Curr Opin Neurol* **27**, 434-441 (2014). https://doi.org:10.1097/WCO.0000000000000112

47 Picillo, M. *et al.* The PRIAMO study: age- and sex-related relationship between prodromal constipation and disease phenotype in early Parkinson's disease. *J Neurol* **268**, 448-454 (2021). https://doi.org:10.1007/s00415-020-10156-3

48 Suttrup, I. & Warnecke, T. Dysphagia in Parkinson's Disease. *Dysphagia* **31**, 24-32 (2016). https://doi.org:10.1007/s00455-015-9671-9

49 Kim, J. S. & Sung, H. Y. Gastrointestinal Autonomic Dysfunction in Patients with Parkinson's Disease. *J Mov Disord* **8**, 76-82 (2015). https://doi.org:10.14802/jmd.15008

50 Edwards, L. L., Pfeiffer, R. F., Quigley, E. M., Hofman, R. & Balluff, M. Gastrointestinal symptoms in Parkinson's disease. *Mov Disord* **6**, 151-156 (1991). https://doi.org:10.1002/mds.870060211

51 Fasano, A. *et al.* The role of small intestinal bacterial overgrowth in Parkinson's disease. *Mov Disord* **28**, 1241-1249 (2013). https://doi.org:10.1002/mds.25522

52 Gabrielli, M. *et al.* Prevalence of small intestinal bacterial overgrowth in Parkinson's disease. *Mov Disord* **26**, 889-892 (2011). https://doi.org:10.1002/mds.23566

53 Russillo, M. C. *et al.* Sex Differences in Parkinson's Disease: From Bench to Bedside. *Brain Sci* **12** (2022). https://doi.org:10.3390/brainsci12070917

54 Jurado-Coronel, J. C. *et al.* Sex differences in Parkinson's disease: Features on clinical symptoms, treatment outcome, sexual hormones and genetics. *Front Neuroendocrinol* **50**, 18-30 (2018). https://doi.org:10.1016/j.yfrne.2017.09.002

55 Cattaneo, C. & Pagonabarraga, J. Sex Differences in Parkinson's Disease: A Narrative Review. *Neurol Ther* **14**, 57-70 (2025). https://doi.org:10.1007/s40120-024-00687-6

56 Gillies, G. E., Pienaar, I. S., Vohra, S. & Qamhawi, Z. Sex differences in Parkinson's disease. *Front Neuroendocrinol* **35**, 370-384 (2014). https://doi.org:10.1016/j.yfrne.2014.02.002

57 Chang, H. J. *et al.* Sex differences in gastrointestinal dysfunction among patients with Parkinson's disease. *Neurol Sci* **44**, 2375-2384 (2023). https://doi.org:10.1007/s10072-023-06710-2

58 Calabresi, P., Di Lazzaro, G., Marino, G., Campanelli, F. & Ghiglieri, V. Advances in understanding the function of alpha-synuclein: implications for Parkinson's disease. *Brain* **146**, 3587-3597 (2023). https://doi.org:10.1093/brain/awad150

59 Warnecke, T., Schafer, K. H., Claus, I., Del Tredici, K. & Jost, W. H. Gastrointestinal involvement in Parkinson's disease: pathophysiology, diagnosis, and management. *NPJ Parkinsons Dis* **8**, 31 (2022). https://doi.org:10.1038/s41531-022-00295-x

60 Wallen, Z. D. *et al.* Metagenomics of Parkinson's disease implicates the gut microbiome in multiple disease mechanisms. *Nat Commun* **13**, 6958 (2022). https://doi.org:10.1038/s41467-022-34667-x

61 Hill-Burns, E. M. *et al.* Parkinson's disease and Parkinson's disease medications have distinct signatures of the gut microbiome. *Mov Disord* **32**, 739-749 (2017). https://doi.org:10.1002/mds.26942

62 Vascellari, S. *et al.* Gut Microbiota and Metabolome Alterations Associated with Parkinson's Disease. *mSystems* **5** (2020). https://doi.org:10.1128/mSystems.00561-20

63 Scheperjans, F. *et al.* Gut microbiota are related to Parkinson's disease and clinical phenotype. *Mov Disord* **30**, 350-358 (2015). https://doi.org:10.1002/mds.26069

64 Cirstea, M. S. *et al.* Microbiota Composition and Metabolism Are Associated With Gut Function in Parkinson's Disease. *Mov Disord* **35**, 1208-1217 (2020). https://doi.org:10.1002/mds.28052

65 Shao, Y. *et al.* Comprehensive metabolic profiling of Parkinson's disease by liquid chromatography-mass spectrometry. *Mol Neurodegener* **16**, 4 (2021). https://doi.org:10.1186/s13024-021-00425-8

66 Keshavarzian, A. *et al.* Colonic bacterial composition in Parkinson's disease. *Mov Disord* **30**, 1351-1360 (2015). https://doi.org:10.1002/mds.26307

67 Palacios, N. *et al.* Metagenomics of the Gut Microbiome in Parkinson's Disease: Prodromal Changes. *Ann Neurol* **94**, 486-501 (2023). https://doi.org:10.1002/ana.26719

68 Romano, S. *et al.* Meta-analysis of the Parkinson's disease gut microbiome suggests alterations linked to intestinal inflammation. *NPJ Parkinsons Dis* **7**, 27 (2021). https://doi.org:10.1038/s41531-021-00156-z

69 Yan, Z. *et al.* Alterations of gut microbiota and metabolome with Parkinson's disease. *Microb Pathog* **160**, 105187 (2021). https://doi.org:10.1016/j.micpath.2021.105187

70 Chen, S. J. *et al.* Association of Fecal and Plasma Levels of Short-Chain Fatty Acids With Gut Microbiota and Clinical Severity in Patients With Parkinson Disease. *Neurology* **98**, e848-e858 (2022). https://doi.org:10.1212/WNL.0000000000013225

71 Sampson, T. R. *et al.* Gut Microbiota Regulate Motor Deficits and Neuroinflammation in a Model of Parkinson's Disease. *Cell* **167**, 1469-1480 e1412 (2016). https://doi.org:10.1016/j.cell.2016.11.018

72 Koh, A., De Vadder, F., Kovatcheva-Datchary, P. & Backhed, F. From Dietary Fiber to Host Physiology: Short-Chain Fatty Acids as Key Bacterial Metabolites. *Cell* **165**, 1332-1345 (2016). https://doi.org:10.1016/j.cell.2016.05.041

73 Grider, J. R. & Piland, B. E. The peristaltic reflex induced by short-chain fatty acids is mediated by sequential release of 5-HT and neuronal CGRP but not BDNF. *Am J Physiol Gastrointest Liver Physiol* **292**, G429-437 (2007). https://doi.org:10.1152/ajpgi.00376.2006

74 Zhang, J. M. *et al.* SCFAs-Induced GLP-1 Secretion Links the Regulation of Gut Microbiome on Hepatic Lipogenesis in Chickens. *Front Microbiol* **10**, 2176 (2019). https://doi.org:10.3389/fmicb.2019.02176

75 Yang, D. *et al.* Nociceptor neurons direct goblet cells via a CGRP-RAMP1 axis to drive mucus production and gut barrier protection. *Cell* **185**, 4190-4205 e4125 (2022). https://doi.org:10.1016/j.cell.2022.09.024

76 Schwerdtfeger, L. A. & Tobet, S. A. Vasoactive intestinal peptide regulates ileal goblet cell production in mice. *Physiol Rep* **8**, e14363 (2020). https://doi.org:10.14814/phy2.14363

77 Conlin, V. S. *et al.* Vasoactive intestinal peptide ameliorates intestinal barrier disruption associated with Citrobacter rodentium-induced colitis. *Am J Physiol Gastrointest Liver Physiol* **297**, G735-750 (2009). https://doi.org:10.1152/ajpgi.90551.2008

78 Neunlist, M. *et al.* Human ENS regulates the intestinal epithelial barrier permeability and a tight junction-associated protein ZO-1 via VIPergic pathways. *Am J Physiol Gastrointest Liver Physiol* **285**, G1028-1036 (2003). https://doi.org:10.1152/ajpgi.00066.2003

79 Ning, W. *et al.* Calcitonin gene-related peptide ameliorates sepsis-induced intestinal injury by suppressing NLRP3 inflammasome activation. *Int Immunopharmacol* **116**, 109747 (2023). https://doi.org:10.1016/j.intimp.2023.109747

80 Hwang, D. Y., Kim, S. & Hong, H. S. Substance-P Ameliorates Dextran Sodium Sulfate-Induced Intestinal Damage by Preserving Tissue Barrier Function. *Tissue Eng Regen Med* **15**, 63-73 (2018). https://doi.org:10.1007/s13770-017-0085-7

81 Pascual-Mato, M. *et al.* Unravelling the role of beta-CGRP in inflammatory bowel disease and its potential role in gastrointestinal homeostasis. *BMC Gastroenterol* **24**, 262 (2024). https://doi.org:10.1186/s12876-024-03366-w

82 Casado-Bedmar, M., Heil, S. D. S., Myrelid, P., Soderholm, J. D. & Keita, A. V. Upregulation of intestinal mucosal mast cells expressing VPAC1 in close proximity to vasoactive intestinal polypeptide in inflammatory bowel disease and murine colitis. *Neurogastroenterol Motil* **31**, e13503 (2019). https://doi.org:10.1111/nmo.13503

83 Keranen, U. *et al.* Changes in substance P-immunoreactive innervation of human colon associated with ulcerative colitis. *Dig Dis Sci* **40**, 2250-2258 (1995). https://doi.org:10.1007/BF02209015

84 Michalski, C. W. *et al.* Increase in substance P precursor mRNA in noninflamed small-bowel sections in patients with Crohn's disease. *Am J Surg* **193**, 476-481 (2007). https://doi.org:10.1016/j.amjsurg.2006.08.075

85 Wenzel, T. J., Gates, E. J., Ranger, A. L. & Klegeris, A. Short-chain fatty acids (SCFAs) alone or in combination regulate select immune functions of microglia-like cells. *Mol Cell Neurosci* **105**, 103493 (2020). https://doi.org:10.1016/j.mcn.2020.103493

86 Erny, D. *et al.* Host microbiota constantly control maturation and function of microglia in the CNS. *Nat Neurosci* **18**, 965-977 (2015). https://doi.org:10.1038/nn.4030

87 Paul, K. C. *et al.* Untargeted serum metabolomics reveals novel metabolite associations and disruptions in amino acid and lipid metabolism in Parkinson's disease. *Mol Neurodegener* **18**, 100 (2023). https://doi.org:10.1186/s13024-023-00694-5

88 Gao, J. M. *et al.* Multiomics of parkinsonism cynomolgus monkeys highlights significance of metabolites in interaction between host and microbiota. *NPJ Biofilms Microbiomes* **10**, 61 (2024). https://doi.org:10.1038/s41522-024-00535-3

89 Postuma, R. B. *et al.* Identifying prodromal Parkinson's disease: pre-motor disorders in Parkinson's disease. *Mov Disord* **27**, 617-626 (2012). https://doi.org:10.1002/mds.24996

90 Beach, T. G. *et al.* Multicenter Assessment of Immunohistochemical Methods for Pathological Alpha-Synuclein in Sigmoid Colon of Autopsied Parkinson's Disease and Control Subjects. *J Parkinsons Dis* **6**, 761-770 (2016). https://doi.org:10.3233/JPD-160888

91 Lebouvier, T. *et al.* Colonic biopsies to assess the neuropathology of Parkinson's disease and its relationship with symptoms. *PLoS One* **5**, e12728 (2010). https://doi.org:10.1371/journal.pone.0012728

92 Pouclet, H. *et al.* A comparison between colonic submucosa and mucosa to detect Lewy pathology in Parkinson's disease. *Neurogastroenterol Motil* **24**, e202-205 (2012). https://doi.org:10.1111/j.1365-2982.2012.01887.x

93 Sanchez-Ferro, A. *et al.* In vivo gastric detection of alpha-synuclein inclusions in Parkinson's disease. *Mov Disord* **30**, 517-524 (2015). https://doi.org:10.1002/mds.25988

94 Rota, L. *et al.* Constipation, deficit in colon contractions and alpha-synuclein inclusions within the colon precede motor abnormalities and neurodegeneration in the central nervous system in a mouse model of alpha-synucleinopathy. *Transl Neurodegener* **8**, 5 (2019). https://doi.org:10.1186/s40035-019-0146-z

95 Bohorquez, D. V. *et al.* Neuroepithelial circuit formed by innervation of sensory enteroendocrine cells. *J Clin Invest* **125**, 782-786 (2015). https://doi.org:10.1172/JCI78361

96 Kaelberer, M. M. *et al.* A gut-brain neural circuit for nutrient sensory transduction. *Science* **361** (2018). https://doi.org:10.1126/science.aat5236

97 Chandra, R., Hiniker, A., Kuo, Y. M., Nussbaum, R. L. & Liddle, R. A. alpha-Synuclein in gut endocrine cells and its implications for Parkinson's disease. *JCI Insight* **2** (2017). https://doi.org:10.1172/jci.insight.92295

98 Chandra, R. *et al.* Gut mucosal cells transfer alpha-synuclein to the vagus nerve. *JCI Insight* **8** (2023). https://doi.org:10.1172/jci.insight.172192

99 Liu, B. *et al.* Vagotomy and Parkinson disease: A Swedish register-based matched-cohort study. *Neurology* **88**, 1996-2002 (2017). https://doi.org:10.1212/WNL.0000000000003961

100 Svensson, E. *et al.* Vagotomy and subsequent risk of Parkinson's disease. *Ann Neurol* **78**, 522-529 (2015). https://doi.org:10.1002/ana.24448

101 Tysnes, O. B. *et al.* Does vagotomy reduce the risk of Parkinson's disease? *Ann Neurol* **78**, 1011-1012 (2015). https://doi.org:10.1002/ana.24531

102 Zhang, H. *et al.* Transcutaneous auricular vagus nerve stimulation improves gait and cortical activity in Parkinson's disease: A pilot randomized study. *CNS Neurosci Ther* **29**, 3889-3900 (2023). https://doi.org:10.1111/cns.14309

103 Marano, M. *et al.* Transcutaneous Auricular Vagus Stimulation Improves Gait and Reaction Time in Parkinson's Disease. *Mov Disord* **37**, 2163-2164 (2022). https://doi.org:10.1002/mds.29166

104 Arotcarena, M. L. *et al.* Bidirectional gut-to-brain and brain-to-gut propagation of synucleinopathy in non-human primates. *Brain* **143**, 1462-1475 (2020). https://doi.org:10.1093/brain/awaa096

105 McFleder, R. L. *et al.* Brain-to-gut trafficking of alpha-synuclein by CD11c(+) cells in a mouse model of Parkinson's disease. *Nat Commun* **14**, 7529 (2023). https://doi.org:10.1038/s41467-023-43224-z

106 Delgado, M., Reduta, A., Sharma, V. & Ganea, D. VIP/PACAP oppositely affects immature and mature dendritic cell expression of CD80/CD86 and the stimulatory activity for CD4(+) T cells. *J Leukoc Biol* **75**, 1122-1130 (2004). https://doi.org:10.1189/jlb.1203626

107 Perner, C. *et al.* Substance P Release by Sensory Neurons Triggers Dendritic Cell Migration and Initiates the Type-2 Immune Response to Allergens. *Immunity* **53**, 1063-1077 e1067 (2020). https://doi.org:10.1016/j.immuni.2020.10.001

108 Lu, X. *et al.* Type 1 Angiotensin Receptors on CD11c-Expressing Cells Protect Against Hypertension by Regulating Dendritic Cell-Mediated T Cell Activation. *Hypertension* **79**, 1227-1236 (2022). https://doi.org:10.1161/HYPERTENSIONAHA.121.18734

109 Lotti, T., D'Erme, A. M. & Hercogova, J. The role of neuropeptides in the control of regional immunity. *Clin Dermatol* **32**, 633-645 (2014). https://doi.org:10.1016/j.clindermatol.2014.04.011

110 Stasi, C. *et al.* Neuroendocrine Dysregulation in Irritable Bowel Syndrome Patients: A Pilot Study. *J Neurogastroenterol Motil* **23**, 428-434 (2017). https://doi.org:10.5056/jnm16155

111 Ishioh, M., Nozu, T. & Okumura, T. Brain Neuropeptides, Neuroinflammation, and Irritable Bowel Syndrome. *Digestion* **105**, 34-39 (2024). https://doi.org:10.1159/000533275

112 Gross, K. J. & Pothoulakis, C. Role of neuropeptides in inflammatory bowel disease. *Inflamm Bowel Dis* **13**, 918-932 (2007). https://doi.org:10.1002/ibd.20129

113 Na, H. *et al.* Characterization of the effects of calcitonin gene-related peptide receptor antagonist for Alzheimer's disease. *Neuropharmacology* **168**, 108017 (2020). https://doi.org:10.1016/j.neuropharm.2020.108017

114 Chung, C. Y. *et al.* Cell type-specific gene expression of midbrain dopaminergic neurons reveals molecules involved in their vulnerability and protection. *Hum Mol Genet* **14**, 1709-1725 (2005). https://doi.org:10.1093/hmg/ddi178

115 Reglodi, D., Lubics, A., Tamas, A., Szalontay, L. & Lengvari, I. Pituitary adenylate cyclase activating polypeptide protects dopaminergic neurons and improves behavioral deficits in a rat model of Parkinson's disease. *Behav Brain Res* **151**, 303-312 (2004). https://doi.org:10.1016/j.bbr.2003.09.007

116 Watson, M. B. *et al.* PACAP deficiency sensitizes nigrostriatal dopaminergic neurons to paraquat-induced damage and modulates central and peripheral inflammatory activation in mice. *Neuroscience* **240**, 277-286 (2013). https://doi.org:10.1016/j.neuroscience.2013.03.002

117 Fernandez, A., de Ceballos, M. L., Rose, S., Jenner, P. & Marsden, C. D. Alterations in peptide levels in Parkinson's disease and incidental Lewy body disease. *Brain* **119 (Pt 3)**, 823-830 (1996). https://doi.org:10.1093/brain/119.3.823

118 Orosz, D. & Bennett, J. P., Jr. Baseline and apomorphine-induced extracellular levels of nigral substance P are increased in an animal model of Parkinson's disease. *Eur J Pharmacol* **182**, 509-514 (1990). https://doi.org:10.1016/0014-2999(90)90049-c

119 Schirinzi, T. *et al.* Serum Substance P Is Increased in Parkinson's Disease and Correlates with Motor Impairment. *Mov Disord* **37**, 228-230 (2022). https://doi.org:10.1002/mds.28824

120 Zhang, W. *et al.* Gut-innervating nociceptors regulate the intestinal microbiota to promote tissue protection. *Cell* **185**, 4170-4189 e4120 (2022). https://doi.org:10.1016/j.cell.2022.09.008

121 Schubert, M. L. The effect of vasoactive intestinal polypeptide on gastric acid secretion is predominantly mediated by somatostatin. *Gastroenterology* **100**, 1195-1200 (1991).

122 Holzer, P. & Holzer-Petsche, U. Constipation Caused by Anti-calcitonin Gene-Related Peptide Migraine Therapeutics Explained by Antagonism of Calcitonin Gene-Related Peptide's Motor-Stimulating and Prosecretory Function in the Intestine. *Front Physiol* **12**, 820006 (2021). https://doi.org:10.3389/fphys.2021.820006

123 Ha, W. S. *et al.* The association between migraine and Parkinson's disease: a nationwide cohort study. *Epidemiol Health* **46**, e2024010 (2024). https://doi.org:10.4178/epih.e2024010

124 Patel, M. *et al.* Role of Substance P in the Pathophysiology of Inflammatory Bowel Disease and Its Correlation With the Degree of Inflammation. *Cureus* **12**, e11027 (2020). https://doi.org:10.7759/cureus.11027

125 Ailani, J. *et al.* Role of Calcitonin Gene-Related Peptide on the Gastrointestinal Symptoms of Migraine-Clinical Considerations: A Narrative Review. *Neurology* **99**, 841-853 (2022). https://doi.org:10.1212/WNL.0000000000201332

126 Scher, A. I. *et al.* Midlife migraine and late-life parkinsonism: AGES-Reykjavik study. *Neurology* **83**, 1246-1252 (2014). https://doi.org:10.1212/WNL.0000000000000840

127 Wang, H. I., Ho, Y. C., Huang, Y. P. & Pan, S. L. Migraine is related to an increased risk of Parkinson's disease: A population-based, propensity score-matched, longitudinal follow-up study. *Cephalalgia* **36**, 1316-1323 (2016). https://doi.org:10.1177/0333102416630577

128 Mukai, K. *et al.* PACAP- and PHI-mediated sustained relaxation in circular muscle of gastric fundus: findings obtained in PACAP knockout mice. *Regul Pept* **133**, 54-61 (2006). https://doi.org:10.1016/j.regpep.2005.09.019

129 Falkenberg, K., Bjerg, H. R. & Olesen, J. Two-Hour CGRP Infusion Causes Gastrointestinal Hyperactivity: Possible Relevance for CGRP Antibody Treatment. *Headache* **60**, 929-937 (2020). https://doi.org:10.1111/head.13795

130 Hafstrom, I., Ringertz, B., Lundeberg, T. & Palmblad, J. The effect of endothelin, neuropeptide Y, calcitonin gene-related peptide and substance P on neutrophil functions. *Acta Physiol Scand* **148**, 341-346 (1993). https://doi.org:10.1111/j.1748-1716.1993.tb09565.x

131 Nijhuis, L. E., Olivier, B. J. & de Jonge, W. J. Neurogenic regulation of dendritic cells in the intestine. *Biochem Pharmacol* **80**, 2002-2008 (2010). https://doi.org:10.1016/j.bcp.2010.06.034

132 Schwerdtfeger, L. A. & Tobet, S. A. Sex differences in anatomic plasticity of gut neuronal-mast cell interactions. *Physiol Rep* **9**, e15066 (2021). https://doi.org:10.14814/phy2.15066

133 Bot, I. *et al.* The neuropeptide substance P mediates adventitial mast cell activation and induces intraplaque hemorrhage in advanced atherosclerosis. *Circ Res* **106**, 89-92 (2010). https://doi.org:10.1161/CIRCRESAHA.109.204875

134 Cross, L. J., Heaney, L. G. & Ennis, M. Further characterisation of substance P induced histamine release from human bronchoalveolar lavage mast cells. *Inflamm Res* **45 Suppl 1**, S11-12 (1996). https://doi.org:10.1007/BF03354065

135 Jancso, N., Jancso-Gabor, A. & Szolcsanyi, J. Direct evidence for neurogenic inflammation and its prevention by denervation and by pretreatment with capsaicin. *Br J*

Pharmacol Chemother **31**, 138-151 (1967). https://doi.org:10.1111/j.1476-5381.1967.tb01984.x

136 Wu, X. *et al.* Vasoactive intestinal polypeptide promotes intestinal barrier homeostasis and protection against colitis in mice. *PLoS One* **10**, e0125225 (2015). https://doi.org:10.1371/journal.pone.0125225

137 Fanciullacci, M., Alessandri, M., Figini, M., Geppetti, P. & Michelacci, S. Increase in plasma calcitonin gene-related peptide from the extracerebral circulation during nitroglycerin-induced cluster headache attack. *Pain* **60**, 119-123 (1995). https://doi.org:10.1016/0304-3959(94)00097-X

138 Durham, P. L. Calcitonin gene-related peptide (CGRP) and migraine. *Headache* **46 Suppl 1**, S3-8 (2006). https://doi.org:10.1111/j.1526-4610.2006.00483.x

139 Wimalawansa, S. J. Calcitonin gene-related peptide and its receptors: molecular genetics, physiology, pathophysiology, and therapeutic potentials. *Endocr Rev* **17**, 533-585 (1996). https://doi.org:10.1210/edrv-17-5-533

140 Deutch, A. Y. & Roth, R. H. Calcitonin gene-related peptide in the ventral tegmental area: selective modulation of prefrontal cortical dopamine metabolism. *Neurosci Lett* **74**, 169-174 (1987). https://doi.org:10.1016/0304-3940(87)90144-3

141 Drumheller, A., Menard, D., Fournier, A. & Jolicoeur, F. B. Neurochemical effects of CGRP. *Ann N Y Acad Sci* **657**, 546-548 (1992). https://doi.org:10.1111/j.1749-6632.1992.tb22830.x

142 Buhner, S. *et al.* Calcium Imaging of Nerve-Mast Cell Signaling in the Human Intestine. *Front Physiol* **8**, 971 (2017). https://doi.org:10.3389/fphys.2017.00971

143 Sikora, L. K., Buchan, A. M., Levy, J. G., McIntosh, C. H. & Brown, J. C. VIP-innervation of rat intestine: a developmental study with monoclonal antibodies. *Peptides* **5**, 231-237 (1984). https://doi.org:10.1016/0196-9781(84)90212-2

144 Vaudry, D. *et al.* Pituitary adenylate cyclase-activating polypeptide and its receptors: 20 years after the discovery. *Pharmacol Rev* **61**, 283-357 (2009). https://doi.org:10.1124/pr.109.001370

145 Lu, J. *et al.* Targeting VIP and PACAP Receptor Signaling: New Insights into Designing Drugs for the PACAP Subfamily of Receptors. *Int J Mol Sci* **23** (2022). https://doi.org:10.3390/ijms23158069

146 Said, S. I. & Mutt, V. Isolation from porcine-intestinal wall of a vasoactive octacosapeptide related to secretin and to glucagon. *Eur J Biochem* **28**, 199-204 (1972). https://doi.org:10.1111/j.1432-1033.1972.tb01903.x

147 Waschek, J. A. VIP and PACAP: neuropeptide modulators of CNS inflammation, injury, and repair. *Br J Pharmacol* **169**, 512-523 (2013). https://doi.org:10.1111/bph.12181

148 Brenneman, D. E. Neuroprotection: a comparative view of vasoactive intestinal peptide and pituitary adenylate cyclase-activating polypeptide. *Peptides* **28**, 1720-1726 (2007). https://doi.org:10.1016/j.peptides.2007.04.002

149 Dejda, A., Jozwiak-Bebenista, M. & Nowak, J. Z. PACAP, VIP, and PHI: effects on AC-, PLC-, and PLD-driven signaling systems in the primary glial cell cultures. *Ann N Y Acad Sci* **1070**, 220-225 (2006). https://doi.org:10.1196/annals.1317.018

150 Reglodi, D. *et al.* Protective effects of pituitary adenylate cyclase activating polypeptide against neurotoxic agents. *Neurotoxicology* **66**, 185-194 (2018). https://doi.org:10.1016/j.neuro.2018.03.010

151 Pascal, M. *et al.* The neuropeptide VIP potentiates intestinal innate type 2 and type 3 immunity in response to feeding. *Mucosal Immunol* **15**, 629-641 (2022). https://doi.org:10.1038/s41385-022-00516-9

152 Delgado, M. & Ganea, D. Neuroprotective effect of vasoactive intestinal peptide (VIP) in a mouse model of Parkinson's disease by blocking microglial activation. *FASEB J* **17**, 944-946 (2003). https://doi.org:10.1096/fj.02-0799fje

153 Anderson, G. *et al.* Loss of enteric dopaminergic neurons and associated changes in colon motility in an MPTP mouse model of Parkinson's disease. *Exp Neurol* **207**, 4-12 (2007). https://doi.org:10.1016/j.expneurol.2007.05.010

154 Drolet, R. E., Cannon, J. R., Montero, L. & Greenamyre, J. T. Chronic rotenone exposure reproduces Parkinson's disease gastrointestinal neuropathology. *Neurobiol Dis* **36**, 96-102 (2009). https://doi.org:10.1016/j.nbd.2009.06.017

155 Greene, J. G., Noorian, A. R. & Srinivasan, S. Delayed gastric emptying and enteric nervous system dysfunction in the rotenone model of Parkinson's disease. *Exp Neurol* **218**, 154-161 (2009). https://doi.org:10.1016/j.expneurol.2009.04.023

156 Giancola, F. *et al.* Downregulation of neuronal vasoactive intestinal polypeptide in Parkinson's disease and chronic constipation. *Neurogastroenterol Motil* **29** (2017). https://doi.org:10.1111/nmo.12995

157 Shultz, J. M. *et al.* Neurotoxin-Induced Catecholaminergic Loss in the Colonic Myenteric Plexus of Rhesus Monkeys. *J Alzheimers Dis Parkinsonism* **6** (2016). https://doi.org:10.4172/2161-0460.1000279

158 Colucci, M. *et al.* Intestinal dysmotility and enteric neurochemical changes in a Parkinson's disease rat model. *Auton Neurosci* **169**, 77-86 (2012). https://doi.org:10.1016/j.autneu.2012.04.005

159 Edvinsson, J. C. *et al.* Neurokinins and their receptors in the rat trigeminal system: Differential localization and release with implications for migraine pain. *Mol Pain* **17**, 17448069211059400 (2021). https://doi.org:10.1177/17448069211059400

160 Ribeiro-da-Silva, A. & Hokfelt, T. Neuroanatomical localisation of Substance P in the CNS and sensory neurons. *Neuropeptides* **34**, 256-271 (2000). https://doi.org:10.1054/npep.2000.0834

161 Brownstein, M. J., Mroz, E. A., Kizer, J. S., Palkovits, M. & Leeman, S. E. Regional distribution of substance P in the brain of the rat. *Brain Res* **116**, 299-305 (1976). https://doi.org:10.1016/0006-8993(76)90907-0

162 Hong, J. S., Yang, H. Y., Racagni, G. & Costa, E. Projections of substance P containing neurons from neostriatum to substantia nigra. *Brain Res* **122**, 541-544 (1977). https://doi.org:10.1016/0006-8993(77)90464-4

163 Ljungdahl, A., Hokfelt, T. & Nilsson, G. Distribution of substance P-like immunoreactivity in the central nervous system of the rat--I. Cell bodies and nerve terminals. *Neuroscience* **3**, 861-943 (1978). https://doi.org:10.1016/0306-4522(78)90116-1

164 Brownstein, M. J., Mroz, E. A., Tappaz, M. L. & Leeman, S. E. On the origin of substance P and glutamic acid decarboxylase (GAD) in the substantia nigra. *Brain Res* **135**, 315-323 (1977). https://doi.org:10.1016/0006-8993(77)91034-4

165 Mroz, E. A., Brownstein, M. J. & Leeman, S. E. Evidence for substance P in the striato-nigral tract. *Brain Res* **125**, 305-311 (1977). https://doi.org:10.1016/0006-8993(77)90623-0

166 Kanazawa, I., Emson, P. C. & Cuello, A. C. Evidence for the existence of substance P-containing fibres in striato-nigral and pallido-nigral pathways in rat brain. *Brain Res* **119**, 447-453 (1977). https://doi.org:10.1016/0006-8993(77)90323-7

167 Thornton, E. & Vink, R. Treatment with a substance P receptor antagonist is neuroprotective in the intrastriatal 6-hydroxydopamine model of early Parkinson's disease. *PLoS One* **7**, e34138 (2012). https://doi.org:10.1371/journal.pone.0034138

168 Tirassa, P. *et al.* What substance P might tell us about the prognosis and mechanism of Parkinson's disease? *Neurosci Biobehav Rev* **131**, 899-911 (2021). https://doi.org:10.1016/j.neubiorev.2021.10.008

169 Lorente, L. *et al.* Serum substance P levels and early mortality of spontaneous intracerebral haemorrhage patients. *J Stroke Cerebrovasc Dis* **29**, 104893 (2020). https://doi.org:10.1016/j.jstrokecerebrovasdis.2020.104893

170 Kennedy, P. G. *et al.* A substance P antagonist, RP-67,580, ameliorates a mouse meningoencephalitic response to Trypanosoma brucei brucei. *Proc Natl Acad Sci U S A* **94**, 4167-4170 (1997). https://doi.org:10.1073/pnas.94.8.4167

171 Burmeister, A. R. *et al.* Human microglia and astrocytes constitutively express the neurokinin-1 receptor and functionally respond to substance P. *J Neuroinflammation* **14**, 245 (2017). https://doi.org:10.1186/s12974-017-1012-5

172 Pellegrini, C. *et al.* Alteration of colonic excitatory tachykininergic motility and enteric inflammation following dopaminergic nigrostriatal neurodegeneration. *J Neuroinflammation* **13**, 146 (2016). https://doi.org:10.1186/s12974-016-0608-5

173 Sharrad, D. F., de Vries, E. & Brookes, S. J. Selective expression of alpha-synuclein-immunoreactivity in vesicular acetylcholine transporter-immunoreactive axons in the guinea pig rectum and human colon. *J Comp Neurol* **521**, 657-676 (2013). https://doi.org:10.1002/cne.23198

174 Sato, T. *et al.* Structure, regulation and function of ghrelin. *J Biochem* **151**, 119-128 (2012). https://doi.org:10.1093/jb/mvr134

175 Pradhan, G., Samson, S. L. & Sun, Y. Ghrelin: much more than a hunger hormone. *Curr Opin Clin Nutr Metab Care* **16**, 619-624 (2013). https://doi.org:10.1097/MCO.0b013e328365b9be

176 Tack, J. *et al.* Influence of ghrelin on interdigestive gastrointestinal motility in humans. *Gut* **55**, 327-333 (2006). https://doi.org:10.1136/gut.2004.060426

177 Masuda, Y. *et al.* Ghrelin stimulates gastric acid secretion and motility in rats. *Biochem Biophys Res Commun* **276**, 905-908 (2000). https://doi.org:10.1006/bbrc.2000.3568

178 Song, N. *et al.* Assessments of plasma ghrelin levels in the early stages of parkinson's disease. *Mov Disord* **32**, 1487-1491 (2017). https://doi.org:10.1002/mds.27095

179 Liu, Y. *et al.* Ghrelin Bridges DMV Neuropathology and GI Dysfunction in the Early Stages of Parkinson's Disease. *Adv Sci (Weinh)* **9**, e2203020 (2022). https://doi.org:10.1002/advs.202203020

180 Bayliss, J. A. *et al.* Ghrelin-AMPK Signaling Mediates the Neuroprotective Effects of Calorie Restriction in Parkinson's Disease. *J Neurosci* **36**, 3049-3063 (2016). https://doi.org:10.1523/JNEUROSCI.4373-15.2016

181 Andrews, Z. B. *et al.* Ghrelin promotes and protects nigrostriatal dopamine function via a UCP2-dependent mitochondrial mechanism. *J Neurosci* **29**, 14057-14065 (2009). https://doi.org:10.1523/JNEUROSCI.3890-09.2009

182 Moon, M. *et al.* Neuroprotective effect of ghrelin in the 1-methyl-4-phenyl-1,2,3,6-tetrahydropyridine mouse model of Parkinson's disease by blocking microglial activation. *Neurotox Res* **15**, 332-347 (2009). https://doi.org:10.1007/s12640-009-9037-x

183 Liu, S., Chen, S., Ren, J., Li, B. & Qin, B. Ghrelin protects retinal ganglion cells against rotenone via inhibiting apoptosis, restoring mitochondrial function, and activating AKT-mTOR signaling. *Neuropeptides* **67**, 63-70 (2018). https://doi.org:10.1016/j.npep.2017.11.007

184 Yu, J., Xu, H., Shen, X. & Jiang, H. Ghrelin protects MES23.5 cells against rotenone via inhibiting mitochondrial dysfunction and apoptosis. *Neuropeptides* **56**, 69-74 (2016). https://doi.org:10.1016/j.npep.2015.09.011

185 Suda, Y. *et al.* Down-regulation of ghrelin receptors on dopaminergic neurons in the substantia nigra contributes to Parkinson's disease-like motor dysfunction. *Mol Brain* **11**, 6 (2018). https://doi.org:10.1186/s13041-018-0349-8

186 Schicho, R., Schemann, M., Pabst, M. A., Holzer, P. & Lippe, I. T. Capsaicin-sensitive extrinsic afferents are involved in acid-induced activation of distinct myenteric neurons in the rat stomach. *Neurogastroenterol Motil* **15**, 33-44 (2003). https://doi.org:10.1046/j.1365-2982.2003.00384.x

187 Tough, I. R. *et al.* Endogenous peptide YY and neuropeptide Y inhibit colonic ion transport, contractility and transit differentially via Y(1) and Y(2) receptors. *Br J Pharmacol* **164**, 471-484 (2011). https://doi.org:10.1111/j.1476-5381.2011.01401.x

188 Shibata, M., Hisajima, T., Nakano, M., Goris, R. C. & Funakoshi, K. Morphological relationships between peptidergic nerve fibers and immunoglobulin A-producing lymphocytes in the mouse intestine. *Brain Behav Immun* **22**, 158-166 (2008). https://doi.org:10.1016/j.bbi.2007.08.013

189 Goto, S. *et al.* Defects in the striatal neuropeptide Y system in X-linked dystonia-parkinsonism. *Brain* **136**, 1555-1567 (2013). https://doi.org:10.1093/brain/awt084

190 Hansel, D. E., Eipper, B. A. & Ronnett, G. V. Regulation of olfactory neurogenesis by amidated neuropeptides. *J Neurosci Res* **66**, 1-7 (2001). https://doi.org:10.1002/jnr.1191

191 Curtis, M. A., Eriksson, P. S. & Faull, R. L. Progenitor cells and adult neurogenesis in neurodegenerative diseases and injuries of the basal ganglia. *Clin Exp Pharmacol Physiol* **34**, 528-532 (2007). https://doi.org:10.1111/j.1440-1681.2007.04609.x

192 Xapelli, S., Agasse, F., Ferreira, R., Silva, A. P. & Malva, J. O. Neuropeptide Y as an endogenous antiepileptic, neuroprotective and pro-neurogenic peptide. *Recent Pat CNS Drug Discov* **1**, 315-324 (2006). https://doi.org:10.2174/157488906778773689

193 Decressac, M. & Barker, R. A. Neuropeptide Y and its role in CNS disease and repair. *Exp Neurol* **238**, 265-272 (2012). https://doi.org:10.1016/j.expneurol.2012.09.004

194 Martignoni, E. *et al.* Cerebrospinal fluid norepinephrine, 3-methoxy-4-hydroxyphenylglycol and neuropeptide Y levels in Parkinson's disease, multiple system atrophy and dementia of the Alzheimer type. *J Neural Transm Park Dis Dement Sect* **4**, 191-205 (1992). https://doi.org:10.1007/BF02260903

195 Cannizzaro, C., Tel, B. C., Rose, S., Zeng, B. Y. & Jenner, P. Increased neuropeptide Y mRNA expression in striatum in Parkinson's disease. *Brain Res Mol Brain Res* **110**, 169-176 (2003). https://doi.org:10.1016/s0169-328x(02)00555-7

196 Kerkerian, L., Bosler, O., Pelletier, G. & Nieoullon, A. Striatal neuropeptide Y neurones are under the influence of the nigrostriatal dopaminergic pathway: immunohistochemical evidence. *Neurosci Lett* **66**, 106-112 (1986). https://doi.org:10.1016/0304-3940(86)90174-6

197 Kerkerian, L., Salin, P. & Nieoullon, A. Pharmacological characterization of dopaminergic influence on expression of neuropeptide Y immunoreactivity by rat striatal neurons. *Neuroscience* **26**, 809-817 (1988). https://doi.org:10.1016/0306-4522(88)90101-7

198 Decressac, M. *et al.* Neuroprotection by neuropeptide Y in cell and animal models of Parkinson's disease. *Neurobiol Aging* **33**, 2125-2137 (2012). https://doi.org:10.1016/j.neurobiolaging.2011.06.018

199 Pain, S. *et al.* Inflammatory process in Parkinson disease: neuroprotection by neuropeptide Y. *Fundam Clin Pharmacol* **33**, 544-548 (2019). https://doi.org:10.1111/fcp.12464

200 Krieger, J. P. Intestinal glucagon-like peptide-1 effects on food intake: Physiological relevance and emerging mechanisms. *Peptides* **131**, 170342 (2020). https://doi.org:10.1016/j.peptides.2020.170342

201 Li, Y. *et al.* GLP-1 receptor stimulation preserves primary cortical and dopaminergic neurons in cellular and rodent models of stroke and Parkinsonism. *Proc Natl Acad Sci U S A* **106**, 1285-1290 (2009). https://doi.org:10.1073/pnas.0806720106

202 Wu, P. *et al.* Liraglutide Regulates Mitochondrial Quality Control System Through PGC-1alpha in a Mouse Model of Parkinson's Disease. *Neurotox Res* **40**, 286-297 (2022). https://doi.org:10.1007/s12640-021-00460-9

203 Bergkvist, L. *et al.* An extended release GLP-1 analogue increases alpha-synuclein accumulation in a mouse model of prodromal Parkinson's disease. *Exp Neurol* **341**, 113693 (2021). https://doi.org:10.1016/j.expneurol.2021.113693

204 Yun, S. P. *et al.* Block of A1 astrocyte conversion by microglia is neuroprotective in models of Parkinson's disease. *Nat Med* **24**, 931-938 (2018). https://doi.org:10.1038/s41591-018-0051-5

205 Su, Y. *et al.* A GLP-2 Analogue Protects SH-SY5Y and Neuro-2a Cells Against Mitochondrial Damage, Autophagy Impairments and Apoptosis in a Parkinson Model. *Drug Res (Stuttg)* **71**, 43-50 (2021). https://doi.org:10.1055/a-1266-3263

206 Fang, X., Tian, P., Zhao, X., Jiang, C. & Chen, T. Neuroprotective effects of an engineered commensal bacterium in the 1-methyl-4-phenyl-1, 2, 3, 6-tetrahydropyridine Parkinson disease mouse model via producing glucagon-like peptide-1. *J Neurochem* **150**, 441-452 (2019). https://doi.org:10.1111/jnc.14694

207 Su, Y. *et al.* Cholecystokinin and glucagon-like peptide-1 analogues regulate intestinal tight junction, inflammation, dopaminergic neurons and alpha-synuclein accumulation in the colon of two Parkinson's disease mouse models. *Eur J Pharmacol* **926**, 175029 (2022). https://doi.org:10.1016/j.ejphar.2022.175029

208 Manfready, R. A. *et al.* Attenuated Postprandial GLP-1 Response in Parkinson's Disease. *Front Neurosci* **15**, 660942 (2021). https://doi.org:10.3389/fnins.2021.660942

209 Liddle, R. A. Cholecystokinin cells. *Annu Rev Physiol* **59**, 221-242 (1997). https://doi.org:10.1146/annurev.physiol.59.1.221

210 Hokfelt, T. *et al.* Evidence for coexistence of dopamine and CCK in meso-limbic neurones. *Nature* **285**, 476-478 (1980). https://doi.org:10.1038/285476a0

211 Zhang, Z. *et al.* Neuroprotective Effects of a Cholecystokinin Analogue in the 1-Methyl-4-Phenyl-1,2,3,6-Tetrahydropyridine Parkinson's Disease Mouse Model. *Front Neurosci* **16**, 814430 (2022). https://doi.org:10.3389/fnins.2022.814430

212 Taylor, M. D., De Ceballos, M. L., Rose, S., Jenner, P. & Marsden, C. D. Effects of a unilateral 6-hydroxydopamine lesion and prolonged L-3,4-dihydroxyphenylalanine treatment on peptidergic systems in rat basal ganglia. *Eur J Pharmacol* **219**, 183-192 (1992). https://doi.org:10.1016/0014-2999(92)90295-f

213 Nilsson, A. *et al.* Striatal alterations of secretogranin-1, somatostatin, prodynorphin, and cholecystokinin peptides in an experimental mouse model of Parkinson disease. *Mol Cell Proteomics* **8**, 1094-1104 (2009). https://doi.org:10.1074/mcp.M800454-MCP200

214 Saia, R. S., Ribeiro, A. B. & Giusti, H. Cholecystokinin Modulates the Mucosal Inflammatory Response and Prevents the Lipopolysaccharide-Induced Intestinal Epithelial Barrier Dysfunction. *Shock* **53**, 242-251 (2020). https://doi.org:10.1097/SHK.0000000000001355

215 Choi, J. G. *et al.* Reduced Levels of Intestinal Neuropeptides and Neurotrophins in Neurotoxin-Induced Parkinson Disease Mouse Models. *J Neuropathol Exp Neurol* **80**, 15-20 (2021). https://doi.org:10.1093/jnen/nlaa113

216 Tobet, L. A. S. a. S. A. in *Precision Medicine for Investigators, Practitioners and Providers* (ed Joel Faintuch and Salomao Faintuch) 97-104 (Academic Press, 2020).

217 Davies, K. N., King, D., Billington, D. & Barrett, J. A. Intestinal permeability and orocaecal transit time in elderly patients with Parkinson's disease. *Postgrad Med J* **72**, 164-167 (1996). https://doi.org:10.1136/pgmj.72.845.164

218 Schwiertz, A. *et al.* Fecal markers of intestinal inflammation and intestinal permeability are elevated in Parkinson's disease. *Parkinsonism Relat Disord* **50**, 104-107 (2018). https://doi.org:10.1016/j.parkreldis.2018.02.022

219 Clairembault, T. *et al.* Structural alterations of the intestinal epithelial barrier in Parkinson's disease. *Acta Neuropathol Commun* **3**, 12 (2015). https://doi.org:10.1186/s40478-015-0196-0

220 Walker, R. I. & Porvaznik, M. J. Disruption of the permeability barrier (zonula occludens) between intestinal epithelial cells by lethal doses of endotoxin. *Infect Immun* **21**, 655-658 (1978). https://doi.org:10.1128/iai.21.2.655-658.1978

221 Kelly, L. P. *et al.* Progression of intestinal permeability changes and alpha-synuclein expression in a mouse model of Parkinson's disease. *Mov Disord* **29**, 999-1009 (2014). https://doi.org:10.1002/mds.25736

222 Dodiya, H. B. *et al.* Chronic stress-induced gut dysfunction exacerbates Parkinson's disease phenotype and pathology in a rotenone-induced mouse model of Parkinson's disease. *Neurobiol Dis* **135**, 104352 (2020). https://doi.org:10.1016/j.nbd.2018.12.012

223 Turner, D. J. *et al.* Substance P regulates migration in rat intestinal epithelial cells. *Ann Surg* **245**, 408-414 (2007). https://doi.org:10.1097/01.sla.0000245549.57076.db

224 van, I. S. C. D. & Derkinderen, P. The Intestinal Barrier in Parkinson's Disease: Current State of Knowledge. *J Parkinsons Dis* **9**, S323-S329 (2019). https://doi.org:10.3233/JPD-191707

225 Perez-Pardo, P. *et al.* Role of TLR4 in the gut-brain axis in Parkinson's disease: a translational study from men to mice. *Gut* **68**, 829-843 (2019). https://doi.org:10.1136/gutjnl-2018-316844

226 Perez-Pardo, P. *et al.* Gut-brain and brain-gut axis in Parkinson's disease models: Effects of a uridine and fish oil diet. *Nutr Neurosci* **21**, 391-402 (2018). https://doi.org:10.1080/1028415X.2017.1294555

227 Adams, B. *et al.* Parkinson's Disease: A Systemic Inflammatory Disease Accompanied by Bacterial Inflammagens. *Front Aging Neurosci* **11**, 210 (2019). https://doi.org:10.3389/fnagi.2019.00210

228 Craig, D. W. *et al.* RNA sequencing of whole blood reveals early alterations in immune cells and gene expression in Parkinson's disease. *Nat Aging* **1**, 734-747 (2021). https://doi.org:10.1038/s43587-021-00088-6

229 Bayati, A. *et al.* Modeling Parkinson's disease pathology in human dopaminergic neurons by sequential exposure to alpha-synuclein fibrils and proinflammatory cytokines. *Nat Neurosci* (2024). https://doi.org:10.1038/s41593-024-01775-4

230 Sun, C. *et al.* Abnormal subpopulations of peripheral blood lymphocytes are involved in Parkinson's disease. *Ann Transl Med* **7**, 637 (2019). https://doi.org:10.21037/atm.2019.10.105

231 Harms, A. S. *et al.* alpha-Synuclein fibrils recruit peripheral immune cells in the rat brain prior to neurodegeneration. *Acta Neuropathol Commun* **5**, 85 (2017). https://doi.org:10.1186/s40478-017-0494-9

232 Chesne, J., Cardoso, V. & Veiga-Fernandes, H. Neuro-immune regulation of mucosal physiology. *Mucosal Immunol* **12**, 10-20 (2019). https://doi.org:10.1038/s41385-018-0063-y

233 Verheijden, S. & Boeckxstaens, G. E. Neuroimmune interaction and the regulation of intestinal immune homeostasis. *Am J Physiol Gastrointest Liver Physiol* **314**, G75-G80 (2018). https://doi.org:10.1152/ajpgi.00425.2016

234 Mertsalmi, T. H. *et al.* More than constipation - bowel symptoms in Parkinson's disease and their connection to gut microbiota. *Eur J Neurol* **24**, 1375-1383 (2017). https://doi.org:10.1111/ene.13398

235 Park, S. *et al.* Patients with Inflammatory Bowel Disease Are at an Increased Risk of Parkinson's Disease: A South Korean Nationwide Population-Based Study. *J Clin Med* **8** (2019). https://doi.org:10.3390/jcm8081191

236 Grozdanov, V. *et al.* Increased Immune Activation by Pathologic alpha-Synuclein in Parkinson's Disease. *Ann Neurol* **86**, 593-606 (2019). https://doi.org:10.1002/ana.25557

237 Christophi, G. P., Rong, R., Holtzapple, P. G., Massa, P. T. & Landas, S. K. Immune markers and differential signaling networks in ulcerative colitis and Crohn's disease. *Inflamm Bowel Dis* **18**, 2342-2356 (2012). https://doi.org:10.1002/ibd.22957

238 Schnell, A. *et al.* Stem-like intestinal Th17 cells give rise to pathogenic effector T cells during autoimmunity. *Cell* **184**, 6281-6298 e6223 (2021). https://doi.org:10.1016/j.cell.2021.11.018

239 Haghikia, A. *et al.* Dietary Fatty Acids Directly Impact Central Nervous System Autoimmunity via the Small Intestine. *Immunity* **43**, 817-829 (2015). https://doi.org:10.1016/j.immuni.2015.09.007

240 Yan, Y. *et al.* Interleukin-6 produced by enteric neurons regulates the number and phenotype of microbe-responsive regulatory T cells in the gut. *Immunity* **54**, 499-513 e495 (2021). https://doi.org:10.1016/j.immuni.2021.02.002

241 Cox, L. M. *et al.* Gamma-delta T cells suppress microbial metabolites that activate striatal neurons and induce repetitive/compulsive behavior in mice. *Brain Behav Immun* **117**, 242-254 (2024). https://doi.org:10.1016/j.bbi.2024.01.214

242 Eftekhari, S., Warfvinge, K., Blixt, F. W. & Edvinsson, L. Differentiation of nerve fibers storing CGRP and CGRP receptors in the peripheral trigeminovascular system. *J Pain* **14**, 1289-1303 (2013). https://doi.org:10.1016/j.jpain.2013.03.010

243 Mikami, N. *et al.* Calcitonin gene-related peptide enhances experimental autoimmune encephalomyelitis by promoting Th17-cell functions. *Int Immunol* **24**, 681-691 (2012). https://doi.org:10.1093/intimm/dxs075

244 Fernandez, S., Knopf, M. A., Bjork, S. K. & McGillis, J. P. Bone marrow-derived macrophages express functional CGRP receptors and respond to CGRP by increasing transcription of c-fos and IL-6 mRNA. *Cell Immunol* **209**, 140-148 (2001). https://doi.org:10.1006/cimm.2001.1795

245 An, Q. *et al.* Calcitonin gene-related peptide regulates spinal microglial activation through the histone H3 lysine 27 trimethylation via enhancer of zeste homolog-2 in rats with neuropathic pain. *J Neuroinflammation* **18**, 117 (2021). https://doi.org:10.1186/s12974-021-02168-1

246 Juhasz, G. *et al.* Sumatriptan causes parallel decrease in plasma calcitonin gene-related peptide (CGRP) concentration and migraine headache during nitroglycerin induced migraine attack. *Cephalalgia* **25**, 179-183 (2005). https://doi.org:10.1111/j.1468-2982.2005.00836.x

247 Steenbergh, P. H. *et al.* Structure and expression of the human calcitonin/CGRP genes. *FEBS Lett* **209**, 97-103 (1986). https://doi.org:10.1016/0014-5793(86)81091-2

248 Noguchi, K., Senba, E., Morita, Y., Sato, M. & Tohyama, M. Alpha-CGRP and beta-CGRP mRNAs are differentially regulated in the rat spinal cord and dorsal root ganglion.

Brain Res Mol Brain Res **7**, 299-304 (1990). https://doi.org:10.1016/0169-328x(90)90080-w

249 Mulderry, P. K. *et al.* Differential expression of alpha-CGRP and beta-CGRP by primary sensory neurons and enteric autonomic neurons of the rat. *Neuroscience* **25**, 195-205 (1988). https://doi.org:10.1016/0306-4522(88)90018-8

250 Goadsby, P. J., Edvinsson, L. & Ekman, R. Vasoactive peptide release in the extracerebral circulation of humans during migraine headache. *Ann Neurol* **28**, 183-187 (1990). https://doi.org:10.1002/ana.410280213

251 Cady, R. J., Glenn, J. R., Smith, K. M. & Durham, P. L. Calcitonin gene-related peptide promotes cellular changes in trigeminal neurons and glia implicated in peripheral and central sensitization. *Mol Pain* **7**, 94 (2011). https://doi.org:10.1186/1744-8069-7-94

252 Kamm, K., Straube, A. & Ruscheweyh, R. Calcitonin gene-related peptide levels in tear fluid are elevated in migraine patients compared to healthy controls. *Cephalalgia* **39**, 1535-1543 (2019). https://doi.org:10.1177/0333102419856640

253 van Dongen, R. M. *et al.* Migraine biomarkers in cerebrospinal fluid: A systematic review and meta-analysis. *Cephalalgia* **37**, 49-63 (2017). https://doi.org:10.1177/0333102415625614

254 Raddant, A. C. & Russo, A. F. Calcitonin gene-related peptide in migraine: intersection of peripheral inflammation and central modulation. *Expert Rev Mol Med* **13**, e36 (2011). https://doi.org:10.1017/S1462399411002067

255 Edvinsson, L., Haanes, K. A., Warfvinge, K. & Krause, D. N. CGRP as the target of new migraine therapies - successful translation from bench to clinic. *Nat Rev Neurol* **14**, 338-350 (2018). https://doi.org:10.1038/s41582-018-0003-1

256 Benemei, S., Nicoletti, P., Capone, J. G. & Geppetti, P. CGRP receptors in the control of pain and inflammation. *Curr Opin Pharmacol* **9**, 9-14 (2009). https://doi.org:10.1016/j.coph.2008.12.007

257 Barbara, G. *et al.* Activated mast cells in proximity to colonic nerves correlate with abdominal pain in irritable bowel syndrome. *Gastroenterology* **126**, 693-702 (2004). https://doi.org:10.1053/j.gastro.2003.11.055

258 Kempuraj, D. *et al.* Cross-Talk between Glia, Neurons and Mast Cells in Neuroinflammation Associated with Parkinson's Disease. *J Neuroimmune Pharmacol* **13**, 100-112 (2018). https://doi.org:10.1007/s11481-017-9766-1

259 Arizono, N. *et al.* Anatomical variation in mast cell nerve associations in the rat small intestine, heart, lung, and skin. Similarities of distances between neural processes and mast cells, eosinophils, or plasma cells in the jejunal lamina propria. *Lab Invest* **62**, 626-634 (1990).

260 Stead, R. H., Dixon, M. F., Bramwell, N. H., Riddell, R. H. & Bienenstock, J. Mast cells are closely apposed to nerves in the human gastrointestinal mucosa. *Gastroenterology* **97**, 575-585 (1989). https://doi.org:10.1016/0016-5085(89)90627-6

261 van Diest, S. A., Stanisor, O. I., Boeckxstaens, G. E., de Jonge, W. J. & van den Wijngaard, R. M. Relevance of mast cell-nerve interactions in intestinal nociception. *Biochim Biophys Acta* **1822**, 74-84 (2012). https://doi.org:10.1016/j.bbadis.2011.03.019

262 Nuutinen, S. & Panula, P. Histamine in neurotransmission and brain diseases. *Adv Exp Med Biol* **709**, 95-107 (2010). https://doi.org:10.1007/978-1-4419-8056-4_10

263 Coelho, M. H., Silva, I. J., Azevedo, M. S. & Manso, C. F. Decrease in blood histamine in drug-treated parkinsonian patients. *Mol Chem Neuropathol* **14**, 77-85 (1991). https://doi.org:10.1007/BF03159928

264 Prell, G. D. & Green, J. P. Histamine metabolites and pros-methylimidazoleacetic acid in human cerebrospinal fluid. *Agents Actions Suppl* **33**, 343-363 (1991). https://doi.org:10.1007/978-3-0348-7309-3_25

265 Futagami, S. *et al.* Nizatidine improves clinical symptoms and gastric emptying in patients with functional dyspepsia accompanied by impaired gastric emptying. *Digestion* **86**, 114-121 (2012). https://doi.org:10.1159/000339111

266 Doi, H. *et al.* Nizatidine ameliorates gastroparesis in Parkinson's disease: a pilot study. *Mov Disord* **29**, 562-566 (2014). https://doi.org:10.1002/mds.25777

267 Stefanova, N. Microglia in Parkinson's Disease. *J Parkinsons Dis* **12**, S105-S112 (2022). https://doi.org:10.3233/JPD-223237

268 Sanchez-Guajardo, V., Febbraro, F., Kirik, D. & Romero-Ramos, M. Microglia acquire distinct activation profiles depending on the degree of alpha-synuclein neuropathology in a rAAV based model of Parkinson's disease. *PLoS One* **5**, e8784 (2010). https://doi.org:10.1371/journal.pone.0008784

269 Barkholt, P., Sanchez-Guajardo, V., Kirik, D. & Romero-Ramos, M. Long-term polarization of microglia upon alpha-synuclein overexpression in nonhuman primates. *Neuroscience* **208**, 85-96 (2012). https://doi.org:10.1016/j.neuroscience.2012.02.004

270 Imamura, K. *et al.* Distribution of major histocompatibility complex class II-positive microglia and cytokine profile of Parkinson's disease brains. *Acta Neuropathol* **106**, 518-526 (2003). https://doi.org:10.1007/s00401-003-0766-2

271 Kam, T. I., Hinkle, J. T., Dawson, T. M. & Dawson, V. L. Microglia and astrocyte dysfunction in parkinson's disease. *Neurobiol Dis* **144**, 105028 (2020). https://doi.org:10.1016/j.nbd.2020.105028

272 Rocha, S. M. *et al.* Microglia-specific knock-out of NF-kappaB/IKK2 increases the accumulation of misfolded alpha-synuclein through the inhibition of p62/sequestosome-

1-dependent autophagy in the rotenone model of Parkinson's disease. *Glia* **71**, 2154-2179 (2023). https://doi.org:10.1002/glia.24385

273 Delgado, M., Leceta, J. & Ganea, D. Vasoactive intestinal peptide and pituitary adenylate cyclase-activating polypeptide inhibit the production of inflammatory mediators by activated microglia. *J Leukoc Biol* **73**, 155-164 (2003). https://doi.org:10.1189/jlb.0702372

274 Karunia, J. *et al.* PACAP and VIP Modulate LPS-Induced Microglial Activation and Trigger Distinct Phenotypic Changes in Murine BV2 Microglial Cells. *Int J Mol Sci* **22** (2021). https://doi.org:10.3390/ijms222010947

275 McGeer, P. L., Itagaki, S. & McGeer, E. G. Expression of the histocompatibility glycoprotein HLA-DR in neurological disease. *Acta Neuropathol* **76**, 550-557 (1988). https://doi.org:10.1007/BF00689592

276 Consonni, A., Morara, S., Codazzi, F., Grohovaz, F. & Zacchetti, D. Inhibition of lipopolysaccharide-induced microglia activation by calcitonin gene related peptide and adrenomedullin. *Mol Cell Neurosci* **48**, 151-160 (2011). https://doi.org:10.1016/j.mcn.2011.07.006

277 Nieto, F. R., Clark, A. K., Grist, J., Chapman, V. & Malcangio, M. Calcitonin gene-related peptide-expressing sensory neurons and spinal microglial reactivity contribute to pain states in collagen-induced arthritis. *Arthritis Rheumatol* **67**, 1668-1677 (2015). https://doi.org:10.1002/art.39082

278 Wang, Q. *et al.* Substance P exacerbates dopaminergic neurodegeneration through neurokinin-1 receptor-independent activation of microglial NADPH oxidase. *J Neurosci* **34**, 12490-12503 (2014). https://doi.org:10.1523/JNEUROSCI.2238-14.2014

CHAPTER 4 –SEX SPECIFIC EFFECTS OF ENVIONMENTAL TOXIN-DERIVED ALPHA SYNUCLEIN ON ENTERIC NEURONAL-EPITHELIAL INTERACTIONS[4]

Overview:

Parkinson's Disease (PD) is a neurodegenerative disorder with prodromal gastrointestinal (GI) issues often emerging decades before motor symptoms. Pathologically, PD can be driven by accumulation of misfolded alpha synuclein (aSyn) protein in the brain and periphery, including the GI tract. Disease epidemiology differs by sex, with men twice as likely to develop PD. Women, however, experience faster disease progression, higher mortality, and more severe GI symptoms. Gut calcitonin gene related peptide (CGRP) is a key regulator of intestinal contractions and visceral pain. The current study tests the hypothesis that sex differences in GI symptomology in PD are the result of aSyn aggregation altering enteric CGRP signaling pathways. To facilitate peripheral aSyn aggregation, the pesticide rotenone was administered intraperitoneally once daily for two weeks to male and female mice. Mice were sacrificed two weeks after the last rotenone injection and immunohistochemistry was performed on sections of proximal colon. Levels of aSyn were heightened in myenteric plexus neurons and a subset of neurons immunoreactive to CGRP in rotenone treated mice. Female mice exhibited 153% more myenteric aSyn, 26% more apical CGRP immunoreactivity, and 66.7% more aSyn in apical $CGRP^+$ fibers after rotenone when compared to males. Goblet cell numbers were diminished but the individual cells were larger in the apical regions of crypts in the colons of rotenone treated mice. This study used a mouse model of PD to uncover sex specific alterations in enteric neuronal and epithelial populations, underscoring the importance of considering sex as a biological variable while investigating prodromal GI symptoms.

[4] Templeton HA, Ehrlich AT, Schwerdtfeger LA, Sheng JA, Tjalkens RB, Tobet SA. Sex specific effects of environmental toxin-derived alpha synuclein on enteric neuronal-epithelial interactions. *Neurogastroenterology and Motility. In Press*. 2025

Introduction:

Parkinson's disease (PD) is a neurodegenerative disorder with prodromal symptoms that emerge decades before motor dysfunction. Gastrointestinal (GI) symptoms including bloating, visceral pain, gastroparesis, and constipation, are seen in 10 – 70% of PD subjects[1,2] and can manifest up to 20 years before diagnosis.[3] GI symptoms impact quality of life, and pose significant health risks including, malnutrition, intestinal obstruction, and impaired medication effectiveness.[4,5] PD is driven pathologically by the accumulation of misfolded alpha synuclein (aSyn) protein in the brain and periphery, including the GI tract. Environmental toxins such as rotenone exacerbate aSyn aggregation, producing PD-like pathology and symptoms when administered to rodents.[6] Gut pathology in rotenone PD models includes peripheral gastroparesis[7] and decreased intestinal transit,[8,9] creating a viable murine model for investigating mechanisms of GI dysfunction in PD.

Females with PD exhibit faster disease progression and higher mortality rates than males[10]. In addition, females with PD report more GI symptoms with higher severity,[11-13] including constipation and abdominal pain, symptoms that heavily impact quality of life[14] and are among the earliest PD symptoms.[15,16] Aggregation of aSyn in the intestinal wall alters gut immune populations[17], and sex differences in immune responses are abundant systemically,[18] and peripherally in the gut mucosal immune system.[19] Roles of peripheral immune influence on enteric neurons and epithelial populations involved in prodromal PD gut symptomology are not well elucidated. Evidence on the role of sex in neurodegenerative disease[11,20,21] along with the current study underscores the importance of including sex as a biological variable in gut focused PD investigations.

[4] Templeton HA, Ehrlich AT, Schwerdtfeger LA, Sheng JA, Tjalkens RB, Tobet SA. Sex specific effects of environmental toxin-derived alpha synuclein on enteric neuronal-epithelial interactions. *Neurogastroenterology and Motility. In Press*. 2025

Calcitonin gene related peptide (CGRP) is a neuropeptide implicated in regulation of GI motility, inflammation, and nociception through dorsal root ganglia (DRG) afferents[22] and intrinsic enteric neurons.[23,24] There are two forms of CGRP, α and β, which share around 90% homology[25] and have nearly identical biological activity.[26,27] While not extensively characterized, there are likely classes of intrinsic sensory neurons (IPANs) in the myenteric plexus that express βCGRP[28,29] and αCGRP[30]. Therapeutic interventions targeting αCGRP significantly inhibit colonic transit, leading to constipation,[31,32] while elevated αCGRP is associated with diarrhea suggesting that αCGRP plays a role in GI motility.[31] Gut mucus regulates intestinal transit by acting as a lubricant to decrease physical resistance, and altered mucus levels influence GI transit time.[33,34] CGRP produced by enteric neurons modulates goblet cell mucus secretion,[35] as well as motility[36], further pointing towards CGRP involvement in intestinal transit regulation. Accumulation of aSyn in enteric neurons likely influences gut motility, driven by cholinergic neurons.[37,38] However, the impact of aSyn accumulation in subsets of enteric cholinergic neurons, including $CGRP^+$ cells, on mucosal neuroepithelial signaling remains to be seen. Determining if enteric $CGRP^+$ neurons and mucosal projecting fibers accumulate aSyn in a mouse model of PD would provide valuable data towards understanding the altered GI function observed in PD.

To investigate the relationship of sex in aSyn accumulation in enteric CGRP fibers and provide a read out of goblet cell morphological alterations, a rotenone model of PD was utilized. Levels of aSyn were quantified in CGRP expressing myenteric neurons and mucosal fibers. In addition, goblet cell anatomic localization and morphology were analyzed. Data from the present study underscores the importance of examining sex selective mechanisms in PD related GI dysfunction, providing crucial insights into some of the earliest prodromal symptoms in PD.

[4] Templeton HA, Ehrlich AT, Schwerdtfeger LA, Sheng JA, Tjalkens RB, Tobet SA. Sex specific effects of environmental toxin-derived alpha synuclein on enteric neuronal-epithelial interactions. *Neurogastroenterology and Motility. In Press*. 2025

Materials and Methods:

Animals. Male and female C57BL/6J background mice aged 3-4 months were used for these studies. All animal protocols were approved by the Institutional Animal Care and Use Committee (IACUC) and Colorado State University Lab Animal Resources under protocol CoA # 1657. Mice were housed on a 12-h light/dark cycle with access to standard chow (Envigo TD.2918) and water *ad libitum*.

Rotenone Preparation and Injections. Rotenone was prepared as a 50x stock dissolved in 100% dimethyl sulfoxide (DMSO) and stored in amber septa vials at -20°C. This solution was then diluted in medium-chain triglyceride, Miglyol 812 N, to obtain a final concentration of 2.5 mg/mL rotenone in 98% Miglyol 812 N, 2% DMSO. Rotenone was prepared fresh every other day. Mice were weighed every day and received intraperitoneal injections at a dose of 2µL/g body weight once daily for 14 days. The optimal dose was determined in a previous publication.[39] Fourteen days after the last rotenone injection, mice were deeply anesthetized with isoflurane and terminated via decapitation. The intestine was removed from stomach to colon and placed in 4% paraformaldehyde (PFA) at 4°C for 24 h. Tissue was subsequently placed in 1X phosphate buffered saline (PBS) at 4°C until sectioning.

Immunohistochemistry. 50 µm thick sections were prepared from 1-3 mm pieces of proximal colon and submerged in 4% agarose. The tissue was in agarose for a total of 9 minutes: 5 min on a room temperature shaker, and 4 min at 4°C to ensure polymerization. Tissue was cut at a thickness of 50 µm on a vibrating microtome (VT1000S; Leica microsystems, Wetzlar, Germany). Sections were washed in 1x PBS for 10 minutes at 4°C and incubated in 0.1M glycine for 30 min at 4°C, followed by three 5 min PBS washes. Next, tissue sections were

[4] Templeton HA, Ehrlich AT, Schwerdtfeger LA, Sheng JA, Tjalkens RB, Tobet SA. Sex specific effects of environmental toxin-derived alpha synuclein on enteric neuronal-epithelial interactions. *Neurogastroenterology and Motility. In Press*. 2025

incubated in 0.5% sodium borohydride at 4°C for 15 min, followed by three 5 min PBS washes. Sections were blocked in PBS with 5% normal goat serum (NGS; Lampire Biological, Pipersville, PA), 1% hydrogen peroxide, and 0.3% Triton X (Tx) for 1 hr at 4°C with a change of solution at 30 min. Following blocking, sections were placed into primary antisera or lectin outlined in Table 3.

Table 3. Primary antibodies/lectin used.

Primary Antibody/Lectin	Immunizing Antigen	Raised	Dilution	Source	Catalog Number
PGP9.5	Recombinant full length human UCHL1 purified from E. coli	Chicken	1:500	Novus Biologicals	NB110-58872SS
CGRP	Full length rat α-CGRP	Rabbit	0.625µg/mL	ImmunoStar	24112
aSyn	Rabbit α-synuclein (D37A6)	Rabbit	1:500	Cell Signaling	4179
UEA-1, Rhodamine	N/A	N/A	0.625µg/mL	Vector Labs	RL-1062-2

Goblet Cell Lectin Histochemistry

The lectin Ulex Europaeus Agglutinin I conjugated with Rhodamine (UEA-1; Vector Labs) was used at a concentration of 0.625µg/mL in PBS containing 5% NGS and 0.3% Tx for 2 days at 4°C. Sections were then washed four times at 15 min intervals in PBS with 0.02% Tx, followed by four PBS washes. Finally, sections were mounted on slides, and cover slipped with an aqueous mounting medium (Aqua-Poly/Mount, Polysciences, Warrington, PA).

PGP9.5 and aSyn Immunohistochemistry

Sections were incubated for 2 days at 4°C in primary antisera containing anti-Protein Gene Product (PGP) 9.5 (Novus Biologicals, Centennial, CO) at 1:500 and anti-alpha-Synuclein (Cell

[4] Templeton HA, Ehrlich AT, Schwerdtfeger LA, Sheng JA, Tjalkens RB, Tobet SA. Sex specific effects of environmental toxin-derived alpha synuclein on enteric neuronal-epithelial interactions. *Neurogastroenterology and Motility. In Press*. 2025

Signaling, Danvers, MA) at 1:500 in PBS containing 5% NGS and 0.3% Tx. The aSyn antibody labels total aSyn per the vendor and several publications.[40-42] Following primary antisera incubation, sections were washed at room temperature in PBS with 1% NGS and 0.32% Tx four times at 15 min intervals. Sections were then incubated for two hours in secondary antibodies to the appropriate species (Alexa Fluor 405 anti-rabbit and Alexa Fluor 568 anti-chicken; Table 4) at 1:500 constituted in PBS with 0.32% Tx. Following secondary antibody incubation, sections were washed four times at 15 min intervals in PBS with 0.02% Tx, followed by four PBS washes. Finally, sections were mounted on slides, and cover slipped with an aqueous mounting medium (Aqua-Poly/Mount, Polysciences, Warrington, PA).

Table 4. Secondary antibodies used.

Secondary Antibody	Conjugate	Dilution	Source	Catalog Number
Goat anti-rabbit IgG	Alexa Fluor 405	1:500	Invitrogen	A-31556
Goat anti-chicken IgY	Alexa Fluor 568	1:500	Abcam	ab175477
Goat anti-rabbit IgG	Alexa Fluor 594	1:500	Invitrogen	A-11037
Goat anti-rabbit IgG	Alexa Fluor 647	1:500	Invitrogen	A-31573
Biotin-SP donkey anti-rabbit IGG	Biotin-SP	1:2500	Jackson ImmunoResearch	711065152

CGRP and aSyn *Immunohistochemistry*

Sections were incubated for 2 days at 4°C in primary antisera containing anti-aSyn (Cell Signaling, Danvers, MA) at 1:500 in PBS containing 5% normal donkey serum (NDS) and 0.3% Tx. A negative control of the aSyn antibody revealed no signal (**Fig. 10C**). Sections were then

[4] Templeton HA, Ehrlich AT, Schwerdtfeger LA, Sheng JA, Tjalkens RB, Tobet SA. Sex specific effects of environmental toxin-derived alpha synuclein on enteric neuronal-epithelial interactions. *Neurogastroenterology and Motility. In Press*. 2025

washed four times at 15 min intervals in PBS with 1% NDS and 0.32% Tx at room temperature. Next, sections were incubated for 2 hr at room temperature in biotinylated donkey-anti-rabbit (Table 2, Jackson ImmunoResearch Laboratories Inc, West Grove, PA) at 1:2500 constituted in PBS with 0.32% Tx. Sections were washed four times at 15 min intervals in PBS with 0.02% Tx at room temperature before incubation in Alexa Fluor 594-streptavidin (Invitrogen) at 1:500 for 1 hr. Sections were then washed four times at 15 min intervals in PBS with 0.02% Tx at room temperature. Sections were incubated for 2 days at 4°C in primary antisera containing anti-αCGRP (ImmunoStar, Hudson, WI) at 0.625µg/mL in PBS containing 5% NGS and 0.3% Tx. Of note, this antibody likely labels a small percentage of βCGRP, however, signal was only partially extinguished in βCGRP pre-absorption studies performed by the vendor. A pre-absorption with full length αCGRP peptide (AnaSpec, Fremont, CA) eliminated signal (**Fig. 10A**) and there was no signal in controls with secondary antisera omitted (**Fig. 10B**). Following primary antibody incubation, sections were then washed four times at 15 min intervals in PBS with 0.02% Tx before incubation in Alexa Fluor 647 (Table 2, Invitrogen, Waltham, MA) at 1:500 for 2 hr at room temperature. Sections were then washed four times at 15 min intervals in PBS with 0.02% Tx, followed by four PBS washes. Finally, sections were mounted on slides, and cover slipped with an aqueous mounting medium (Aqua-Poly/Mount, Polysciences, Warrington, PA).

[4] Templeton HA, Ehrlich AT, Schwerdtfeger LA, Sheng JA, Tjalkens RB, Tobet SA. Sex specific effects of environmental toxin-derived alpha synuclein on enteric neuronal-epithelial interactions. *Neurogastroenterology and Motility. In Press*. 2025

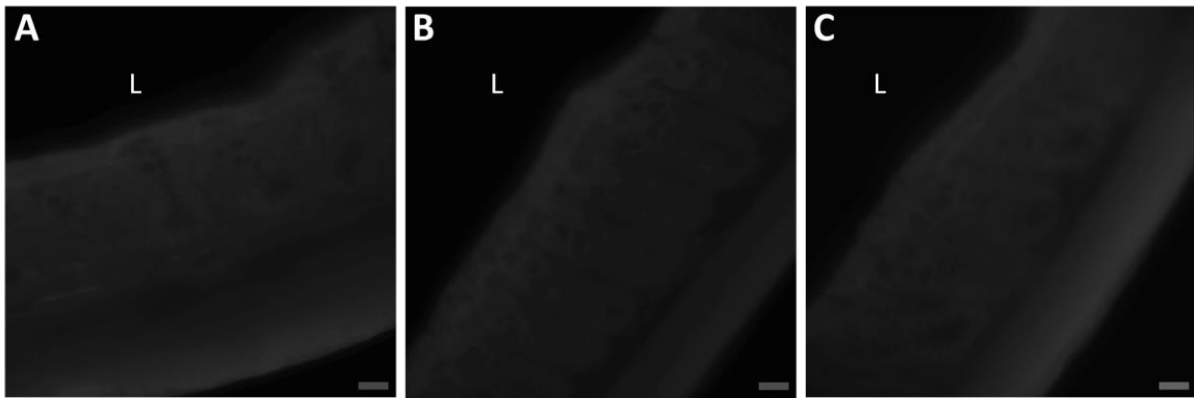

Figure 10. Images of control studies of αCGRP and aSyn antibodies. (**A**) Pre-absorption with full length αCGRP peptide revealed no signal. (**B**) αCGRP primary antibody with secondary antisera omitted revealed no signal. (**C**) aSyn primary antibody with secondary antisera omitted revealed no signal.

Tissue Imaging & Analysis. Images were taken using a Zeiss LSM800 upright confocal laser scanning microscope and a 40x or 63x (EC Plan-Neofluar) oil immersion objective. High resolution images were taken using a Zeiss LSM880 upright confocal microscope with an Axiocam 503 monochromatic camera and a 63x (Plan-Apochromat) oil immersion objective. Data for CGRP and aSyn and goblet cell analyses was gathered from confocal Z-stacks with 15 planes 1 µm apart with the top and bottom planes set from the focus of labeling. Max intensity Z-projections were performed, and regions of interest (ROIs) were defined as the apical or basal half of a crypt. Apical and basal regions were defined by measuring the length of a crypt and dividing it into two equal parts. ROIs were gathered from 12 crypts per animal and averaged. aSyn and PGP 9.5 analyses were gathered from individual, single plane confocal images. Control areas for aSyn and PGP9.5 colocalization were initially defined as muscle regions with no PGP9.5-ir. These regions had no aSyn-ir. Twelve 50 µm x 50 µm ROIs containing aSyn and PGP 9.5 double labeling were selected per sample. aSyn and CGRP analyses were gathered from 20 µm z-projection confocal images. The apical half of six crypts and six myenteric neurons containing aSyn and CGRP double labeling were selected per animal from 20 µm z-

[4] Templeton HA, Ehrlich AT, Schwerdtfeger LA, Sheng JA, Tjalkens RB, Tobet SA. Sex specific effects of environmental toxin-derived alpha synuclein on enteric neuronal-epithelial interactions. *Neurogastroenterology and Motility. In Press*. 2025

projection confocal and subsequently averaged. All image acquisition and analyses were performed by a researcher blinded to treatment. All image analyses were performed using Fiji (v1.0; NIH). Goblet cell quantity and size was measured using the analyze particles tool in Fiji. Images were thresholded based on optical density and a binary watershed was applied prior to quantification. Mean goblet cell size was calculated based off of the area as measured by analyze particles for individual anatomic ROIs as described above. Immunoreactive percentage of area labeled was calculated using the 'measure' tool in Fiji on thresholded images restricted to the defined ROI for each respective analysis. To determine the % area of aSyn in CGRP neurons/fibers, thresholded CGRP-IR images were used to generate ROIs using the analyze particles tool. Thresholded aSyn-IR images were then analyzed using CGRP ROIs as area restrictions. Then, the percentage of total CGRP-IR area that contained aSyn-IR was calculated.

2.5 Statistics. All statistical analyses were performed using Graphpad Prism version 10.1.2 (Graphpad Software, La Jolla, CA). For aSyn and PGP 9.5 average area, CGRP area, and percent area of aSyn in CGRP, a two-way ANOVA was performed by treatment and sex. For goblet cell number and size, a three-way ANOVA was performed by treatment, region, and sex. All data are presented as means +/- standard error of the mean (SEM). In all instances where p values are noted, a post hoc Tukey's multiple comparison test was performed to compare individual means. A Brown-Forsythe equality of variance test was performed for all two-way ANOVAs to confirm variances were not significantly different across groups. For three-way ANOVAs, a Spearman's test for heteroscedasticity was used to confirm equal error.

[4] Templeton HA, Ehrlich AT, Schwerdtfeger LA, Sheng JA, Tjalkens RB, Tobet SA. Sex specific effects of environmental toxin-derived alpha synuclein on enteric neuronal-epithelial interactions. *Neurogastroenterology and Motility. In Press*. 2025

Results:

Rotenone Treatment Increased Myenteric Plexus aSyn

To verify that mice responded to rotenone treatment, body weight was measured daily throughout the entirety of the experiment. The experimental timeline is outlined in **Figure 11A**. Mice had similar starting body weights regardless of treatment group (vehicle: 24.2 g +/-5, rotenone: 21.8 g +/- 0.8) (**Fig.11B**). Change in weight was measured by subtracting starting weight from each daily weight measurement. Rotenone treatment resulted in blunted weight gain in males (**Fig. 11C**) and females (**Fig. 11D**). As a further measurement of rotenone impact, a researcher blind to treatment correctly identified treatment groups based on a five-minute open field behavior test. Rotenone treated mice exhibited decreased exploratory movement and alterations in gait, similar to our previous findings.[39]

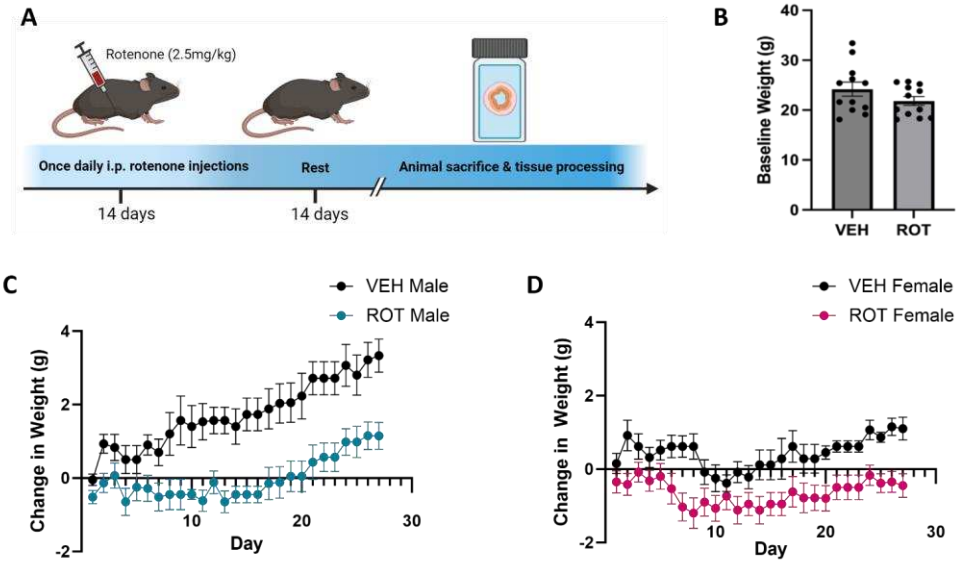

Figure 11. Rotenone blunted weight gain in males and females. (**A**) Overview of experimental timeline. (**B**) Baseline weights of male and female vehicle vs. rotenone mice. (**C**) Average change in weight from baseline in males. (**D**) Average change in weight from baseline in females. VEH = vehicle, ROT = rotenone.

[4] Templeton HA, Ehrlich AT, Schwerdtfeger LA, Sheng JA, Tjalkens RB, Tobet SA. Sex specific effects of environmental toxin-derived alpha synuclein on enteric neuronal-epithelial interactions. *Neurogastroenterology and Motility. In Press*. 2025

Following behavioral confirmation of impairment, intestinal sections were analyzed for myenteric neuronal changes using a peripheral neuronal marker, PGP 9.5. Total aSyn area increased in myenteric PGP 9.5^{+} neurons in males and females after 2 weeks of rotenone treatment, with an increase in immunoreactive (ir) aSyn of 203% in females (1.5 µm^2 +/- 0.1, $p<0.0001$) and 50% in males (1.3 µm^2 +/- 0.04, $p<0.05$) (**Fig. 12A,B**) compared to vehicle treated animals (females: 0.49 +/- 0.10, $p > 0.05$; males: 0.84 +/-0.11, $p > 0.05$). A two-way ANOVA revealed a main effect of rotenone treatment ($F(1,20) = 60.50$, $p < 0.0001$) and a

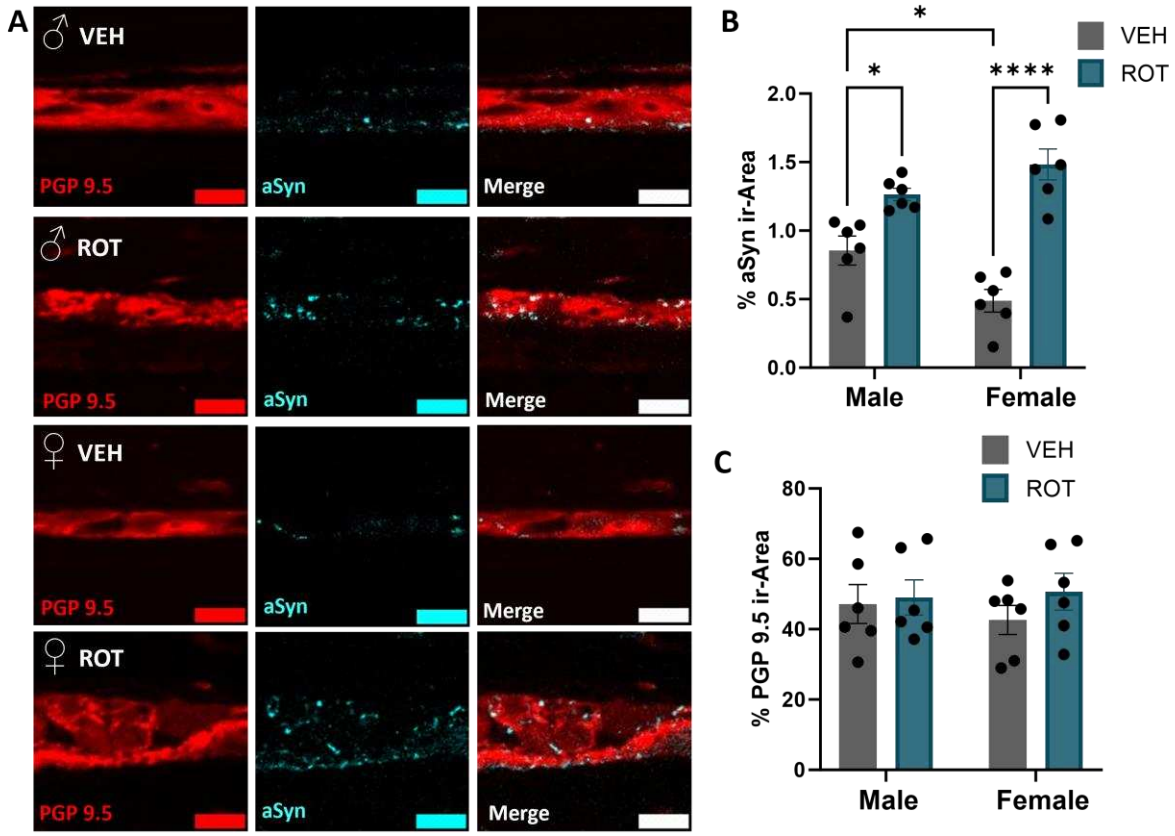

Figure 12. Myenteric plexus aSyn was greater in colons from rotenone treated mice. (**A**) Compared to vehicle both male and female proximal colon showed greater aSyn immunoreactivity in myenteric neurons with rotenone treatment. Females exhibited larger a larger increase in myenteric aSyn than males. (**B**) Quantification of aSyn immunoreactivity in the myenteric plexus. (**C**) Quantification of PGP 9.5 immunoreactivity in the myenteric plexus. Scale bars are 15 µm, *p<0.05, **p<0.003 ****p<0.0001. VEH = vehicle, ROT = rotneone, aSyn = alpha synuclein, PGP9.5 = protein gene product 9.5.

[4] Templeton HA, Ehrlich AT, Schwerdtfeger LA, Sheng JA, Tjalkens RB, Tobet SA. Sex specific effects of environmental toxin-derived alpha synuclein on enteric neuronal-epithelial interactions. *Neurogastroenterology and Motility. In Press*. 2025

significant interaction between sex and rotenone ($F(1,20) = 10.55$, $p < 0.01$) indicating that rotenone's impact was reliably greater in females. This was due in part to vehicle treated females starting with 58% (0.49 μm^2 +/- 0.07) less immunoreactive myenteric aSyn than vehicle treated males ($p<0.05$, **Fig. 12B**). PGP 9.5-ir area was not different in males vs. females after rotenone treatment (Interaction effect: $F(1,17) = 0.177$, $p > 0.05$) (**Fig. 12**) indicating that increases in aSyn area were not a result of elevated ir-PGP 9.5^+ cell area.

Apical CGRP Fiber Quantities Elevated in Rotenone Treated Mice

CGRP fiber immunoreactivity was interrogated by crypt region (i.e., apical crypt vs. basal crypt) in separate two-way ANOVAs. In apical crypts, CGRP levels were greater in rotenone treated animals ($F(1,20) = 61.93$, $p < 0.0001$) (**Fig. 13A,C**). This increase was 26% higher in females compared to males ($F(1,20) = 9.74$, $p < 0.01$) (**Fig. 13C**), driven by the rotenone treated groups, as there was no difference by sex in vehicle ($F(1,20) = 2.89$, $p > 0.05$) and no sex by treatment interaction.

In basal crypt regions, the average percent area of CGRP-ir was low in males and females. There was, however, a main effect of sex ($F(1,20) = 13.2$, $p < 0.05$) where male vehicle treated animals had elevated basal CGRP-ir compared to vehicle treated females (**Fig. 13D**). The interaction of sex by treatment was not statistically significant suggesting some reliability to the sex effect even though the sex difference between treated mice was small.

[4] Templeton HA, Ehrlich AT, Schwerdtfeger LA, Sheng JA, Tjalkens RB, Tobet SA. Sex specific effects of environmental toxin-derived alpha synuclein on enteric neuronal-epithelial interactions. *Neurogastroenterology and Motility. In Press*. 2025

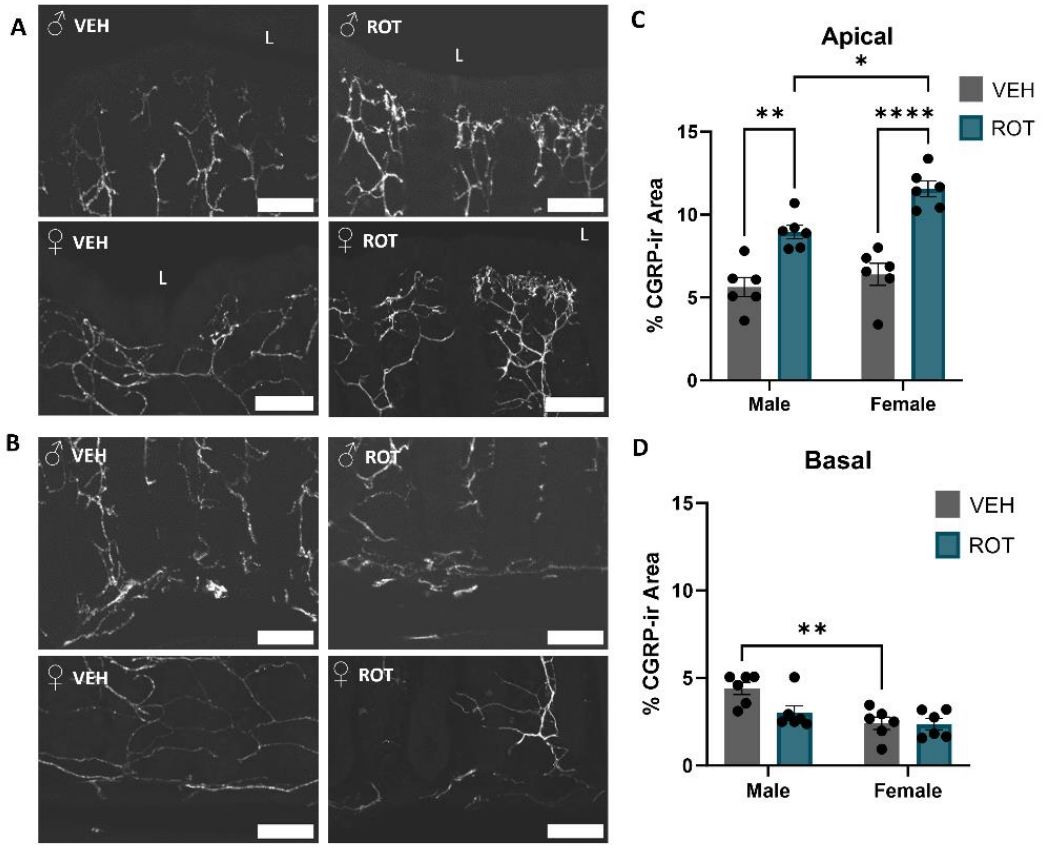

Figure 13. Apical CGRP⁺ fiber quantities were elevated in colon crypts from rotenone treated mice. (**A**) Rotenone treatment increased the apical percent area of CGRP⁺ fibers in males and females. (**B**) Rotenone treatment did not alter basal percent area of CGRP⁺ fibers in males and females. (**C**) Quantification of average perecent area of CGRP immunoreactivity in the apical crypt. (**D**) Quantification of average perecent area of CGRP immunoreacity in the basal crypt. Scale bars are 50 µm, L = lumen, *p<0.05, **p<0.003 ****p<0.0001. VEH = vehicle, ROT = rotenone, CGRP = calcitonin gene related peptide.

Rotenone Treatment Increased aSyn in CGRP⁺ Myenteric Neurons and Apical Fibers

Immunoreactive aSyn was colocalized with CGRP⁺ myenteric neurons and apical mucosal fibers in a sex selective manner (**Fig. 14**). Two-way ANOVA investigating aSyn in CGRP⁺ myenteric neurons revealed a main effect of rotenone treatment ($F(1,20) = 58.37$, $p < 0.0001$). The percent area of aSyn in myenteric CGRP neurons (**Fig. 14A,B**) was greater in males and

[4] Templeton HA, Ehrlich AT, Schwerdtfeger LA, Sheng JA, Tjalkens RB, Tobet SA. Sex specific effects of environmental toxin-derived alpha synuclein on enteric neuronal-epithelial interactions. *Neurogastroenterology and Motility. In Press*. 2025

females treated with rotenone (male 12% +/- 1.2; female 10% +/-0.6) compared to vehicle (male 4.8% +/- 0.7, $p < 0.0001$; female 4.7% +/- 0.7, $p < 0.005$) (**Fig. 14A**). Levels of aSyn in apical $CGRP^+$ fibers (**Fig. 14C,D,E**) were increased in rotenone treated mice ($F(1,20) = 116.7$, $p < 0.0001$), of both sexes ($F(1,20) = 6.21$, $p < 0.05$), however, females had a larger increase as demonstrated by a statistically significant interaction between sex and treatment ($F(1,20) = 6.57$, $p < 0.05$). The percent area of aSyn in apical CGRP fibers was elevated in males (vehicle: 0.04% +/- 0.02, rotenone: 0.9% +/- 0.1, $p < 0.0001$) and females (vehicle: female 0.04% +/- 0.02, rotenone: 1.5% +/- 0.2, $p < 0.0001$) (**Fig. 14E**). This increase was 66.57% higher in female animals compared to males ($p < 0.01$) (**Fig. 14E**). To confirm this increase was not due to greater apical $CGRP^+$-IR in rotenone treated animals, the ratio of aSyn-IR to apical CGRP was assessed. The ratio of aSyn-IR to apical CGRP-IR (**Fig. 14F**) was increased in rotenone treated mice ($F(1,20) = 47.94$, $p < 0.0001$), of both sexes ($F(1,20) = 4.88$, $p = 0.05$), however, females had a larger increase as demonstrated by a statistically significant interaction between sex and treatment ($F(1,20) = 4.879$, $p < 0.05$). The ratio of aSyn-IR to CGRP-IR was elevated in males (vehicle: 0.0002 +/- 0.0001, rotenone: 0.003 +/- 0.007) and females (vehicle: 9.8e-05 +/- 5e-05, rotenone: 0.006 +/- 0.001) in rotenone treated mice compared to vehicle. This increase was 50% higher in female animals compared to males ($p < 0.05$).

[4] Templeton HA, Ehrlich AT, Schwerdtfeger LA, Sheng JA, Tjalkens RB, Tobet SA. Sex specific effects of environmental toxin-derived alpha synuclein on enteric neuronal-epithelial interactions. *Neurogastroenterology and Motility. In Press*. 2025

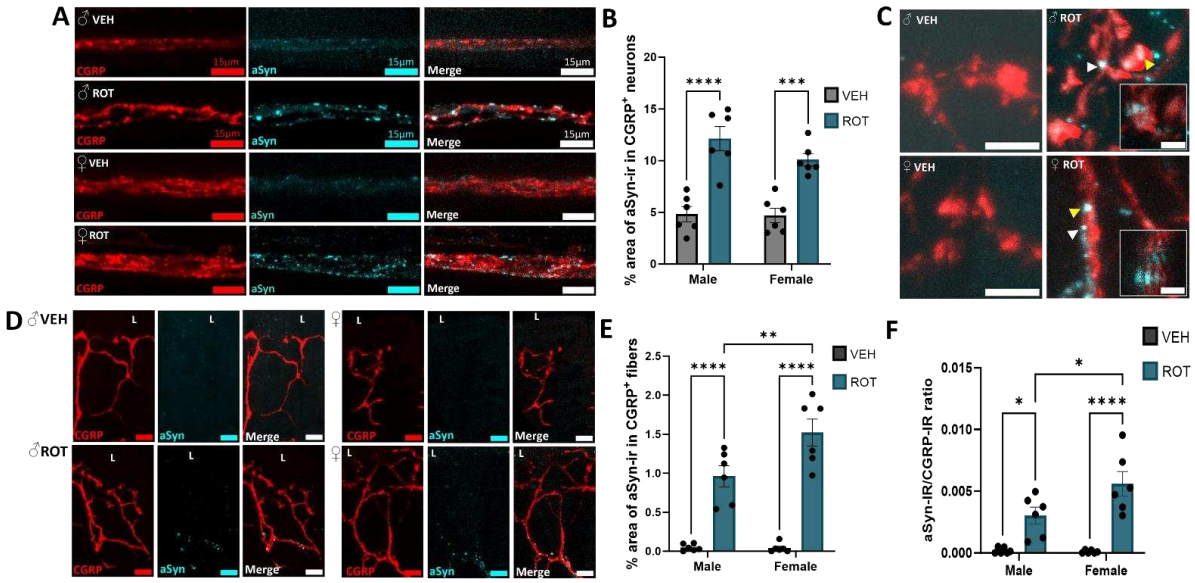

Figure 14. Rotenone treatment increased aSyn in CGRP+ myenteric neurons and apical fibers. (**A**) Rotenone treatement increased the percent area of aSyn in myenteric CGRP neurons in males and females. (**B**) Rotenone treatment increased the percent area of aSyn in apical CGRP fibers in males and females. (**C**) High resolution images of aSyn-ir in apcial CGRP varicosities. Arrows indicate areas of CGRP and aSyn colocalization, white arrows indicate region of inset. Insets are volume rendered cross-sections taken at a 60 degree angle. (**D**) Quantification of percent area of aSyn immunoreactivy in myenteric CGRP^{+} neurons. (**E**) Quantification of percent area of aSyn immunoreactivity in apical CGRP^{+} fibers. (**F**) Quantification of ratio of aSyn-IR in CGRP-IR fibers. Scale bars are 15 µm for A & D, for C scale bars are 5 µm and 2 µm for insets. L = lumen, * p<0.05, **p<0.01, ****p<0.0001. VEH = vehicle, ROT = rotenone, CGRP = calcitonin gene related peptide, aSyn = alpha synuclein.

Goblet Cells Altered Morphologically After Rotenone Treatment

Mucopolysaccharides were fluorescently labeled with the lectin Ulex Europaeus Agglutinin I (UEA1) and goblet cell size and number were analyzed by crypt region (i.e., apical vs. basal, **Fig. 15**). A three-way ANOVA revealed a main effect of region ($F(1,40) = 82.41$, $p < 0.001$) where apical goblet cell numbers were lower in animals treated with rotenone ($F(1,40) = 12.92$, $p < 0.001$) regardless of sex ($F(1,40) = 1.4$, $p > 0.05$) (**Fig. 15A-C**). Males treated with rotenone had 53% fewer apical goblet cells (5.0 +/- 0.1) (**Fig. 15B**) compared to vehicle (10.0 +/- 0.4, $p < 0.0001$) (**Fig. 15A, C**) and rotenone treated females had 48% fewer cells (4.0 +/- 0.2)

[4] Templeton HA, Ehrlich AT, Schwerdtfeger LA, Sheng JA, Tjalkens RB, Tobet SA. Sex specific effects of environmental toxin-derived alpha synuclein on enteric neuronal-epithelial interactions. *Neurogastroenterology and Motility. In Press*. 2025

compared to vehicle (8.0 +/- 0.5, $p < 0.0001$). Vehicle treated males had 20% higher baseline goblet cell counts compared to females restricted to the apical region ($F(1,40) = 13.07$, $p < 0.001$) (**Fig. 15C)**. There were 20% fewer basal goblet cells after rotenone treatment in males (10.0 +/- 0.6) (**Fig. 15B'**) compared to vehicle (8.0 +/- 0.3, $p < 0.05$) (**Fig. 15A'**) that did not reach statistical significance by posthoc testing in females (**Fig. 15C**).

In contrast to fewer goblet cells after rotenone, those goblet cells that remained were larger. A three-way ANOVA investigating goblet cell size revealed a main effect of region ($F(1,40) = 34.34$, $p < 0.001$) where goblet cell size was greater in rotenone treated animals selectively in the apical crypt regions ($F(1,40) = 12.36$, $p < 0.001$), with no main effect of sex ($F(1,40) = 1.14$, $p > 0.05$) (**Fig. 15D**). There was a main effect of treatment ($F(1,40) = 40.95$, $p <$

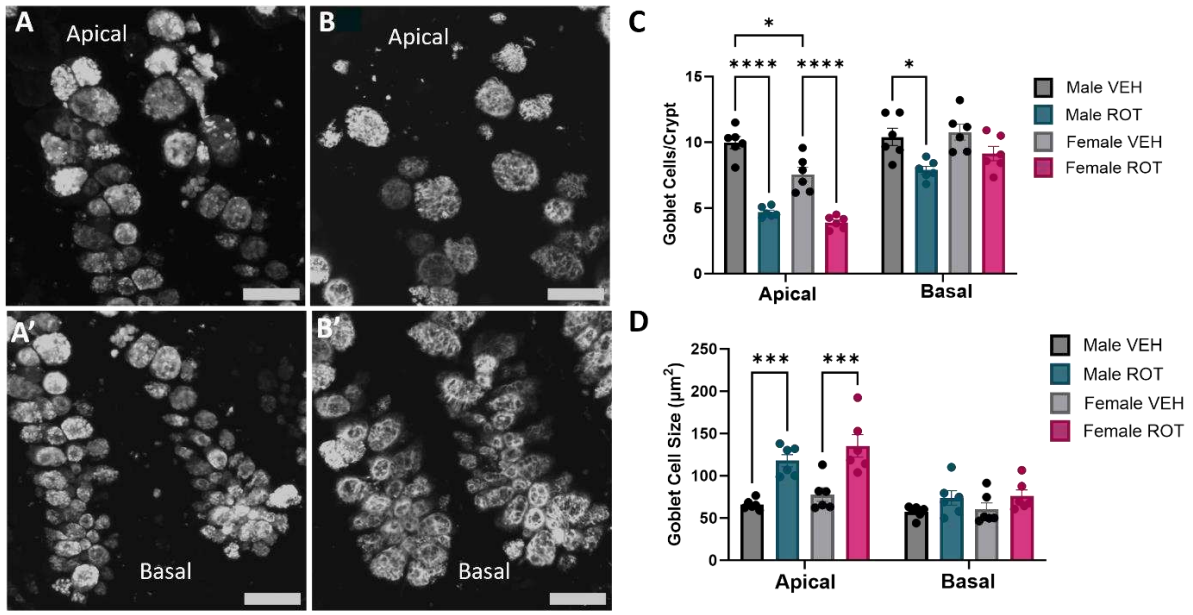

Figure 15. UEA1⁺ goblet cells altered morphologically after rotenone treatment. (**A**) UEA1⁺ goblet cells at the apex and (**A'**) base of the crypt in vehicle treated tissue have a smaller average immunoreactive area and are fewer in number than (**B**) UEA1⁺ goblet cells at the apex and (**B'**) base of the crypt in rotenone treated tissue. (**C**) Quantification of UEA1⁺ goblet cell number and (**D**) UEA1⁺ immunoreactive area. Scale bars 25 µm, representative images are male, *p<0.05, ***p<0.001, ****p<0.0001. VEH = vehicle, ROT = rotenone, UEA1 = Ulex Europaeus Agglutinin I.

[4] Templeton HA, Ehrlich AT, Schwerdtfeger LA, Sheng JA, Tjalkens RB, Tobet SA. Sex specific effects of environmental toxin-derived alpha synuclein on enteric neuronal-epithelial interactions. *Neurogastroenterology and Motility. In Press*. 2025

0.0001) where apical goblet cell size was 79% greater in rotenone treated males (117.7 μm^2 +/ 6.1) (**Fig. 15B**) compared to vehicle treated males (65.9 μm^2 +/- 2.1, $p < 0.001$) (**Fig. 15A**) and 74% greater in rotenone treated females (135.3 μm^2 +/- 11.2) compared to those treated with vehicle (77.8 μm^2 +/- 6.7, $p < 0.001$).

Discussion:

Females with PD exhibit faster disease progression and higher mortality rates than males[10]. Using a rotenone mouse model of PD, the results of the current study point towards sex selective changes in enteric aSyn levels, alterations in CGRP distribution, and changes in goblet cell morphology, potentially influencing the more severe outcomes in females with PD. These findings contribute to our understanding of the link between intestinal homeostasis and aSyn aggregation in peripheral PD pathology and may provide insights for advancing early diagnostic strategies. Few studies of peripheral aSyn aggregation or PD pathological etiology include sex as a biological variable. Given that females with PD exhibit a higher mortality rate and report increased severity of GI symptoms,[10,11,43] the present studies provide an indication of potential sex-selective targets of a disease process.

Enteric aSyn levels are elevated in PD,[44] and the pesticide rotenone increases aSyn in the central nervous system[39] and the GI tract.[45] The present study demonstrated that intraperitoneal rotenone injections increased total aSyn in myenteric plexus neurons consistent with pathology found after oral rotenone administration.[45] There was a basal sex difference in myenteric aSyn levels, with males having higher quantities. When treated with rotenone, aSyn levels rose significantly in both sexes, but more so in females. This finding potentially implicates the female myenteric neuronal population as having an altered neurochemical phenotype at baseline, akin to the estrus cycle dependent change in neuronal nitric oxide synthase (nNOS)

[4] Templeton HA, Ehrlich AT, Schwerdtfeger LA, Sheng JA, Tjalkens RB, Tobet SA. Sex specific effects of environmental toxin-derived alpha synuclein on enteric neuronal-epithelial interactions. *Neurogastroenterology and Motility. In Press*. 2025

neuron phenotype.[46] The lower baseline but subsequent post-rotenone compensation of aSyn levels in female CGRP neurons and fibers may influence GI motility and goblet cell secretory function. Together, these data provide a potential explanation for the more severe GI transit dysfunction in PD females. Further investigations of the impact of aSyn on GI motility and neuroepithelial signaling within the context of sex are clearly warranted.[11,14]

Neurons utilizing the neuropeptide CGRP for signaling may be critically involved in regulating intestinal motility and nociception.[31,47,48] Visceral pain is regulated by gut wall components, including the secretions from the microbiome adjacent to the colonic wall, and via enteric neuronal afferent CGRP signaling to the dorsal root ganglia.[22,35,48] Further, agonizing colonic CGRP receptors prior to colonic distention yields elevated visceral pain responses in conventionally colonized mice[22]. The increased $CGRP^+$ apical fiber density observed in this study may contribute to elevated sensitivity to noxious stimuli from the lumen, however, receptor expression patterns for noxious ligands on apical $CGRP^+$ fibers were not investigated in this study. The greater increase in apical CGRP in rotenone-treated females provides a focal point highlighting CGRPs potential involvement in the higher incidence of visceral pain observed in female PD patients. Studies examining CGRP receptor populations along with peptide release in these anatomically distinct enteric regions are needed to identify functional connections among the gut circuits identified here.

Alpha-synuclein aggregation can elicit morphological and firing pattern changes in neuronal populations.[49] Increased aSyn in $CGRP^+$ enteric neurons may modulate downstream CGRP anatomical alterations and signaling patterns. CGRP production is upregulated in damaged nerves[25] and intraperitoneal injections of the CGRP antagonist BIBN 4096 BS decreased central aSyn expression in a mouse model of Alzheimer's disease.[50] Rotenone treated males and females had increased aSyn in $CGRP^+$ myenteric neurons and apical $CGRP^+$

[4] Templeton HA, Ehrlich AT, Schwerdtfeger LA, Sheng JA, Tjalkens RB, Tobet SA. Sex specific effects of environmental toxin-derived alpha synuclein on enteric neuronal-epithelial interactions. *Neurogastroenterology and Motility. In Press*. 2025

fibers, suggesting that aSyn levels may be related to alterations in gut CGRP neuronal immunoreactivity akin to those seen in PD patient derived neuronal cultures.[49,51] Female mice showed a greater increase in aSyn in apical CGRP$^+$ fibers, a greater increase in immunoreactive CGRP in apical regions of colonic crypts, and lower baseline levels of myenteric aSyn compared to males suggesting that females might be more susceptible to aSyn and CGRP localization within neuronal fibers following rotenone treatment.

Underlying causes of constipation, one of the earliest symptoms of PD,[15,16] are multifaceted and treatment with anti-CGRP monoclonal antibodies decreases GI transit.[31,32] Similarly, animal studies with rotenone report decreased intestinal transit.[8,9] In the present study, rotenone treated mice exhibited increased area of CGRP immunoreactive fibers at the apical crypt. One explanation for the association between elevated gut mucosal CGRP and potential aSyn driven constipation is through regulation of mucus production by goblet cells. In the current study there were fewer goblet cells that were larger following rotenone treatment. The impact was stronger apically, coinciding with the greater CGRP fiber density after rotenone. Goblet cells originate from progenitor cells at the base of the crypts and mature as they migrate apically where they acquire the ability to synthesize and secrete mucoplysaccharides.[52] Mature goblet cells are located in the upper third of crypts[53,54] potentially making them more susceptible to morphological changes due to local environmental factors like dense CGRP producing neuronal fibers. While acute stimulation of goblet cells serves as a protective mechanism to bolster the mucosal barrier in response to pathogens,[55] chronic stimulation may lead to goblet cell mucus depletion. Impacts of aSyn driven alterations to goblet cell mucus production and secretion remains unclear. The current results suggest a need to investigate goblet cell mucus production and mucosal thickness to determine if altered CGRP signaling after rotenone leads to mucosal barrier dysfunction.

[4] Templeton HA, Ehrlich AT, Schwerdtfeger LA, Sheng JA, Tjalkens RB, Tobet SA. Sex specific effects of environmental toxin-derived alpha synuclein on enteric neuronal-epithelial interactions. *Neurogastroenterology and Motility. In Press*. 2025

Conclusions:

In conclusion, rotenone treatment reproduced PD clinical findings of increased aSyn in the myenteric plexus and extended these findings to show increases in apical CGRP immunoreactivity and altered goblet cell morphology in colonic crypts. Enteric aSyn may alter CGRP neuronal interactions with goblet cells that are critical for mucus production or secretion. These findings demonstrate a potential pathway for sex selective neuronal-epithelial interaction between CGRP and goblet cells secondary to elevated enteric aSyn, identifying a potential contributor to GI dysfunction in PD. Since GI symptoms arise in a sex specific manner, years before motor dysfunction, understanding mechanisms of enteric aSyn pathophysiology is crucial for identifying early diagnostic markers and novel therapeutic targets.

[4] Templeton HA, Ehrlich AT, Schwerdtfeger LA, Sheng JA, Tjalkens RB, Tobet SA. Sex specific effects of environmental toxin-derived alpha synuclein on enteric neuronal-epithelial interactions. *Neurogastroenterology and Motility. In Press*. 2025

References:

1 de Lau, L. M. & Breteler, M. M. Epidemiology of Parkinson's disease. *Lancet Neurol* **5**, 525-535 (2006). https://doi.org:10.1016/S1474-4422(06)70471-9

2 Fasano, A., Visanji, N. P., Liu, L. W., Lang, A. E. & Pfeiffer, R. F. Gastrointestinal dysfunction in Parkinson's disease. *Lancet Neurol* **14**, 625-639 (2015). https://doi.org:10.1016/S1474-4422(15)00007-1

3 Travagli, R. A., Browning, K. N. & Camilleri, M. Parkinson disease and the gut: new insights into pathogenesis and clinical relevance. *Nat Rev Gastroenterol Hepatol* **17**, 673-685 (2020). https://doi.org:10.1038/s41575-020-0339-z

4 Calabresi, P. *et al.* Alpha-synuclein in Parkinson's disease and other synucleinopathies: from overt neurodegeneration back to early synaptic dysfunction. *Cell Death Dis* **14**, 176 (2023). https://doi.org:10.1038/s41419-023-05672-9

5 Warnecke, T., Schafer, K. H., Claus, I., Del Tredici, K. & Jost, W. H. Gastrointestinal involvement in Parkinson's disease: pathophysiology, diagnosis, and management. *NPJ Parkinsons Dis* **8**, 31 (2022). https://doi.org:10.1038/s41531-022-00295-x

6 Cannon, J. R. *et al.* A highly reproducible rotenone model of Parkinson's disease. *Neurobiol Dis* **34**, 279-290 (2009). https://doi.org:10.1016/j.nbd.2009.01.016

7 Johnson, M. E., Stringer, A. & Bobrovskaya, L. Rotenone induces gastrointestinal pathology and microbiota alterations in a rat model of Parkinson's disease. *Neurotoxicology* **65**, 174-185 (2018). https://doi.org:10.1016/j.neuro.2018.02.013

8 Pan-Montojo, F. *et al.* Environmental toxins trigger PD-like progression via increased alpha-synuclein release from enteric neurons in mice. *Sci Rep* **2**, 898 (2012). https://doi.org:10.1038/srep00898

9 Drolet, R. E., Cannon, J. R., Montero, L. & Greenamyre, J. T. Chronic rotenone exposure reproduces Parkinson's disease gastrointestinal neuropathology. *Neurobiol Dis* **36**, 96-102 (2009). https://doi.org:10.1016/j.nbd.2009.06.017

10 Dahodwala, N., Pei, Q. & Schmidt, P. Sex Differences in the Clinical Progression of Parkinson's Disease. *J Obstet Gynecol Neonatal Nurs* **45**, 749-756 (2016). https://doi.org:10.1016/j.jogn.2016.05.002

11 Chang, H. J. *et al.* Sex differences in gastrointestinal dysfunction among patients with Parkinson's disease. *Neurol Sci* **44**, 2375-2384 (2023). https://doi.org:10.1007/s10072-023-06710-2

12 Xiao-Ling, Q. *et al.* Gender Was Associated with Depression but Not with Gastrointestinal Dysfunction in Patients with Parkinson's Disease. *Parkinsons Dis* **2021**, 3118948 (2021). https://doi.org:10.1155/2021/3118948

13 Picillo, M. *et al.* The PRIAMO study: age- and sex-related relationship between prodromal constipation and disease phenotype in early Parkinson's disease. *J Neurol* **268**, 448-454 (2021). https://doi.org:10.1007/s00415-020-10156-3

14 Pilipovich, A. A., Vorob'eva, O. V., Makarov, S. A., Shindryaeva, N. N. & Vorob'eva, Y. D. Gastrointestinal Dysfunction Impact on Life Quality in a Cohort of Russian Patients with Parkinson's Disease I-III H&Y Stage. *Parkinsons Dis* **2022**, 1571801 (2022). https://doi.org:10.1155/2022/1571801

15 Adams-Carr, K. L. *et al.* Constipation preceding Parkinson's disease: a systematic review and meta-analysis. *J Neurol Neurosurg Psychiatry* **87**, 710-716 (2016). https://doi.org:10.1136/jnnp-2015-311680

16 Cersosimo, M. G. *et al.* Gastrointestinal manifestations in Parkinson's disease: prevalence and occurrence before motor symptoms. *J Neurol* **260**, 1332-1338 (2013). https://doi.org:10.1007/s00415-012-6801-2

17 Perez-Pardo, P. *et al.* Gut-brain and brain-gut axis in Parkinson's disease models: Effects of a uridine and fish oil diet. *Nutr Neurosci* **21**, 391-402 (2018). https://doi.org:10.1080/1028415X.2017.1294555

18 Klein, S. L. & Flanagan, K. L. Sex differences in immune responses. *Nat Rev Immunol* **16**, 626-638 (2016). https://doi.org:10.1038/nri.2016.90

19 Schwerdtfeger, L. A. & Tobet, S. A. Sex differences in anatomic plasticity of gut neuronal-mast cell interactions. *Physiol Rep* **9**, e15066 (2021). https://doi.org:10.14814/phy2.15066

20 Ullah, M. F. *et al.* Impact of sex differences and gender specificity on behavioral characteristics and pathophysiology of neurodegenerative disorders. *Neurosci Biobehav Rev* **102**, 95-105 (2019). https://doi.org:10.1016/j.neubiorev.2019.04.003

21 Philipe de Souza Ferreira, L. *et al.* Sex differences in Parkinson's Disease: An emerging health question. *Clinics (Sao Paulo)* **77**, 100121 (2022). https://doi.org:10.1016/j.clinsp.2022.100121

22 Pujo, J. *et al.* Gut microbiota modulates visceral sensitivity through calcitonin gene-related peptide (CGRP) production. *Gut Microbes* **15**, 2188874 (2023). https://doi.org:10.1080/19490976.2023.2188874

23 Delvalle, N. M. *et al.* Communication Between Enteric Neurons, Glia, and Nociceptors Underlies the Effects of Tachykinins on Neuroinflammation. *Cell Mol Gastroenterol Hepatol* **6**, 321-344 (2018). https://doi.org:10.1016/j.jcmgh.2018.05.009

24 Buckinx, R. *et al.* Transient receptor potential vanilloid type 1 channel (TRPV1) immunolocalization in the murine enteric nervous system is affected by the targeted C-terminal epitope of the applied antibody. *J Histochem Cytochem* **61**, 421-432 (2013). https://doi.org:10.1369/0022155413484764

25 Russell, F. A., King, R., Smillie, S. J., Kodji, X. & Brain, S. D. Calcitonin gene-related peptide: physiology and pathophysiology. *Physiol Rev* **94**, 1099-1142 (2014). https://doi.org:10.1152/physrev.00034.2013

26 Mulderry, P. K. *et al.* Differential expression of alpha-CGRP and beta-CGRP by primary sensory neurons and enteric autonomic neurons of the rat. *Neuroscience* **25**, 195-205 (1988). https://doi.org:10.1016/0306-4522(88)90018-8

27 Noguchi, K., Senba, E., Morita, Y., Sato, M. & Tohyama, M. Alpha-CGRP and beta-CGRP mRNAs are differentially regulated in the rat spinal cord and dorsal root ganglion. *Brain Res Mol Brain Res* **7**, 299-304 (1990). https://doi.org:10.1016/0169-328x(90)90080-w

28 Morarach, K. *et al.* Diversification of molecularly defined myenteric neuron classes revealed by single-cell RNA sequencing. *Nat Neurosci* **24**, 34-46 (2021). https://doi.org:10.1038/s41593-020-00736-x

29 Wright, C. M. *et al.* scRNA-Seq Reveals New Enteric Nervous System Roles for GDNF, NRTN, and TBX3. *Cell Mol Gastroenterol Hepatol* **11**, 1548-1592 e1541 (2021). https://doi.org:10.1016/j.jcmgh.2020.12.014

30 Nestor-Kalinoski, A. *et al.* Unique Neural Circuit Connectivity of Mouse Proximal, Middle, and Distal Colon Defines Regional Colonic Motor Patterns. *Cell Mol Gastroenterol Hepatol* **13**, 309-337 e303 (2022). https://doi.org:10.1016/j.jcmgh.2021.08.016

31 Ailani, J. *et al.* Role of Calcitonin Gene-Related Peptide on the Gastrointestinal Symptoms of Migraine-Clinical Considerations: A Narrative Review. *Neurology* **99**, 841-853 (2022). https://doi.org:10.1212/WNL.0000000000201332

32 Haanes, K. A., Edvinsson, L. & Sams, A. Understanding side-effects of anti-CGRP and anti-CGRP receptor antibodies. *J Headache Pain* **21**, 26 (2020). https://doi.org:10.1186/s10194-020-01097-3

33 Fang, F. *et al.* Slowed Intestinal Transit Induced by Less Mucus in Intestinal Goblet Cell Piezo1-Deficient Mice through Impaired Epithelial Homeostasis. *Int J Mol Sci* **24** (2023). https://doi.org:10.3390/ijms241814377

34 Gao, C. C. *et al.* Rhubarb extract relieves constipation by stimulating mucus production in the colon and altering the intestinal flora. *Biomed Pharmacother* **138**, 111479 (2021). https://doi.org:10.1016/j.biopha.2021.111479

35 Yang, D. *et al.* Nociceptor neurons direct goblet cells via a CGRP-RAMP1 axis to drive mucus production and gut barrier protection. *Cell* **185**, 4190-4205 e4125 (2022). https://doi.org:10.1016/j.cell.2022.09.024

36 Grider, J. R. CGRP as a transmitter in the sensory pathway mediating peristaltic reflex. *Am J Physiol* **266**, G1139-1145 (1994). https://doi.org:10.1152/ajpgi.1994.266.6.G1139

37 Sharrad, D. F., de Vries, E. & Brookes, S. J. Selective expression of alpha-synuclein-immunoreactivity in vesicular acetylcholine transporter-immunoreactive axons in the guinea pig rectum and human colon. *J Comp Neurol* **521**, 657-676 (2013). https://doi.org:10.1002/cne.23198

38 Swaminathan, M., Fung, C., Finkelstein, D. I., Bornstein, J. C. & Foong, J. P. P. alpha-Synuclein Regulates Development and Function of Cholinergic Enteric Neurons in the Mouse Colon. *Neuroscience* **423**, 76-85 (2019). https://doi.org:10.1016/j.neuroscience.2019.10.029

39 Rocha, S. M. *et al.* Rotenone induces regionally distinct alpha-synuclein protein aggregation and activation of glia prior to loss of dopaminergic neurons in C57Bl/6 mice. *Neurobiol Dis* **167**, 105685 (2022). https://doi.org:10.1016/j.nbd.2022.105685

40 Cao, B. *et al.* PDCD4 triggers alpha-synuclein accumulation and motor deficits via co-suppressing TFE3 and TFEB translation in a model of Parkinson's disease. *NPJ Parkinsons Dis* **10**, 146 (2024). https://doi.org:10.1038/s41531-024-00760-9

41 Yu, M. *et al.* Functional screening of lysosomal storage disorder genes identifies modifiers of alpha-synuclein neurotoxicity. *PLoS Genet* **19**, e1010760 (2023). https://doi.org:10.1371/journal.pgen.1010760

42 Uemura, N. *et al.* alpha-Synuclein aggregates amplified from patient-derived Lewy bodies recapitulate Lewy body diseases in mice. *Nat Commun* **14**, 6892 (2023). https://doi.org:10.1038/s41467-023-42705-5

43 Cerri, S., Mus, L. & Blandini, F. Parkinson's Disease in Women and Men: What's the Difference? *J Parkinsons Dis* **9**, 501-515 (2019). https://doi.org:10.3233/JPD-191683

44 Gold, A., Turkalp, Z. T. & Munoz, D. G. Enteric alpha-synuclein expression is increased in Parkinson's disease but not Alzheimer's disease. *Mov Disord* **28**, 237-240 (2013). https://doi.org:10.1002/mds.25298

45 Dodiya, H. B. *et al.* Chronic stress-induced gut dysfunction exacerbates Parkinson's disease phenotype and pathology in a rotenone-induced mouse model of Parkinson's disease. *Neurobiol Dis* **135**, 104352 (2020). https://doi.org:10.1016/j.nbd.2018.12.012

46 Balasuriya, G. K., Nugapitiya, S. S., Hill-Yardin, E. L. & Bornstein, J. C. Nitric Oxide Regulates Estrus Cycle Dependent Colonic Motility in Mice. *Front Neurosci* **15**, 647555 (2021). https://doi.org:10.3389/fnins.2021.647555

47 Iyengar, S., Ossipov, M. H. & Johnson, K. W. The role of calcitonin gene-related peptide in peripheral and central pain mechanisms including migraine. *Pain* **158**, 543-559 (2017). https://doi.org:10.1097/j.pain.0000000000000831

48 Clifton, M. S. *et al.* Role of calcitonin receptor-like receptor in colonic motility and inflammation. *Am J Physiol Gastrointest Liver Physiol* **293**, G36-44 (2007). https://doi.org:10.1152/ajpgi.00464.2006

49 Calabresi, P., Di Lazzaro, G., Marino, G., Campanelli, F. & Ghiglieri, V. Advances in understanding the function of alpha-synuclein: implications for Parkinson's disease. *Brain* **146**, 3587-3597 (2023). https://doi.org:10.1093/brain/awad150

50 Na, H. *et al.* Characterization of the effects of calcitonin gene-related peptide receptor antagonist for Alzheimer's disease. *Neuropharmacology* **168**, 108017 (2020). https://doi.org:10.1016/j.neuropharm.2020.108017

51 Lin, M. *et al.* In Parkinson's patient-derived dopamine neurons, the triplication of alpha-synuclein locus induces distinctive firing pattern by impeding D2 receptor autoinhibition. *Acta Neuropathol Commun* **9**, 107 (2021). https://doi.org:10.1186/s40478-021-01203-9

52 Yang, S. & Yu, M. Role of Goblet Cells in Intestinal Barrier and Mucosal Immunity. *J Inflamm Res* **14**, 3171-3183 (2021). https://doi.org:10.2147/JIR.S318327

53 Merzel, J. & Almeida, M. L. Maturation of goblet cells of the mouse small intestine as shown by the uptake of 35S-sodium sulfate. *Anat Rec* **177**, 519-524 (1973). https://doi.org:10.1002/ar.1091770405

54 Noah F. Shroyer, S. A. K. in *Pediatric Gastrointestinal and Liver Disease* (ed Jeffrey S. Hyams Robert Wyllie) Ch. 31, 324-336 (W.B. Saunders, 2011).

55 Newberry, R. D. & Lorenz, R. G. Organizing a mucosal defense. *Immunol Rev* **206**, 6-21 (2005). https://doi.org:10.1111/j.0105-2896.2005.00282.x

CHAPTER 5 – ENTERIC GLIA, NEUROPEPTIDES, AND PARKINSON'S: IMPACTS OF CALCITONIN GENE RELATED PEPTIDE ON GUT ALPHA SYNUCLEIN

Overview:

Parkinson's Disease is a neurodegenerative disorder characterized by accumulation of misfolded a-synuclein in the central and peripheral nervous systems, influencing symptomology at both sites. Alterations to the neuropeptide calcitonin gene-related peptide have been linked with altered central nervous system a-synuclein aggregation. This study examines the role of calcitonin gene-related peptide in modulating enteric a-synuclein accumulation and enteric glia reactivity using an ex vivo slice culture model from A53T$^{+/-}$ human a-synuclein mutant mice. In slices treated with calcitonin gene-related peptide, a-synuclein immunoreactivity was elevated in myenteric neurons. A stark elevation in gut mucosal calcitonin gene-related peptide immunoreactivity was revealed to be predominantly S100β^{+} cells rather than neuronal fibers, pointing towards an active enteric glial phenotype. These data implicate calcitonin gene-related peptide in the accumulation of enteric a-synuclein in a model of Parkinson's disease, an effect potentially driven by an inflammatory environment due to enteric glial activity.

Introduction:

Parkinson's Disease (PD) is a neurodegenerative disorder characterized by the accumulation of misfolded alpha synuclein (aSyn) protein resulting in central and peripheral symptoms. Prodromal gastrointestinal (GI) symptoms are seen in 10-70% of PD patients (de Lau et al, 2006; Fasano et al, 2015) and can arise up to 20 years prior to motor symptoms (Travagli et al, 2020). Genetic studies of PD subjects have identified disease causing missense mutations on the aSyn gene, including A53T, that are linked to early onset PD in European families (Recchia et al, 2008; Anderson et al, 2006). Mice expressing the human aSyn A53T mutant exhibit motor impairments and aSyn accumulation in the brain and GI tract (Farrell et al,

2013). These alterations mirror the phenotype observed in human subjects with the A53T mutation (Giasson et al, 2002) leading to A53T mice being a commonly used model of PD.

The neuropeptide calcitonin gene related peptide (CGRP) is closely linked to diseases commonly comorbid with PD, including IBD (Pascual-Mato et al, 2024) and migraine (An et al, 2021)[1]. Accumulation of aSyn in the central nervous system (CNS) may be influenced by CGRP (Alexoudi et al, 2024) and treatment with CGRP antagonists reduce aSyn aggregation in mouse brain (Na et al, 2020; Benemei et al, 2009). A previous study from our laboratory utilized a rotenone model of PD and demonstrated increased αCGRP immunoreactivity in apical colonic crypts and elevated aSyn levels in αCGRP+ neurons and fibers, suggesting that enteric αCGRP dysregulation may contribute to aSyn aggregation (Templeton et al, 2025). An unexplained, sharp increase in CGRP labelled cells and fibers in colonic mucosa further pointed towards CGRP dysfunction in PD animal models.

Enteric glial cells serve multiple roles in the gut wall, including innate immunity. Enteric glia express multiple canonically astrocytic proteins including glial fibrillary acidic protein (GFAP), and S100β, a calcium-binding protein, that has been associated with the onset and maintenance of inflammation in the gut (Esposito et al, 2007; Cirillo et al, 2009). S100β levels are increased in the cerebral spinal fluid (CSF) and substantia nigra of PD patients (Sathe et al, 2012), and enteric glial expression of GFAP is elevated in the colon of PD subjects (Clairembault et al, 2014). Furthermore, in an N-methyl-4-phenyl-1,2,3,6-tetrahydropyridine (MPTP) model of Parkinson's, genetic ablation of S100β appeared to be neuroprotective by decreasing gliosis in the substantia nigra (Sathe et al, 2012). Both CGRP and aSyn can activate glial cells (Afroz et al, 2019; Harms et al, 2017; Grozdanov et al, 2019). Taken together with previous data pointing towards an elevation of mucosal CGRP, (Templeton et al, 2025) it is possible that alterations in enteric CGRP and aSyn may be the result of an inflammatory environment influenced by enteric glia which could perpetuate PD pathology in the gut.

To investigate the role of CGRP in enteric aSyn accumulation and enteric glial reactivity, an ex vivo organotypic slice model of A53T$^{+/-}$ colon tissue was utilized. Levels of aSyn, CGRP, and S100β were quantified in myenteric and mucosal regions following CGRP treatment. Furthermore, stool was used to investigate levels of CGRP and S100β across genotypes. The present study provides data on the contribution of CGRP to aSyn accumulation and enteric glial alterations in the gut wall.

Materials and Methods:

Animals. Male hA53T aSyn transgenic mice (B6. Cg-3210039L1RikTg $^{(Prnp\text{-}SNCA*A53T)23Mkle}$/J; Jackson Laboratories, strain no. 006823, Bar Harbor, ME, USA) were bred with female wild-type (WT) C57BL/6J mice (Jackson Laboratories, strain no 000664) to obtain male and female WT and hemizygous mice. All studies were done in male and female between 10-12 months of age, except for data in **Figure 19** which were between 3-4 months of age. All animal protocols were approved by the Institutional Animal Care and Use Committee (IACUC) and Colorado State University Lab Animal Resources under protocol CoA #1657. Mice were housed on a 12-h light/dark cycle with access to standard chow (Envigo TD.2918) and water *ad libitum*.

Genotyping. Genotyping was performed using the following primers for polymerase chain reaction (PCR): forward, 5'TCA TGA AAG GAC TTT CAA AGG C-3', transgene reverse, 5′-CCT CCC CCA GCC TAG ACC-3′ (transgene = ~500 bp); internal positive control forward, 5′-CTA GGC CAC AGA ATT GAA AGA TCT-3′; and internal positive control reverse, 5′-GTA GGT GGA AAT TCT AGC ATC C-3′ (internal positive control = 324 bp). PCR was run on a C1000 Touch Thermal Cycler. Master Mix per sample: 12.8 µL milli-Q water, 5 µL 5x buffer, 1.8 µL $MgCl_2$ (25mM), 1 µL DNTPs (10mM), 1.2 µL of 20 µM primers. Taq mix per sample: 4.6 µL milli-Q water, 1 µL 5x buffer, 0.4 µL Taq.

Organotypic slice preparation. Preparation of intestinal slices was similar to that previously described (Schwerdtfeger et al., 2016). Briefly, mice were deeply anesthetized with isoflurane and terminated via decapitation. The intestine was removed from stomach to colon and fecal pellets were removed directly from the colon and kept at -80°C until further experiments were performed. The intestines were then immediately placed into 4°C 1X Krebs buffer (in mM: 2.5 KCl, 2.5 $CaCl_2$, 126 NaCl, 1.2 $MgCl_2$, 1.2 NaH_2PO_4). Remaining mesentery was dissected away, and proximal colon was cut into 2-4mm length pieces. Tissue pieces were submerged in low-melting point 8% agarose (Gold Biotechnology) for 7 minutes total: 5 minutes on a room temperature shaker and 2 minutes at 4°C to ensure polymerization. Using a vibrating microtome (CT1000S; Lieca Microsystems, Wetzlar, Germany), 250 µm slices were cut and collected in ice cold 1X Krebs buffer. The slices were then transferred into a 60-mm plastic bottom dish (Corning, Corning, NY) containing 5 mL of Hibernate media (Life Technologies). Slices were kept at 4°C in Hibernate media for 15 min before being transferred into 5 mL of adult neurobasal media that was custom made in house with 5% B-27 supplement (B-27; Life Technologies), 4 mM glucose, and without phenol red. To help maintain the microbiome, media contained 0.4 mg/ml inulin (soluble fiber). Slices were kept in this media at 37°C for 35 min and plated on 35 mm plastic bottom dishes (Corning, Corning, NY) with excess media siphoned from the dish, and incubated for 10 min at 37°C. Slices were then covered with a thin layer of collagen solution [vol/vol; 10.4% 10X MEM (Minimal Essential Medium, Sigma-Aldrich), 83.5% collagen (PureCol; Inamed), and 4.2% sodium bicarbonate] which polymerized for 15 min. Finally, 1 ml of custom adult neurobasal media was added to the dish and tissue was left in a 37°C, 5% CO_2 incubator until further experiments were performed.

Organotypic slice drug treatments. Tissue was allowed to recover from slicing for 24 hr before addition of drug treatment. Slices were treated with recombinant CGRP (2 µM; AnaSpec) or vehicle at 24 hr ex vivo for a subsequent 24 hr. Doses were chosen based upon preliminary

dose-response analyses where increases in myenteric aSyn were seen within 24 hr. After 48 h culture, slices were fixed in 4% paraformaldehyde for 10 min and washed with 1X PBS 3 times for a total of 9 min.

Slice re-sectioning. To enhance the visualization of cellular components after fixation, 250 µm slices were re-sectioned at 50 µm, as described previously (Schwerdtfeger and Tobet, 2020; Schwerdtfeger and Tobet, 2021). Briefly, slices were placed in 4% agarose and then kept at 4°C for 4 min to ensure agarose polymerization. Using a vibrating microtome; VT1000S; Leica microsystems, Wetzlar, Germany) slices were sectioned at 50 µm thick.

Immunohistochemistry. 50 µm sections of immersion fixed whole colon or 50 µm re-sectioned slices were washed in 1x PBS for 10 minutes at 4°C and incubated in 0.1M glycine for 30 min at 4°C, followed by three 5 min PBS washes. Next, tissue sections were incubated in 0.5% sodium borohydride at 4°C for 15 min, followed by three 5 min PBS washes. Sections were blocked in PBS with 5% normal goat serum (NGS; Lampire Biological, Pipersville, PA), 1% hydrogen peroxide, and 0.3% Triton X (Tx) for 1 hr at 4°C with a change of solution at 30 min. Following blocking, sections were placed into primary antisera for 24 hr as outlined in Table 1 made in PBS 5% NGS and 0.3% Tx. Dual-label reactions were performed in parallel with both antisera being added at the same time. Of note, the aSyn antibody labels total aSyn per the vendor and several publications.[4-6] The CGRP antibody likely labels a small percentage of βCGRP, however, signal was only partially extinguished in βCGRP pre-absorption studies performed by the vendor. A pre-absorption with full length αCGRP peptide (AnaSpec, Fremont, CA) eliminated signal (Templeton et al, 2025). All experiments were performed with a negative control where secondary antisera were omitted. Following primary antisera incubation, sections were washed at room temperature in PBS with 1% NGS and 0.32% Tx four times at 15 min intervals. Sections were then incubated for two hours in Alexa Fluor conjugated secondary

antibodies to the appropriate species (**Table 5**) at 1:500 in PBS with 0.32% Tx. Following secondary antibody incubation, sections were washed four times at 15 min intervals in PBS with 0.02% Tx, followed by four PBS washes. Finally, sections were mounted on slides, and cover slipped with an aqueous mounting medium (Aqua-Poly/Mount, Polysciences, Warrington, PA).

Table 5. Primary and secondary antibodies used.

Primary Antibody	Immunizing Antigen	Raised	Dilution	Source	Catalog Number	Secondary Antibody
PGP9.5	Recombinant full length human UCHL1 purified from E. coli	Chicken	1:500	Novus Biologicals	NB110-58872SS	Goat anti-chicken IgY – Alexa Fluor 568 (Abcam)
CGRP	Full length rat α-CGRP	Rabbit	0.625µg/mL	ImmunoStar	24112	Goat anti-rabbit IgG – Alexa Fluor 647 or 488 (Invitrogen)
aSyn	Rabbit α-synuclein (D37A6)	Rabbit	1:500	Cell Signaling	4179	Biotin-SP donkey anti-rabbit IGG (Jackson Immuno Research)
S100β	Proprietary	Rabbit	1:1200	Abcam	ab52642	Biotin-SP donkey anti-rabbit IGG (Jackson Immuno Research) or Goat anti-rabbit IgG – Alexa Fluor 594 (Invitrogen)

Cell proliferation. To determine the synthesis of new DNA in presumptive dividing cells the incorporation of 5-ethynyl-2'-deoxyuridine (EdU; Invitrogen, Eugene, OR) was used. Mice received 25 mg/kg intraperitoneal injections of EdU 24 hr prior to euthanasia and slice experiments were performed as outlined above. Following IHC, the EdU visualization procedure

began with a 30 min block in 3% bovine serum albumin buffer (BSA; Sigma-Aldrich) and 5% Tx. Sections were then placed in a click-IT cocktail containing 1X click-IT reaction buffer, CuSO4, Alexa-Fluor azide 647, and 1X reaction buffer additive (Invitrogen) for 1 hr. Finally, sections were washed 3 times in 1X PBS for a total of 30 minutes prior to being mounted.

Tissue imaging & analysis. Images were taken using a Zeiss LSM800 upright confocal laser scanning microscope and a 40x or 63x (EC Plan-Neofluar) oil immersion objective. Data for CGRP or PGP9.5 and aSyn, S100β and CGRP, S100β and EdU, and CGRP and EdU analyses was gathered from confocal Z-stacks with 20 planes 1 µm apart with the top and bottom planes set from the focus of labeling. Max intensity Z-projections were performed. Control areas for aSyn and PGP9.5 colocalization were initially defined as muscle regions with no PGP9.5-ir. These regions had no aSyn-ir. All image acquisition and analyses were performed by a researcher blinded to treatment. All image analyses were performed using Fiji (v1.0; NIH). Immunoreactive percentage of area labeled was calculated using the 'measure' tool in Fiji on thresholded images restricted to the defined ROI for each respective analysis. To determine the % area of aSyn in CGRP or PGP9.5 neurons/fibers, thresholded CGRP-ir or PGP9.5-ir images were used to generate ROIs using the analyze particles tool. Thresholded aSyn-ir images were then analyzed using CGRP or PGP9.5 ROIs as area restrictions. Then, the percentage of total CGRP-ir or PGP9.5-ir area that contained aSyn-ir was calculated. To determine the % area of EdU in CGRP-ir or S100β-ir, thresholded CGRP-ir or S100β-ir images were used to generate ROIs using the analyze particles tool. Thresholded EdU-ir images were then analyzed using CGRP-ir or S100β-ir ROIs as area restrictions. Then, the percentage of total CGRP-ir or S100β-ir area that contained EdU-ir was calculated. To determine the % area of CGRP in S100β+ cells, thresholded S100β-ir images were used to generate ROIs using the analyze particles tool. Thresholded CGRP-ir images were then analyzed using S100β-ir ROIs as area restrictions. Then, the percentage of total S100β-ir area that contained CGRP-ir was calculated.

Enzyme-linked immunosorbent assay. The levels of CGRP and S100β in fecal samples were determined using an enzyme-linked immunosorbent assay (ELISA) kit (CGRP EEL090, S100β EEL109, Thermo Fisher Scientific, Waltham, MA) according to the manufacturer's guidelines. Fecal samples were homogenized in triton X-100 buffer at a ratio of 1:10 (g/mL) buffer to sample and centrifuged for 6 min and 10,000 rcf. Standards were prepared in serial dilution according to the Thermo Fisher Scientific user manual. Samples and standards were added to appropriate wells, followed by biotinylated and horseradish peroxidase (HRP) antibodies. The ELISA plate was read on a Cytation 3 plate reader (Agilent Technologies, Inc., Santa Clara, CA) at 450 nm. Concentrations were calculated based on the manufacturers standard curve and final concentrations were adjusted for dilution factors prior to plotting.

2.5 Statistics. All statistical analyses were performed using Graphpad Prism version 10.1.2 (Graphpad Software, La Jolla, CA). Analysis revealed no sex differences, so all data is reported with both males and females. For in vivo aSyn and CGRP average area, CGRP area, percent area of CGRP in S100β, percent area of aSyn in CGRP, and percent area of EdU in CGRP or S100β unpaired t tests were performed. For ex vivo aSyn and CGRP average area, CGRP area, percent area of CGRP in S100β, and percent area of aSyn in CGRP a two-way ANOVA was performed by treatment and genotype. All data are presented as means +/- standard error of the mean (SEM). In all instances where p values are noted, a post hoc Tukey's multiple comparison test was performed to compare individual means. A Brown-Forsythe equality of variance test was performed for all two-way ANOVAs to confirm variances were not significantly different across groups.

Results:

aSyn is elevated CGRP-ir cells in the A53T$^{+/-}$ colon.

Immunoreactive aSyn was colocalized with CGRP^{+} myenteric neurons and apical mucosal fibers in a genotype specific manner in the in vivo colon (**Fig. 16A**). The percentage of aSyn-ir area in CGRP^{+} apical fibers was 458% greater in A53T$^{+/-}$ animals (6.7% +/- 0.8) compared to WT (1.2% +/-0.2; (t(9)= 5.4, p<0.001)) (**Fig. 16B**). The percentage of aSyn-ir area in CGRP^{+}

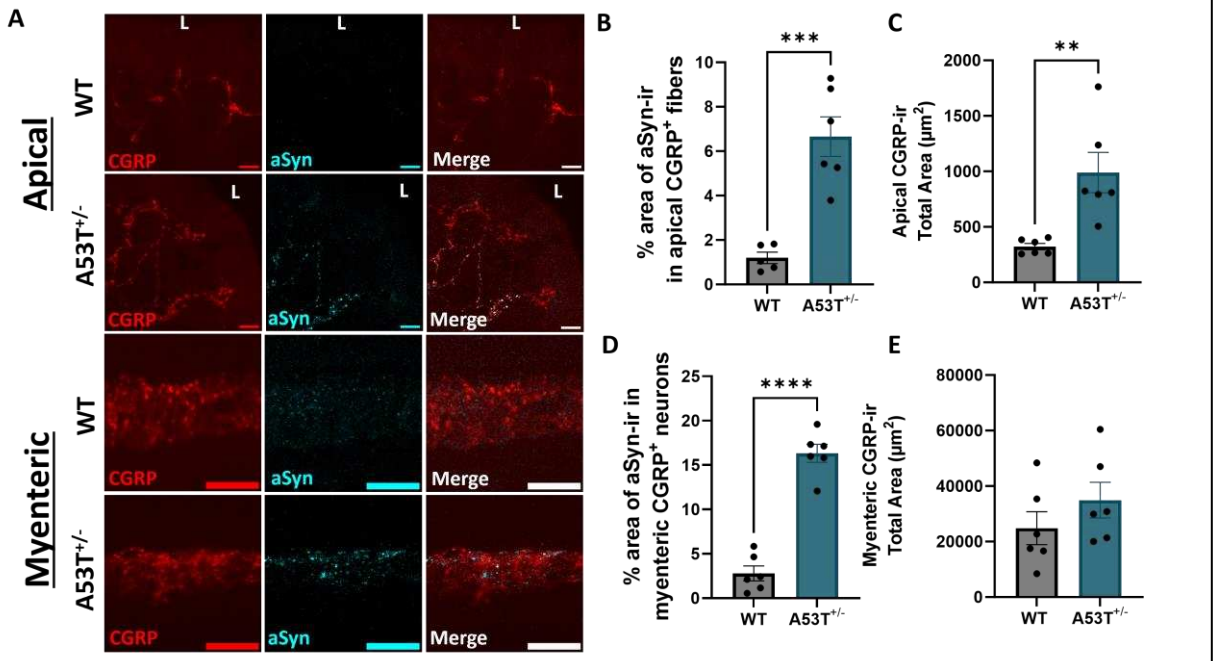

Figure 16. Elevated aSyn in CGRP-ir cells in A53T$^{+/-}$ colon. (**A**) The percent area of aSyn-ir in apical CGRP^{+} fibers and myenteric CGRP^{+} neurons is greater in A53T$^{+/-}$ colon compared to WT. Apical CGRP-ir total area is greater in A53T$^{+/-}$ colon compared to WT, but myenteric CGRP-ir total area is similar in both A54T$^{+/-}$ and WT colon. (**B**) Quantification of % area of aSyn-ir in apical CGRP^{+} fibers. (**C**) Quantification of apical CGRP-ir total area. (**D**) Quantification of % area of aSyn-ir in myenteric CGRP+ neurons. (**E**) Quantification of myenteric CGRP-ir total area. Scale bars are 20 µm, aSyn = alpha synuclein, CGRP = calcitonin gene related peptide, WT = wild type. **p<0.01, ***p<0.001 ****p<0.0001. n = 6 (3 male, 3 female).

myenteric neurons was 471% greater in A53T$^{+/-}$ animals (16% +/- 1) compared to WT (3% +/- 0.8; (t(10)= 910.28, p<0.0001) (**Fig. 16D**). Total CGRP-ir was interrogated by anatomic region, with quantification of CGRP-ir in apical crypts and myenteric plexus. In apical crypts, CGRP levels were 206.2% greater in A53T$^{+/-}$ animals (989 µm^2 +/- 182) compared to WT (323 µm^2 +/-

68; t(10) = 3.6, p < 0.01) (**Fig. 16C**). Myenteric CGRP levels were similar in A53T$^{+/-}$ (24837 µm^2 +/- 5944) and WT animals (34921 µm^2 +/- 6442; t(10) = 1.2, p > 0.05) (**Fig. 16E**).

Ex vivo CGRP treatment increases aSyn in myenteric neurons.

The peripheral neuronal marker PGP 9.5 was used to interrogate the percent area of aSyn-ir in PGP 9.5 myenteric neurons of ex vivo colon slices following vehicle or CGRP treatment. A two-way ANOVA revealed a main effect of treatment (F(1,14) = 30.6, p < 0.0001) where percent

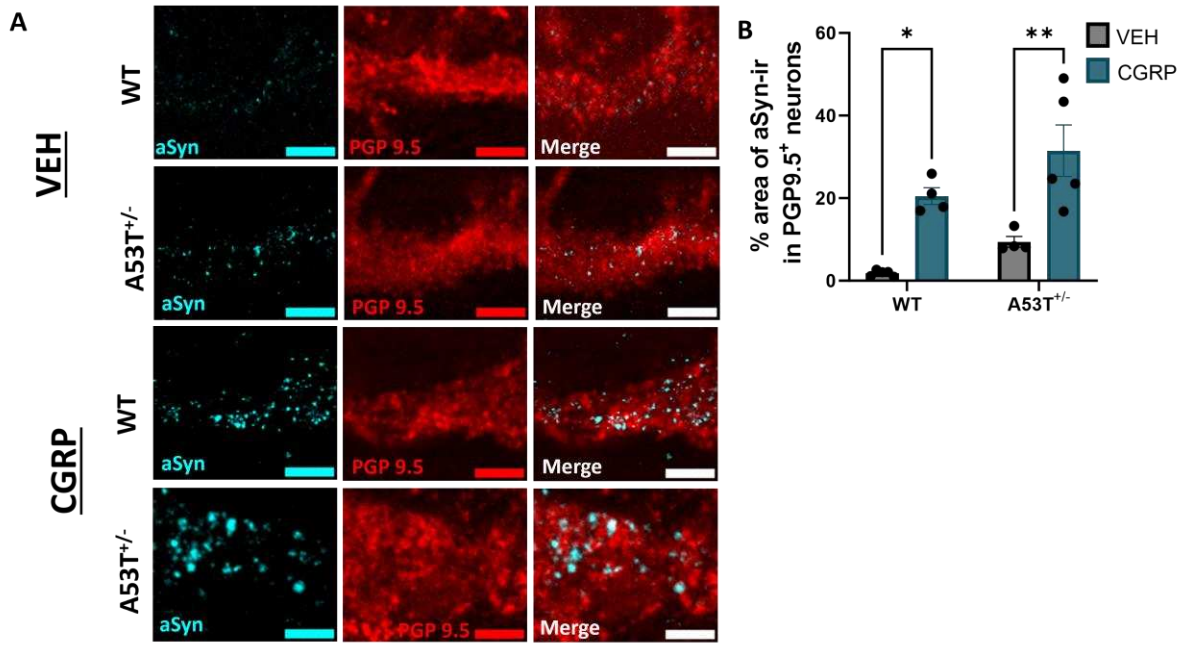

Figure 17. **Myenteric neurons have elevated aSyn following CGRP treatment.** (**A**) CGRP treatment increased levels of aSyn in PGP 9.5$^+$ myenteric neurons in both WT and A53T$^{+/-}$ ex vivo colon slices. (**B**) Quantification of aSyn-ir in PGP 9.5$^+$ myenteric neurons in WT and A53T$^{+/-}$ slices following vehicle or CGRP treatment. Scale bars are 10 µm, aSyn = alpha synuclein, PGP 9.5 = protein gene product 9.5, CGRP = calcitonin gene related peptide, WT = wild type. * p < 0.05, **p<0.01. WT n = 4 (2 male, 2 female), A53T$^{+/-}$ VEH n = 4 (2 male, 2 female), CGRP n = 5 (2 male, 3 female).

area of aSyn-ir was greater in CGRP treated colon in both WT and A53T$^{+/-}$ animals (**Fig. 17A, B**). Following CGRP treatment, WT myenteric neurons (20.5% +/- 2) had a 1039% increase in aSyn-ir compared to vehicle treatment (1.8% +/- 0.3; p < 0.05). Following CGRP treatment (31.5% +/- 6.2) A53T$^{+/-}$ myenteric neurons had a 235% increase in aSyn-ir compared to vehicle treatment (9.4% +/- 1.3; p < 0.05). There was also a main effect of genotype (F(1,14) = 6.4, p <

0.03) where A53T$^{+/-}$ mice had a greater percent area of aSyn-ir in PGP9.5+ myenteric neurons than WT animals.

Enteric glial cells are hyperplastic and express CGRP in A53T$^{+/-}$ colonic mucosa.

To investigate possible mucosal cells expressing CGRP apically, the enteric glial marker, S100β was examined in in vivo sections of colon. A53T$^{+/-}$ mucosa (2.8 +/- 0.2) (**Fig. 18B**) had 87% more S100β^{+} cells per crypt compared to WT (**Fig. 18A**) (1.5 +/-0.2; t(10) = 5.1, p < 0.001) (**Fig. 18A-C**). The percent area of CGRP-ir in S100β+ cells was 159% greater in A53T$^{+/-}$ mucosa (57% +/- 1.7) compared to WT (22% +/- 3.2; t(10) = 9.4, p < 0.0001) (**Fig. 18D**).

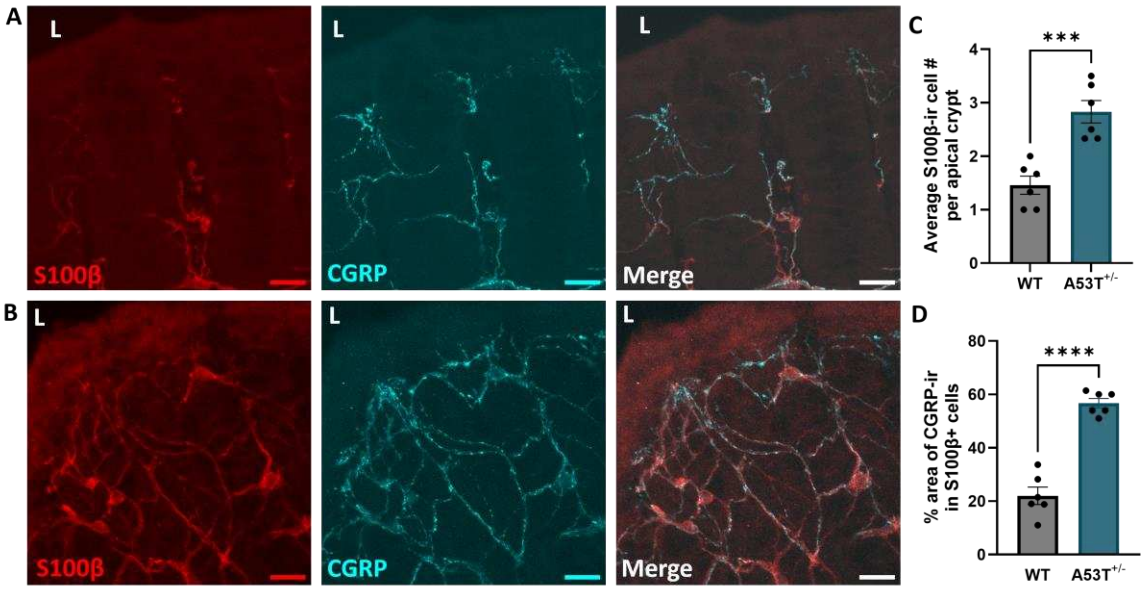

Figure 18. **Enteric glial cells are hyperplastic and express CGRP in A53T colonic mucosa.** (**A**) S100β and CGRP in WT in vivo colon. (**B**) S100β and CGRP in A53T$^{+/-}$ in vivo colon. (**C**) Quantification of average S100β^{+} cell number per crypt in WT and A53T$^{+/-}$ colon. (**D**) Quantification of % area of CGRP-ir in S100β+ cells in WT and A53T$^{+/-}$ colon. Scale bars are 20 µm, S100β = calcium binding protein B, CGRP = calcitonin gene related peptide, WT = wild type. ***p<0.001 ****p<0.0001. n = 6 (3 male, 3 female).

Enteric glial cell quantities and CGRP-ir are elevated to A53T$^{+/-}$ following ex vivo CGRP treatment in WT mice.

Number of S100β^{+} cells per apical crypt were interrogated in ex vivo colon slices following vehicle and CGRP treatment. A two-way ANOVA revealed a main effect of treatment ($F(1,15) = 51.08$, $p < 0.0001$), a main effect of genotype ($F(1,15) = 58.3$, $p < 0.0001$), and a significant interaction between genotype and treatment ($F(1,15) = 16.78$, $p < 0.001$). This indicated that the number of S100β-ir cells was greater when treated with CGRP in both WT and A53T$^{+/-}$ colon, but A53T$^{+/-}$ colon had greater overall S100β-ir cells (**Fig. 19A, B**). Following CGRP treatment (4.1 +/- 0.4), WT colon had around 2.8 more S100β-ir cells per crypt compared to vehicle treatment (1.2 +/- 0.2, $p < 0.0001$). Following CGRP treatment (5 +/- 0.2), A53T$^{+/-}$ colon had around 0.78 more S100β-ir cells per crypt compared to vehicle (4.2 +/- 0.3, $p > 0.05$) (**Fig. 19A, B**). The percent area of CGRP-ir in S100β^{+} cells was also investigated following vehicle or CGRP treatment. A two-way ANOVA revealed a main effect of genotype ($F(1,13)= 12.42$, $p < 0.01$) indicating that A53T$^{+/-}$ colon has a greater percent of CGRP-ir in S100β cells than WT colon, regardless of treatment. Vehicle treated A53T$^{+/-}$ colon (18% +/- 3) had 415% greater percent CGRP-ir in S100β^{+} cells than vehicle treated WT colon (3.6% +/- 1.7, $p < 0.05$) (**Fig. 19C**). CGRP treated A53T$^{+/-}$ colon (24.7% +/- 5) had 90% greater percent CGRP-ir in S100β cells than CGRP treated WT colon (13% +/- 157, $p > 0.05$). A two-way ANOVA also revealed a main effect of treatment ($F(1,13) = 4.9$, $p < 0.05$) indicating that CGRP treatment increased percent area of CGRP-ir in S100β+ cells. Following CGRP treatment, WT colon had 266.2% more CGRP-ir in S100β^{+} cells ($p < 0.5$) and A53T$^{+/-}$ colon had 35% more CGRP-ir in S100β^{+} cells ($p > 0.05$).

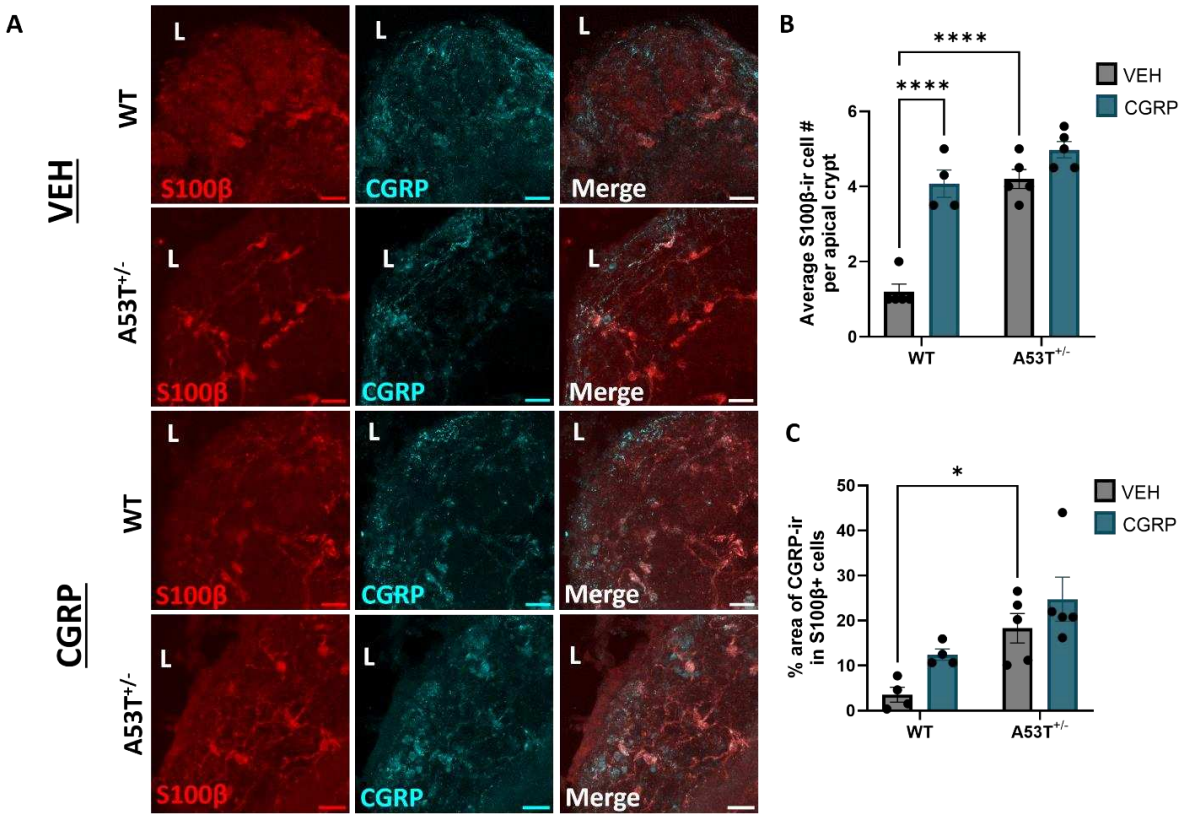

Figure 19. **CGRP treatment alters mucosal S100β cell quantities and CGRP co-localization.** (**A**) A53T$^{+/-}$ colon slices have greater number of S100β^{+} cells regardless of treatment. CGRP treatment increases S100β^{+} cell number in WT colon. (**B**) Quantification of S100β + cell number per apical crypt in WT and A53T colon slices following VEH or CGRP treatment (**C**) Quantification of % area of CGRP-ir in S100β+ cells. Scale bars are 20 µm, S100β = calcium binding protein B, CGRP = calcitonin gene related peptide, WT = wild type, VEH = vehicle. * $p < 0.05$, ****$p<0.0001$. WT n = 4 (2 male, 2 female), A53T$^{+/-}$ n = 5 (2 male, 3 female).

S100b is elevated in A53T$^{+/-}$ mouse stool and CGRP is increased with age.

Quantities of CGRP and S100b in stool were compared between WT and A53T$^{+/-}$ animals. Both WT (196 pg/mL +/- 21) and A53T$^{+/-}$ (209 pg/mL +/- 320) animals had similar quantities of stool CGRP (**Fig. 20A**), however a Spearman's correlation revealed stool CGRP quantity was positively correlated with age in A53T$^{+/-}$ animals (Spearman's $r = 0.89$, $p <0.05$) (**Fig. 20B**) but not correlated in WT animals (**Fig. 20B**). When investigating S100β concentrations in stool, WT animal's stool (63 pg/mL +/- 6.5), had less S100β compared to A53T$^{+/-}$ animals, which showed a

249% increase (219 pg/mL +/- 41; t(10) 3.8, $p < 0.01$). There was no association observed between stool S100β quantities and age in WT (Spearman's r = -0.52, $p > 0.05$) or A53T$^{+/-}$

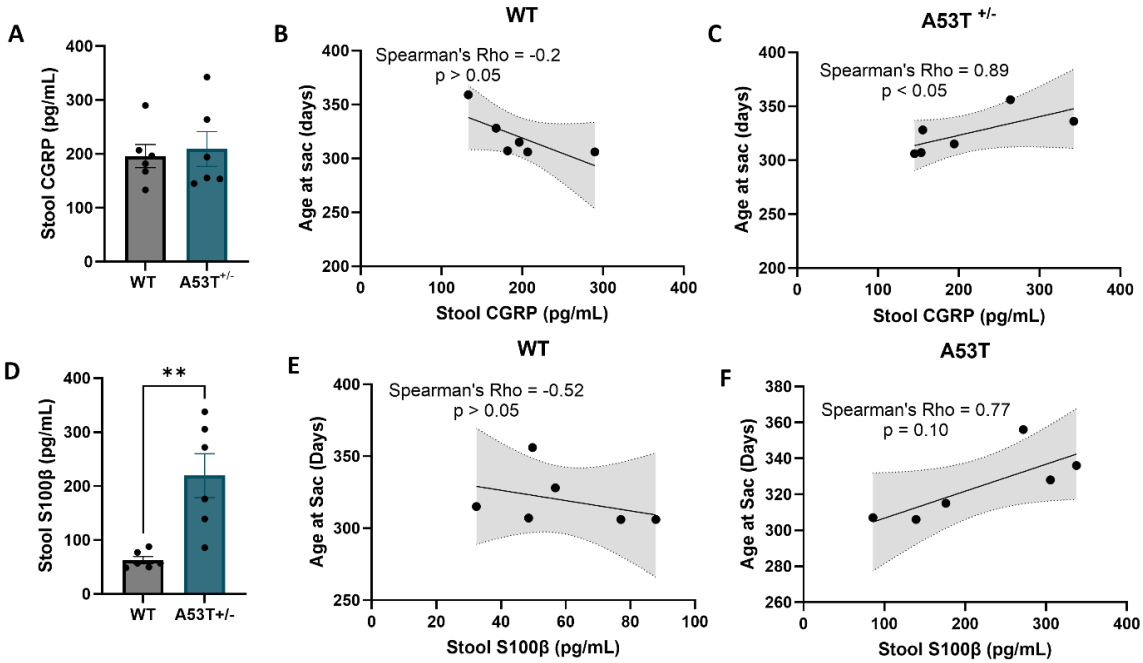

Figure 20. **S100β is elevated in A53T mouse stool and CGRP is increased with age.** (**A**) Stool CGRP levels were similar in WT and A53T+/- animals (**B**) No correlation between age and stool CGRP levels in WT animals. (**C**) Stool CGRP levels increase with age in A53T+/- animals. (**D**) Stool S100β levels were greater in A53T+/- animals compared to WT. (E) No correlation between age and stool S100β levels in WT animals. (F) No correlation between age and stool S100β levels in A53T+/- animals. CGRP = calcitonin gene related peptide, S100β = calcium binding protein B, WT = wild type, **p<0.01. n = 6 (3 male, 3 female).

(Spearman's r = 0.77, p = 0.10) animals as measured by a Spearman's correlation.

To determine if the age effect on stool CGRP was consistent with substantially younger animals, a pilot was performed to view CGRP/S100β phenotypes and aSyn levels at 12 – 14 weeks of age. This preliminary data suggested that young A53T$^{+/-}$ mice exhibit elevations in aSyn in PGP9.5+ myenteric neurons, and apical crypt CGRP-ir and S100β+ cell quantities, similar to old (> 9 mo old) A53T$^{+/-}$ mice (**Fig. 21A, B**). Therefore, further analysis of young vs. old A53T$^{+/-}$ animals was not performed.

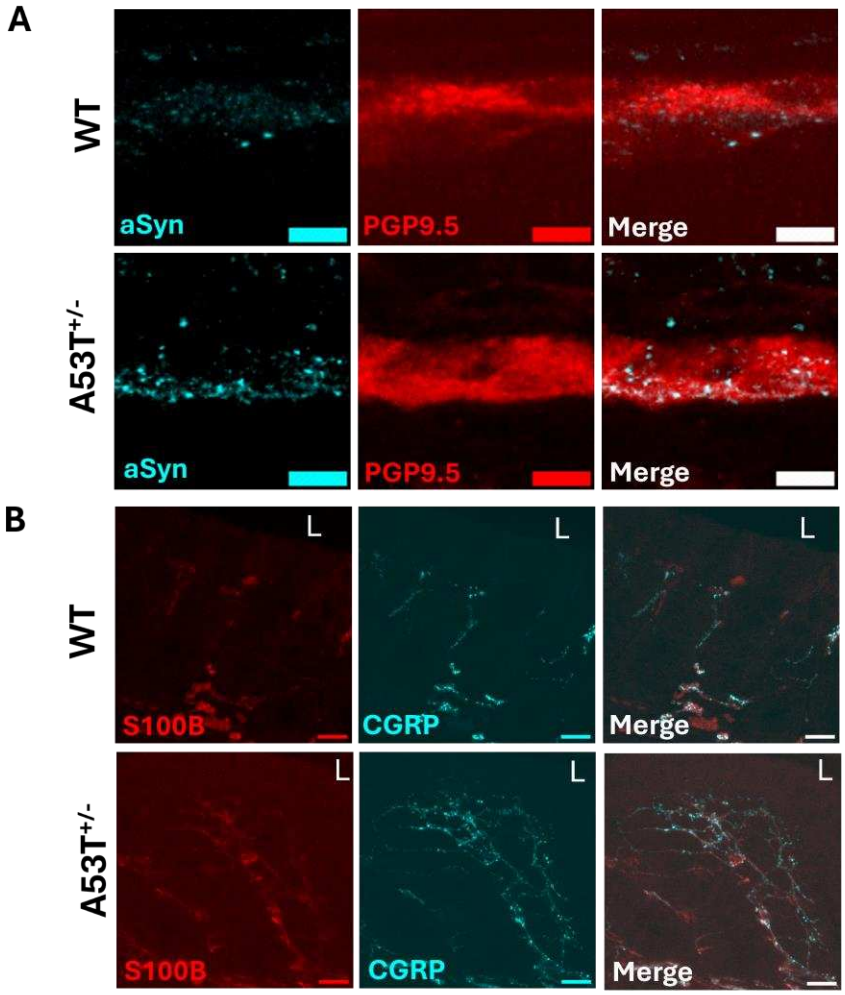

Figure 21. **Young A53T$^{+/-}$ mice exhibit similar aSyn, CGRP, and S100B phenotypes as old A53T$^{+/-}$ mice.** (**A**) Young A53T$^{+/-}$ mice have elevated aSyn levels in PGP9.5+ myenteric neurons similar to old A53T$^{+/-}$ mice. (**B**) Young A53T$^{+/-}$ mice have increased S100B-ir and apical CGRP-ir similar to old A53T$^{+/-}$ mice. Scale bars for A are 10 µm, Scale bars for B are 20 µm S100B = calcium binding protein B, CGRP = calcitonin gene related peptide, WT = wild type.

Apical S100β-ir and CGRP-ir cells are non-proliferative.

Investigations next sought to determine if the apical elevation of CGRP+ / S100β+ cells was due to enteric glial cell proliferation. Animals were treated with EdU 24 hr prior to sac and was developed after post-hoc IHC for anti-S100β (**Fig. 22A, B**) or CGRP (**Fig. 22E, F**) which revealed minimal co-localization between EdU+ cells and S100β+ cells in WT (15.5% +/- 2.8) or

A53T$^{+/-}$ (16.2% +/- 3) (**Fig. 22C**) and CGRP+ cells in WT (7.6 +/- 1.9) or A53T$^{+/-}$ (7 +/- 1) (**Fig. 22G**). There was no difference in total cell proliferation between WT (30 +/- 3.2) and A53T$^{+/-}$

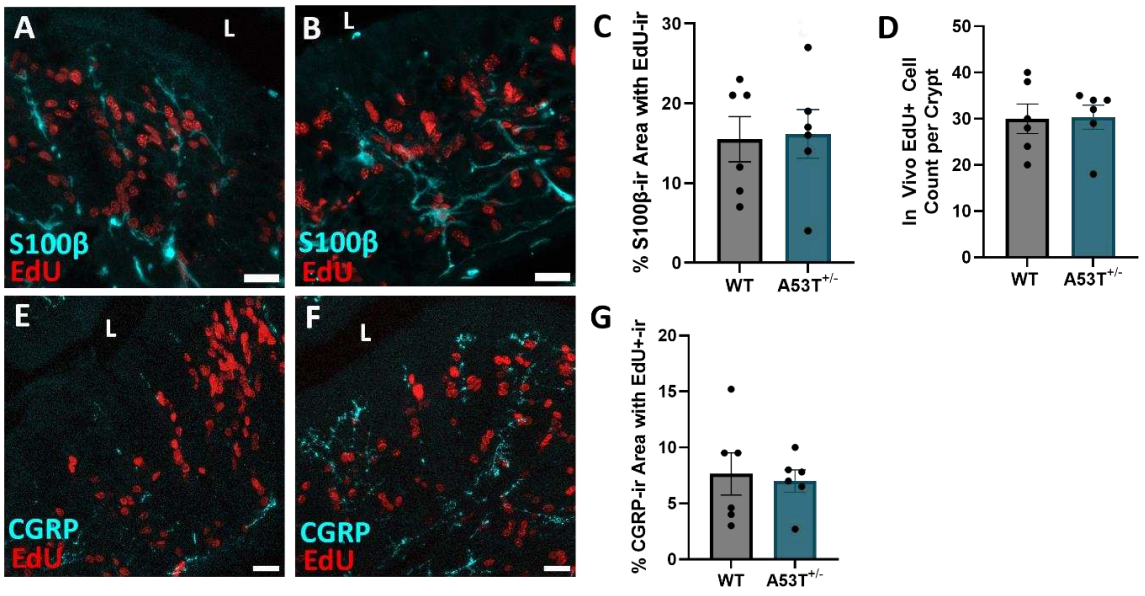

Figure 22. S100β+ and CGRP+ cells are not co-localized with EdU in WT or A53T$^{+/-}$ mice. (**A**) S100β-ir and EdU in WT colon. (**B**) S100β-ir and EdU in A53T$^{+/-}$ colon. (**C**) Quantification of the percentage of S100β-ir area containing EdU. (**D**) Quantification of EdU+ cell count per crypt. (**E**) CGRP and EdU in WT colon. (**F**) CGRP and EdU in A53T$^{+/-}$ colon. (**G**) Quantification of the percentage of CGRP-ir area containing EdU. Scale bars are 25 µm, n = 6 (3 male, 3 female).

(30.3 +/- 2.6) mice (**Fig. 22D**).

Discussion:

The importance of gut-brain signaling in PD has been increasingly recognized, with gastrointestinal dysfunction often preceding motor symptoms. Using a transgenic A53T mouse model of PD, the current study points towards CGRP influencing the accumulation of enteric aSyn, an effect potentially influenced by reactive enteric gliosis. By identifying factors like CGRP that facilitate aSyn accumulation in the gut, this research provides further evidence supporting the gut is a critical area for investigation on the origins of PD.

A pesticide model of PD using rotenone in mice has shown an upregulation of CGRP in myenteric neurons (Templeton et al, 2025) and PD patients have increased levels of CGRP in CSF (Svenningsson et al, 2017). Furthermore, previous work has demonstrated increased αCGRP immunoreactivity in apical colonic crypts and elevated aSyn levels in αCGRP+ neurons and fibers (Templeton et al, 2025). The present study found similar increases in colonic apical CGRP-ir associated with elevated aSyn in A53T mice, suggesting that dysregulation of enteric CGRP may contribute to aSyn aggregation similar to that seen in PD patient derived neuronal cultures (Calabresi et al, 2023; Lin et al, 2021). The observed elevation in myenteric neuronal aSyn in response to CGRP treatment in both wild-type and A53T$^{+/-}$ mutant mice suggests a role for CGRP in facilitation of enteric aSyn aggregation, regardless of pre-existing aSyn levels and PD-like pathology. Additionally, stool levels of CGRP correlated with increased age only in A53T$^{+/-}$ mice suggesting that CGRP is released as aSyn accumulates and disease progresses. Antagonizing CGRP receptors can reduce aSyn levels in the brain (Na et al, 2020), further supporting the role of CGRP in aSyn aggregation dynamics. The CGRP – aSyn interaction observed in the present study opens an arena for investigating peripheral modulation of synuclein aggregation via enteric neuropeptides.

Immune dysregulation resulting in systemic inflammation has been implicated in PD (Harms et al., 2017), yet specific mechanisms through which it modulates disease are not fully understood. Microglia in the CNS and enteric glial cells in the ENS have been implicated in PD pathology (Clairembault et al., 2014; Rocha et al, 2023). The brains of PD subjects have increased levels of activated microglia in areas with increased pathologic aSyn (McGeer et al, 1988), and the distribution of aSyn+ astrocytes parallel the distribution of Lewy bodies (Braak et al, 2007). Additionally, S100β, a calcium-binding protein, expressed on astrocytes and enteric glial cells is increased in the CSF and substantia nigra of PD patients (Sathe et al, 2012). S100β has also been associated with the onset and maintenance of inflammation in the gut (Esposito et al, 2007; Cirillo et al, 2009). Furthermore, PD subjects have elevated GFAP immunoreactivity

in colon biopsy samples, pointing towards an activated glial phenotype (Clairembault et al., 2014; Rosembaum et al., 2016). In the present study, increased quantities of S100β-ir and CGRP-ir in the colonic mucosa of A53T$^{+/-}$ mice was predominantly enteric glial cells that were expressing CGRP, pointing towards an activated enteric glia phenotype. This was further supported by elevated quantities of S100β in stool of A53T$^{+/-}$ mice. When added to colonic slices from wild type animals, CGRP increased mucosal S100β+ cell quantities and CGRP/S100β-ir co-localization in-line with A53T mutant mice. This mirrors clinical phenotypes of PD where subjects have increased quantities of enteric glial cell expression of GFAP in the colonic wall (Clairembault et al, 2014). The observed glial hyperplasia following CGRP treatment was only significant in wild-type colon slices, while slices from A53T$^{+/-}$ mice had higher baseline levels of S100β-ir. One explanation for this could be that A53T$^{+/-}$ mice may have an impaired inflammatory response that alters how enteric glial cells respond to external signals such as CGRP. It is also possible that A53T$^{+/-}$ animals are at a maximum 'capacity' of enteric glial cells at baseline, and treatment with CGRP is done in a tissue environment with minimal physical space for expansion or energy resources. Furthermore, data point towards the elevated quantities of mucosal enteric glial cells as likely being a migration event to the apical mucosa, rather than a proliferative one, as enteric glia and CGRP+ cells did not take up the thymidine analog EdU. There was also no difference in cell proliferation between WT and A53T$^{+/-}$ animals as seen by similar EdU+ cell numbers. Preliminary data pointed towards these enteric neural phenotypes being seen as early as 3-months of age in A53T mice, emphasizing the need for earl development studies in this animal model of PD.

In summary, our findings suggest that CGRP is involved in promoting aSyn accumulation in the enteric nervous system, and its dysregulation, along with glial activation, may play a critical role in PD pathogenesis. Targeting peripheral CGRP signaling pathways could offer a potential therapeutic strategy to reduce enteric aSyn aggregation, an approach

particularly apt for early stages of disease, when peripheral aSyn accumulation may be a precursor to disease progression.

References

1 Afroz, S. *et al.* CGRP Induces Differential Regulation of Cytokines from Satellite Glial Cells in Trigeminal Ganglia and Orofacial Nociception. *Int J Mol Sci* **20** (2019). https://doi.org:10.3390/ijms20030711

2 Alexoudi, A., Donadio, V. & Karageorgiou, E. The potential role of CGRP in synuclein-associated neurodegenerative disorders. *Front Neurosci* **18**, 1479830 (2024). https://doi.org:10.3389/fnins.2024.1479830

3 An, Q. *et al.* Calcitonin gene-related peptide regulates spinal microglial activation through the histone H3 lysine 27 trimethylation via enhancer of zeste homolog-2 in rats with neuropathic pain. *J Neuroinflammation* **18**, 117 (2021). https://doi.org:10.1186/s12974-021-02168-1

4 Anderson, J. P. *et al.* Phosphorylation of Ser-129 is the dominant pathological modification of alpha-synuclein in familial and sporadic Lewy body disease. *J Biol Chem* **281**, 29739-29752 (2006). https://doi.org:10.1074/jbc.M600933200

5 Benemei, S., Nicoletti, P., Capone, J. G. & Geppetti, P. CGRP receptors in the control of pain and inflammation. *Curr Opin Pharmacol* **9**, 9-14 (2009). https://doi.org:10.1016/j.coph.2008.12.007

6 Braak, H., Sastre, M. & Del Tredici, K. Development of alpha-synuclein immunoreactive astrocytes in the forebrain parallels stages of intraneuronal pathology in sporadic Parkinson's disease. *Acta Neuropathol* **114**, 231-241 (2007). https://doi.org:10.1007/s00401-007-0244-3

7 Calabresi, P. *et al.* Alpha-synuclein in Parkinson's disease and other synucleinopathies: from overt neurodegeneration back to early synaptic dysfunction. *Cell Death Dis* **14**, 176 (2023). https://doi.org:10.1038/s41419-023-05672-9

8 Cirillo, C. *et al.* Increased mucosal nitric oxide production in ulcerative colitis is mediated in part by the enteroglial-derived S100B protein. *Neurogastroenterol Motil* **21**, 1209-e1112 (2009). https://doi.org:10.1111/j.1365-2982.2009.01346.x

9 Clairembault, T. *et al.* Enteric GFAP expression and phosphorylation in Parkinson's disease. *J Neurochem* **130**, 805-815 (2014). https://doi.org:10.1111/jnc.12742

10 de Lau, L. M. & Breteler, M. M. Epidemiology of Parkinson's disease. *Lancet Neurol* **5**, 525-535 (2006). https://doi.org:10.1016/S1474-4422(06)70471-9

11 Esposito, G. *et al.* Enteric glial-derived S100B protein stimulates nitric oxide production in celiac disease. *Gastroenterology* **133**, 918-925 (2007). https://doi.org:10.1053/j.gastro.2007.06.009

12 Farrell, K. F. *et al.* Non-motor parkinsonian pathology in aging A53T alpha-synuclein mice is associated with progressive synucleinopathy and altered enzymatic function. *J Neurochem* **128**, 536-546 (2014). https://doi.org:10.1111/jnc.12481

13 Fasano, A., Visanji, N. P., Liu, L. W., Lang, A. E. & Pfeiffer, R. F. Gastrointestinal dysfunction in Parkinson's disease. *Lancet Neurol* **14**, 625-639 (2015). https://doi.org:10.1016/S1474-4422(15)00007-1

14 Giasson, B. I. *et al.* Neuronal alpha-synucleinopathy with severe movement disorder in mice expressing A53T human alpha-synuclein. *Neuron* **34**, 521-533 (2002). https://doi.org:10.1016/s0896-6273(02)00682-7

15 Grozdanov, V. *et al.* Increased Immune Activation by Pathologic alpha-Synuclein in Parkinson's Disease. *Ann Neurol* **86**, 593-606 (2019). https://doi.org:10.1002/ana.25557

16 Harms, A. S. *et al.* alpha-Synuclein fibrils recruit peripheral immune cells in the rat brain prior to neurodegeneration. *Acta Neuropathol Commun* **5**, 85 (2017). https://doi.org:10.1186/s40478-017-0494-9

17 Hayley N Templeton, A. T. E., Luke A Schwerdtfeger, Julietta A Sheng, Ronald B Tjalkens, Stuart A Tobet. Sex specific effects of environmental toxin-derived alpha synuclein on enteric neuronal-epithelial interactions. *Neurogastrol Motil* (2025).

18 Lin, M. *et al.* In Parkinson's patient-derived dopamine neurons, the triplication of alpha-synuclein locus induces distinctive firing pattern by impeding D2 receptor autoinhibition. *Acta Neuropathol Commun* **9**, 107 (2021). https://doi.org:10.1186/s40478-021-01203-9

19 McGeer, P. L., Itagaki, S. & McGeer, E. G. Expression of the histocompatibility glycoprotein HLA-DR in neurological disease. *Acta Neuropathol* **76**, 550-557 (1988). https://doi.org:10.1007/BF00689592

20 Michetti, F. *et al.* Growing role of S100B protein as a putative therapeutic target for neurological- and nonneurological-disorders. *Neurosci Biobehav Rev* **127**, 446-458 (2021). https://doi.org:10.1016/j.neubiorev.2021.04.035

21 Na, H. *et al.* Characterization of the effects of calcitonin gene-related peptide receptor antagonist for Alzheimer's disease. *Neuropharmacology* **168**, 108017 (2020). https://doi.org:10.1016/j.neuropharm.2020.108017

22 Parkinson, J. *An Essay on the Shaking Palsy*. (Edwards & Brune Ltd., 1817).

23 Pascal, M. *et al.* The neuropeptide VIP potentiates intestinal innate type 2 and type 3 immunity in response to feeding. *Mucosal Immunol* **15**, 629-641 (2022). https://doi.org:10.1038/s41385-022-00516-9

24 Recchia, A. *et al.* Generation of a alpha-synuclein-based rat model of Parkinson's disease. *Neurobiol Dis* **30**, 8-18 (2008). https://doi.org:10.1016/j.nbd.2007.11.002

25 Rocha, S. M. *et al.* Microglia-specific knock-out of NF-kappaB/IKK2 increases the accumulation of misfolded alpha-synuclein through the inhibition of p62/sequestosome-1-dependent autophagy in the rotenone model of Parkinson's disease. *Glia* **71**, 2154-2179 (2023). https://doi.org:10.1002/glia.24385

26 Rosenbaum, C. *et al.* Activation of Myenteric Glia during Acute Inflammation In Vitro and In Vivo. *PLoS One* **11**, e0151335 (2016). https://doi.org:10.1371/journal.pone.0151335

27 Sathe, K. *et al.* S100B is increased in Parkinson's disease and ablation protects against MPTP-induced toxicity through the RAGE and TNF-alpha pathway. *Brain* **135**, 3336-3347 (2012). https://doi.org:10.1093/brain/aws250

28 Svenningsson, P., Palhagen, S. & Mathe, A. A. Neuropeptide Y and Calcitonin Gene-Related Peptide in Cerebrospinal Fluid in Parkinson's Disease with Comorbid Depression versus Patients with Major Depressive Disorder. *Front Psychiatry* **8**, 102 (2017). https://doi.org:10.3389/fpsyt.2017.00102

29 Templeton, H., Ehrlich, A., Schwerdtfeger, L., Sheng, J., Tjalkens, R., Tobet, S. Sex specific effects of enviornmental toxin-derived alpha synuclein on enteric neuronal-epithelial interactions. *Neurogastroenterol Motil* (2025).

30 Travagli, R. A., Browning, K. N. & Camilleri, M. Parkinson disease and the gut: new insights into pathogenesis and clinical relevance. *Nat Rev Gastroenterol Hepatol* **17**, 673-685 (2020). https://doi.org:10.1038/s41575-020-0339-z

DISCUSSION

Overview

The gut is essential for overall health, serving not only as the center for digestion and nutrient absorption but also playing a crucial role in immune support, microbial balance, and metabolic regulation. In the last 15-20 years, the concept of gut health has become increasingly popular as the knowledge of the gut's involvement in more than just digestion has become more widely available and accepted (Bischoff, 2011). Scientific investigations along with the food and drug industries have highlighted the importance of maintaining a balanced microbiome and diet to avoid impairment of intestinal barrier as this may lead to increased risk of developing various diseases, including autoimmune disorders (Akobeng et al, 2020; Christovich and Luo, 2022), inflammatory bowel disease (Michielan and D'Inca, 2015), and neurodegenerative conditions like Parkinson's Disease (Braak et al, 2006; Kim et al, 2019; Holmqvist, 2014).

Traditionally, Parkinson's Disease (PD) was thought of as a disorder confined to the central nervous system (CNS). Despite the high prevalence of GI issues in PD, including constipation, visceral pain, and bloating, GI symptoms were largely overlooked in clinical practice until the late 1970s, only becoming clinically relevant due to side effects associated with the use of dopamine pathway modulators like levodopa (Parkes et al., 1971). Not until the new millennium did the search for explanations concerning the potential role of the peripheral nervous system (PNS) and GI involvement in PD pathogenesis gain momentum (Braak et al., 2006; Braak et al., 2003). In 2003, Heiko Braak postulated that PD pathology, and specifically aSyn aggregation, began in the gut and traveled to the brain via the vagus nerve. In support of this hypothesis, aggregated aSyn has been found throughout the GI tract in PD subjects (Braak et al., 2006; Potsuma et al., 2012; Beach et al., 2016; Lebouvier et al., 2010; Pouclet et al., 2012; Sanchez-Ferro et all. 2015). Additionally, pathological aSyn can propagate bidirectionally between the brain and gut via the vagus nerve (Van Den Berge et al., 2019). Four months after

injection of aSyn pre-formed fibrils (PFFs) into the duodenal wall, phosphorylated aSyn pathology was increased in the DMV and several brain areas including the SNpc (Van Den Berge et al., 2019). Fibrils of aSyn injected into the striatum can propagate anterograde to the colon within one month, primarily via the vagus nerve (Wang et al., 2022). Additionally, dysregulation of gut barrier integrity has been described in PD subjects and multiple animal models and may contribute to disease progression. Increased intestinal permeability (Davies et al., 1996; Schwiertz et al., 2018) and barrier structural alterations (Clairembault et al., 2015) have been correlated with increased mucosal aSyn (Forsyth et al., 2011). These results support the hypothesis of vagal bidirectional communication between the gut and brain resulting in propagation of aSyn. While it is clear that there is a gut-brain connection in PD, investigations into the gut-brain axis are relatively new. Therefore, methodologies to study gut homeostasis and pathogenesis are still evolving creating a need to develop models that accurately capitulate in vivo physiology.

Ex Vivo Models

The gut is a complex organ composed of epithelial, immune, and neural elements that work synergistically to digest and absorb nutrients while protecting the body from potentially detrimental external stimuli and pathogens. Ex vivo models of the gut involve removal of the organ from the body while maintaining the patterned 3D architecture of crypts and villi, multi-cellular diversity, and microenvironment seen in vivo. However, when ex vivo tissues are cultured in a dish, the barrier between luminal contents and the gut wall is lost. Utilization of dual-flow microfluidic devices to create two channels separated by gut explants enables this physical barrier to be maintained. This microfluidic device creates a valuable model to study questions related to barrier integrity, however, is more time-consuming, costly, and lower throughput than organotypic slices. Utilization of both microfluidic devices and organotypic slices in my investigations enabled me to study gut physiology within the context of PD using

differential experimental paradigms, one with a maintained epithelial – luminal barrier, allowing studies on perturbations of the barrier itself, and another without barrier maintenance but with neural and immune networks more readily accessible for investigation.

The work discussed in Section 1 built upon previous work in the lab utilizing iterations of a microfluidic device and an organotypic slice model that highlighted the importance of the microbiome on regulation of gut wall health and physiologic oxygen concentrations for preservation of microbiota (Schwerdtfeger et al., 2016; Schwerdtfeger et al. 2019, Richardson et al., 2020; McLean et al., 2018, Martinez et al., 2022). The devices described in Section 1 included the luminal addition of inulin, a soluble fiber to “feed” the microbiome, and sodium sulfite, an oxygen scavenger, to decrease oxygen to more in vivo – like levels. In addition, media was custom-made in house to contain physiological glucose levels of 4 mM versus traditional culture media with ~25 mM glucose. The combination of inulin, lower glucose levels, and in vivo oxygen concentration, resulted in improved maintenance of neuronal populations not accounted for in other ex vivo on-chip device culture systems (van Midwoud et al., 2010; Kim & Ingber, 2013). Despite the benefits of physiological oxygen levels for microbiome and mucosal health, sodium sulfite is an anti-microbial and may impact the microbiome. Another important modification to the previous device design was the use of 50 μm pore Nitex above and below the tissue explant held with quick-setting cyanoacrylate to securely hold the tissue explant in place. This allowed for the elimination of nicardipine, a calcium channel blocker that was previously used to keep the tissue from pulling out of position in the device by eliminating intestinal smooth muscle contractions (Richardson et al., 2020). Nicardipine is an L-type calcium channel blocker used previously in our laboratory to modulate or inhibit muscle contractions in gut organotypic slices (Schwerdtfeger et al., 2016). Calcium channels play vital roles in several cellular physiological functions by allowing controlled transport of calcium across the plasma membrane, such as muscle contraction and neurotransmitter release (Cooper & Dimri, 2022). By eliminating the need for nicardipine, a variable potentially impacting physiological processes

downstream of gut contractions was removed, providing a more accurate modeling of the in vivo physiological environment. Many ex vivo models do not preserve organ structure beyond 24 hr and/or do not maintain a range of cell types including immune and neural components (de Kanter et al., 2005; van Midwoud et al., 2010; Kim & Ingber, 2013). The specifications implemented into our device that accounted for luminal environment, oxygen concentration, nutrient availability, and contractility, resulted in a physiologically relevant model that maintained epithelial cells, immune cells, neuronal fibers, and tight junctions for 72 hr. The microfluidic devices described in Section 1 will enable study of intestinal physiology and disease in a physiologically complex gut culture system with potential for use in the later stages of drug development pipelines.

My work in refining our gut-on-chip ex vivo model instilled an interest in further understanding barrier tissue function within the context of a pathologic phenotype known as leaky gut. Breakdown of the gut epithelial barrier and mucus layers became of particular interest as these tissue elements are associated with multiple diseases including, inflammatory bowel diseases (IBD) (Michielan and D'Inca, 2015), autoimmune diseases such as celiac disease (Akobeng et al, 2020; Christovich and Luo, 2022), neurodegenerative disorders such as Alzheimer's and Parkinson's Disease, (Braak et al, 2006; Kim et al, 2019; Holmqvist, 2014; Caradonna et al, 2024), multiple sclerosis (Schwerdtfeger et al., 2025), and neurodevelopmental disorders such as autism spectrum disorder (Min et al, 2022). When developing a means to trigger leaky gut in our microfluidic organotypic device cultures, it was important that it could be applied to multiple disease states / animal models of disease. Therefore, we chose collagenase, an enzyme naturally secreted by gut bacteria to induce a leaky gut phenotype. Addition of broad-spectrum bacterial collagenase in the luminal media successfully recapitulated hallmarks of leaky gut seen in human patients such as decreased tight junction proteins and increased epithelial permeability (Cherwin & Templeton et al., 2023; Way et al., 2024; Davies et al., 1996; Schwiertz et al., 2018; Clairembault et al., 2015).

Despite its value in recapitulating a ‘leaky gut’ phenotype, the microfluidic organotypic device only provided readouts of barrier breakdown post hoc after culture via immunohistochemistry, or with an outside assay on media effluents to determine fluorescein concentrations in media across flow chambers (Martinez et al., 2022). A highlight of the device described in Chapter 2 was the incorporation of trans-epithelial electrical resistance (TEER) enabling monitoring of barrier permeability in real time. Traditionally, TEER has been used on cell monolayers, devoid of the complex three dimensional and heterogenous cellular environment of barrier tissues in vivo. Existing devices capable of long-term explant viability are limited to data observed after the tissue is removed from the device, 48 h or more after it was dissected from the animal (Dawson et al., 2016; Richardson et al., 2021; Martinez et al., 2022). Incorporating TEER measurements inside our microfluidic device increased the temporal resolution of changes in barrier function that might be caused by external perturbations (e.g., infection or chemical irritation). Preservation of tissue viability and the ability to characterize barrier permeability in real time addresses important drawbacks in existing live tissue barrier permeability devices.

Since the microfluidic device successfully recreated a leaky gut phenotype, future studies will be aimed at utilizing specific matrix metalloproteinases (MMPs) to create a leaky gut model with relevance to peripheral pathogenic mechanisms involved in PD etiology. MMPs are versatile endopeptidases that degrade many extracellular matrix and non-matrix proteins (Rempe et al., 2016) and in the context of PD, MMP1 is a host collagenase found in gut epithelia, mucosa, submucosa and muscularis externa (Biel et al., 2023) that cleaves aSyn into fragments with increased likelihood of aggregation (Levin et al., 2009). GelE is the bacterial equivalent of MMP1 secreted by bacteria including *Enterococcus faecalis* which is routinely reported to be elevated in the microbiome of PD patients (Fan et al., 2022; Weis et al., 2019; Li et al., 2022). GelE also activates host MMPs leading to a further compromised intestinal epithelial barrier and subsequent inflammation (Shogan et al., 2015). Therefore, future studies

harnessing our microfluidic devices to investigate the peripheral production of pathogenic aSyn fragments should utilize MMP1, GelE, or other enzymes with potential to disrupt barrier integrity and induce intestinal neuroinflammation.

CGRP as a key to PD

While disruption of intestinal barrier integrity is a key peripheral phenotype of PD, growing evidence suggests that peripheral and central innate immune responses, cellular inflammation, and antibody production contribute to neurodegeneration in PD (Harms et al, 2017). Recent research suggests that peripheral immune activation can lead to immune cell infiltration in the brain (Greenhalgh et al., 2020) as well as increases in cytokines that can cross the blood brain barrier to activate microglia (Fani Maleki and Rivest, 2019). Elevation of pro-inflammatory cytokines such as, IL1β, IL6, and TNFα have been detected in the serum and cerebral spinal fluid of PD patients (Nagatsu et al., 2000; Schroder et al., 2018). Additionally, aSyn has been shown to trigger immune activation (Alam et al., 2022) and exhibits chemoattractant activity towards macrophages, neutrophils, and dendritic cells in humans, and mouse neutrophils and microglial cells (Stolzenberg et al., 2017; Wang et al., 2015). In the brain, aSyn released from neurons activates microglia which can lead to chronic neuroinflammation (Zhang et al., 2005; Kim et al., 2013). Following immune challenge with norovirus infection, the amount of aSyn in enteric neurons was shown to be correlated with degree of inflammation as measured by increases in polymorphonuclear and mononuclear immune cells, in the intestinal wall. Therefore, it is thought that enteric neuronal aSyn is induced as a consequence of immune challenge (Stolzenberg et al., 2017). However, mechanisms underlying this peripheral immune activation in the GI tract of PD subjects are currently unknown.

Following a pilot experiment using rotenone as a model of PD, the neuropeptide calcitonin gene related peptide (CGRP) stood out as a potential player in enteric PD pathology

due to the presence of apical CGRP immunoreactive “fireworks” in the rotenone treated colon. This phenotype drove me to read deeper into neuropeptide involvement in PD. Alterations in CGRP have been closely linked to various disease states that are strongly associated with PD, including IBD (Pascual-Mato, 2024), migraine (Juhasz et al, 2005), and increased CNS aSyn (Na et al, 2020). CGRP is also thought to play a large role in the neuro-immune axis through inducing shifts in immune cell recruitment, proliferation, and cytokine release (Assas et al., 2014). Results in Section 2 pointed towards CGRP as being critical in aSyn accumulation in the gut as well as regulation of neuro-immune and neuro-epithelial interactions.

Utilizing a rotenone model of PD, results from Chapter 4 revealed elevated apical CGRP following rotenone treatment in both males and females that was associated with elevated aSyn in these fibers. However, females had a greater elevation in both apical CGRP and aSyn in these CGRP fibers. Sex differences in cellular and physiological level functions are common and must be considered in the investigation of disease pathology. Investigating diseases like PD which show sex differences in presentation, incidence, and severity, underscores the necessity to consider basal physiologic sex differences when designing basic science studies on PD or considering therapeutic choices. Females with PD exhibit faster disease progression and higher mortality rates than males (Dahodwala et al., 2016). In addition, females with PD report more GI symptoms with higher severity, (Chang et al., 2023; Xiao-Ling et al., 2021; Picillo et al., 2021) including constipation and abdominal pain. Aggregation of aSyn in the intestinal wall alters gut immune populations (Perez-Pardo et al., 2018), and sex differences in immune responses are abundant systemically (Klein et al., 2016), and peripherally in the gut mucosal immune system (Schwerdtfeger & Tobet, 2021). The greater increase in apical CGRP in rotenone-treated females provides a focal point highlighting CGRPs potential involvement in the higher incidence of visceral pain observed in female PD patients. Uncovering sex specific alterations in enteric neuronal populations, underscores the importance of considering sex as a biological variable while investigating prodromal GI symptoms.

Along with alterations in CGRP and aSyn following rotenone administration, changes were seen in specialized epithelial cells responsible for producing and secreting mucus known as goblet cells. Rotenone treatment resulted in fewer apical goblet cells that were increased cell size. The impact on goblet cells was more pronounced apically, coinciding with the greater CGRP fiber density after rotenone. One explanation for the association between elevated gut mucosal CGRP and aSyn driven constipation is through regulation of mucus production by goblet cells. Not only does enteric mucus play an important role in barrier health, but it also acts as lubrication to promote intestinal transit. One of the earliest symptoms of PD is often constipation (Adams-Carr et al., 2016; Cersosimo et al., 2013). While acute stimulation of goblet cells serves as a protective mechanism to bolster the mucosal barrier in response to pathogens (Newberry & Lorenzo, 2005), chronic stimulation may lead to goblet cell mucus depletion contributing to dysregulation of the intestinal barrier and constipation. The findings described in Chapter 4 demonstrate a potential pathway for sex selective neuronal-epithelial interaction between CGRP and goblet cells secondary to elevated enteric aSyn, identifying a potential contributor to GI dysfunction in PD.

My findings in the rotenone model of PD prompted further investigation into the role of CGRP in aSyn accumulation in the gut. Utilizing a genetic A53T model of PD and ex vivo slices, results from Chapter 5 revealed that CGRP treatment increased aSyn in myenteric plexus neurons in both wild-type and A53T$^{+/-}$ mice suggesting a role for CGRP in facilitation of aSyn aggregation, regardless of whether the animal already had pre-existing aSyn accumulation and PD pathology (e.g., A53T$^{+/-}$ animals). By identifying specific factors like CGRP that may facilitate aSyn accumulation in the gut, this research provides further evidence supporting the gut-brain axis as a critical area for investigation in PD.

Along with elevations in apical CGRP and aSyn, A53T$^{+/-}$ mice exhibited increased numbers of S100b+ glial cells and increased S100b levels in stool consistent with an activated enteric glial cell (Rosenbaum et al., 2016) seen in PD patients with elevated GFAP

immunoreactivity (ir) in colon biopsy samples (Clairembault et al., 2014). Interestingly, A53T$^{+/-}$ mice also had increased colocalization of CGRP and S100b. When treated with CGRP, S100b+ cell number and S100b/CGRP colocalization increased in wild-type mice only. A53T$^{+/-}$ mice had higher levels of S100b-ir than wild-type mice before CGRP treatment. One explanation for this could be that A53T$^{+/-}$ mice may have an impaired inflammatory response that alters how enteric glial cells respond to CGRP. It is also possible that A53T$^{+/-}$ animals are at the maximum carrying capacity of enteric glial cells at baseline, and treatment with CGRP leaves no room or energy resources to expand the already expanded glial population. In contrast, wild-type tissue may have a more controlled inflammatory response and thus show more robust enteric glial response when treated with CGRP.

Finally, I wanted to determine if elevated aSyn preceded changes in CGRP and S100b or if changes in CGRP and S100b preceded elevations in aSyn. A53T$^{+/-}$ mice exhibit linear increases in aSyn load in the substantia nigra with age (Oaks et al., 2013). Therefore, a pilot experiment was performed to ascertain whether the CGRP/S100b phenotypes and aSyn levels were present at young age, 12-14 weeks old, before a heavy aSyn burden appeared. Preliminary data suggested that young A53T$^{+/-}$ mice exhibited elevations in aSyn in PGP9.5+ myenteric neurons, elevated apical CGRP-ir, and increases in mucosal S100b+ cells similar to aged (e.g., 9-12 months) A53T$^{+/-}$ mice. These results suggest that elevated aSyn may precede the CGRP/S100b phenotypes, however, studies using even younger mice will need to be performed in the future. While the relationship between enteric aSyn and CGRP/S100b remains obscure, results from Chapter 4 indicate a clear role for CGRP and S100b in GI pathology seen in mouse models of PD.

Currently, there are no cures for PD and only symptomatic treatments that often become ineffective over time. Since GI symptoms arise years before motor dysfunction, understanding mechanisms of enteric aSyn pathophysiology is crucial for identifying early diagnostic markers and novel therapeutic targets.

References

1 Afroz, S. *et al.* CGRP Induces Differential Regulation of Cytokines from Satellite Glial Cells in Trigeminal Ganglia and Orofacial Nociception. *Int J Mol Sci* **20** (2019). https://doi.org:10.3390/ijms20030711

2 Alexoudi, A., Donadio, V. & Karageorgiou, E. The potential role of CGRP in synuclein-associated neurodegenerative disorders. *Front Neurosci* **18**, 1479830 (2024). https://doi.org:10.3389/fnins.2024.1479830

3 An, Q. *et al.* Calcitonin gene-related peptide regulates spinal microglial activation through the histone H3 lysine 27 trimethylation via enhancer of zeste homolog-2 in rats with neuropathic pain. *J Neuroinflammation* **18**, 117 (2021). https://doi.org:10.1186/s12974-021-02168-1

4 Anderson, J. P. *et al.* Phosphorylation of Ser-129 is the dominant pathological modification of alpha-synuclein in familial and sporadic Lewy body disease. *J Biol Chem* **281**, 29739-29752 (2006). https://doi.org:10.1074/jbc.M600933200

5 Benemei, S., Nicoletti, P., Capone, J. G. & Geppetti, P. CGRP receptors in the control of pain and inflammation. *Curr Opin Pharmacol* **9**, 9-14 (2009). https://doi.org:10.1016/j.coph.2008.12.007

6 Braak, H., Sastre, M. & Del Tredici, K. Development of alpha-synuclein immunoreactive astrocytes in the forebrain parallels stages of intraneuronal pathology in sporadic Parkinson's disease. *Acta Neuropathol* **114**, 231-241 (2007). https://doi.org:10.1007/s00401-007-0244-3

7 Calabresi, P. *et al.* Alpha-synuclein in Parkinson's disease and other synucleinopathies: from overt neurodegeneration back to early synaptic dysfunction. *Cell Death Dis* **14**, 176 (2023). https://doi.org:10.1038/s41419-023-05672-9

8 Cirillo, C. *et al.* Increased mucosal nitric oxide production in ulcerative colitis is mediated in part by the enteroglial-derived S100B protein. *Neurogastroenterol Motil* **21**, 1209-e1112 (2009). https://doi.org:10.1111/j.1365-2982.2009.01346.x

9 Clairembault, T. *et al.* Enteric GFAP expression and phosphorylation in Parkinson's disease. *J Neurochem* **130**, 805-815 (2014). https://doi.org:10.1111/jnc.12742

10 de Lau, L. M. & Breteler, M. M. Epidemiology of Parkinson's disease. *Lancet Neurol* **5**, 525-535 (2006). https://doi.org:10.1016/S1474-4422(06)70471-9

11 Esposito, G. *et al.* Enteric glial-derived S100B protein stimulates nitric oxide production in celiac disease. *Gastroenterology* **133**, 918-925 (2007). https://doi.org:10.1053/j.gastro.2007.06.009

12 Farrell, K. F. *et al.* Non-motor parkinsonian pathology in aging A53T alpha-synuclein mice is associated with progressive synucleinopathy and altered enzymatic function. *J Neurochem* **128**, 536-546 (2014). https://doi.org:10.1111/jnc.12481

13 Fasano, A., Visanji, N. P., Liu, L. W., Lang, A. E. & Pfeiffer, R. F. Gastrointestinal dysfunction in Parkinson's disease. *Lancet Neurol* **14**, 625-639 (2015). https://doi.org:10.1016/S1474-4422(15)00007-1

14 Giasson, B. I. *et al.* Neuronal alpha-synucleinopathy with severe movement disorder in mice expressing A53T human alpha-synuclein. *Neuron* **34**, 521-533 (2002). https://doi.org:10.1016/s0896-6273(02)00682-7

15 Grozdanov, V. *et al.* Increased Immune Activation by Pathologic alpha-Synuclein in Parkinson's Disease. *Ann Neurol* **86**, 593-606 (2019). https://doi.org:10.1002/ana.25557

16 Harms, A. S. *et al.* alpha-Synuclein fibrils recruit peripheral immune cells in the rat brain prior to neurodegeneration. *Acta Neuropathol Commun* **5**, 85 (2017). https://doi.org:10.1186/s40478-017-0494-9

17 Hayley N Templeton, A. T. E., Luke A Schwerdtfeger, Julietta A Sheng, Ronald B Tjalkens, Stuart A Tobet. Sex specific effects of environmental toxin-derived alpha synuclein on enteric neuronal-epithelial interactions. *BioRxiv* (2024).

18 Lin, M. *et al.* In Parkinson's patient-derived dopamine neurons, the triplication of alpha-synuclein locus induces distinctive firing pattern by impeding D2 receptor autoinhibition. *Acta Neuropathol Commun* **9**, 107 (2021). https://doi.org:10.1186/s40478-021-01203-9

19 McGeer, P. L., Itagaki, S. & McGeer, E. G. Expression of the histocompatibility glycoprotein HLA-DR in neurological disease. *Acta Neuropathol* **76**, 550-557 (1988). https://doi.org:10.1007/BF00689592

20 Michetti, F. *et al.* Growing role of S100B protein as a putative therapeutic target for neurological- and nonneurological-disorders. *Neurosci Biobehav Rev* **127**, 446-458 (2021). https://doi.org:10.1016/j.neubiorev.2021.04.035

21 Na, H. *et al.* Characterization of the effects of calcitonin gene-related peptide receptor antagonist for Alzheimer's disease. *Neuropharmacology* **168**, 108017 (2020). https://doi.org:10.1016/j.neuropharm.2020.108017

22 Parkinson, J. *An Essay on the Shaking Palsy*. (Edwards & Brune Ltd., 1817).

23 Pascal, M. *et al.* The neuropeptide VIP potentiates intestinal innate type 2 and type 3 immunity in response to feeding. *Mucosal Immunol* **15**, 629-641 (2022). https://doi.org:10.1038/s41385-022-00516-9

24 Recchia, A. *et al.* Generation of a alpha-synuclein-based rat model of Parkinson's disease. *Neurobiol Dis* **30**, 8-18 (2008). https://doi.org:10.1016/j.nbd.2007.11.002

25 Rocha, S. M. *et al.* Microglia-specific knock-out of NF-kappaB/IKK2 increases the accumulation of misfolded alpha-synuclein through the inhibition of p62/sequestosome-1-dependent autophagy in the rotenone model of Parkinson's disease. *Glia* **71**, 2154-2179 (2023). https://doi.org:10.1002/glia.24385

26 Rosenbaum, C. *et al.* Activation of Myenteric Glia during Acute Inflammation In Vitro and In Vivo. *PLoS One* **11**, e0151335 (2016). https://doi.org:10.1371/journal.pone.0151335

27 Sathe, K. *et al.* S100B is increased in Parkinson's disease and ablation protects against MPTP-induced toxicity through the RAGE and TNF-alpha pathway. *Brain* **135**, 3336-3347 (2012). https://doi.org:10.1093/brain/aws250

28 Svenningsson, P., Palhagen, S. & Mathe, A. A. Neuropeptide Y and Calcitonin Gene-Related Peptide in Cerebrospinal Fluid in Parkinson's Disease with Comorbid Depression versus Patients with Major Depressive Disorder. *Front Psychiatry* **8**, 102 (2017). https://doi.org:10.3389/fpsyt.2017.00102

29 Templeton, H., Ehrlich, A., Schwerdtfeger, L., Sheng, J., Tjalkens, R., Tobet, S. Sex specific effects of enviornmental toxin-derived alpha synuclein on enteric neuronal-epithelial interactions. *Neurogastroenterol Motil* (2025).

30 Travagli, R. A., Browning, K. N. & Camilleri, M. Parkinson disease and the gut: new insights into pathogenesis and clinical relevance. *Nat Rev Gastroenterol Hepatol* **17**, 673-685 (2020). https://doi.org:10.1038/s41575-020-0339-z

APPENDIX

A. Permission to reproduce manuscript entitled “Microfluidic organotypic device to test intestinal mucosal barrier permeability ex vivo”
B. Permission to reproduce sections from manuscript entitled “A microphysiological system for studying barrier health of live tissues in real time”

A. Reproduced from "Microfluidic organotypic device to test intestinal mucosal barrier permeability ex vivo" with permission from the Ryal Society of Chemistry

Per the Royal Society of Chemistry: https://www.rsc.org/journals-books-databases/journal-authors-reviewers/licences-copyright-permissions/#reuse-permission-requests

You do not need to request permission to reuse your own figures, diagrams, etc., that were originally published in a Royal Society of Chemistry publication. However, permission should be requested for use of the whole article or chapter except if reusing it in a thesis. If you are including an article or book chapter published by us in your thesis please ensure that your co-authors are aware of this.

All authors have been notified via email, and appropriate citations are included in the footer for the chapter where this manuscript appears.

C. Permission to reproduce manuscript entitled "A microphysiological system for studying barrier health of live tissues in real time"

Per Nature Portfolio: https://www.nature.com/nature-portfolio/reprints-and-permissions/permissions-requests#get-permission

Authors have the right to reuse their article's Version of Record, in whole or in part, in their own thesis. Additionally, they may reproduce and make available their thesis, including Springer Nature content, as required by their awarding academic institution.

The article has been properly cited in this thesis according to current citation standards.